Measurement of g-2 of the muon

René Reimann

Flavour Physics Workshop, Neckarzimmern

April 6-8, 2022

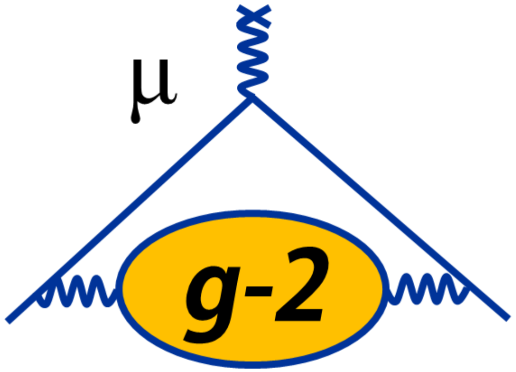

PRiSMA+ Cluster of Excellence
Precision Physics, Fundamental Interactions and Structure of Matter

JOHANNES GUTENBERG UNIVERSITÄT MAINZ
JG|U

Outline

Part 1

- General introduction to precision physics
- Properties of the muon
- Dipole moments, g-2, and how to measure it in principle

Part 2

- How to measure the anomalous precession frequency
- Beam dynamics and major systematic uncertainties

Break

Part 3

- Preparation and measurement of the magnetic field

Part 4

- Result of Run 1
- Comparison with theory prediction
- Other experiments

Standard Model of Elementary Particles

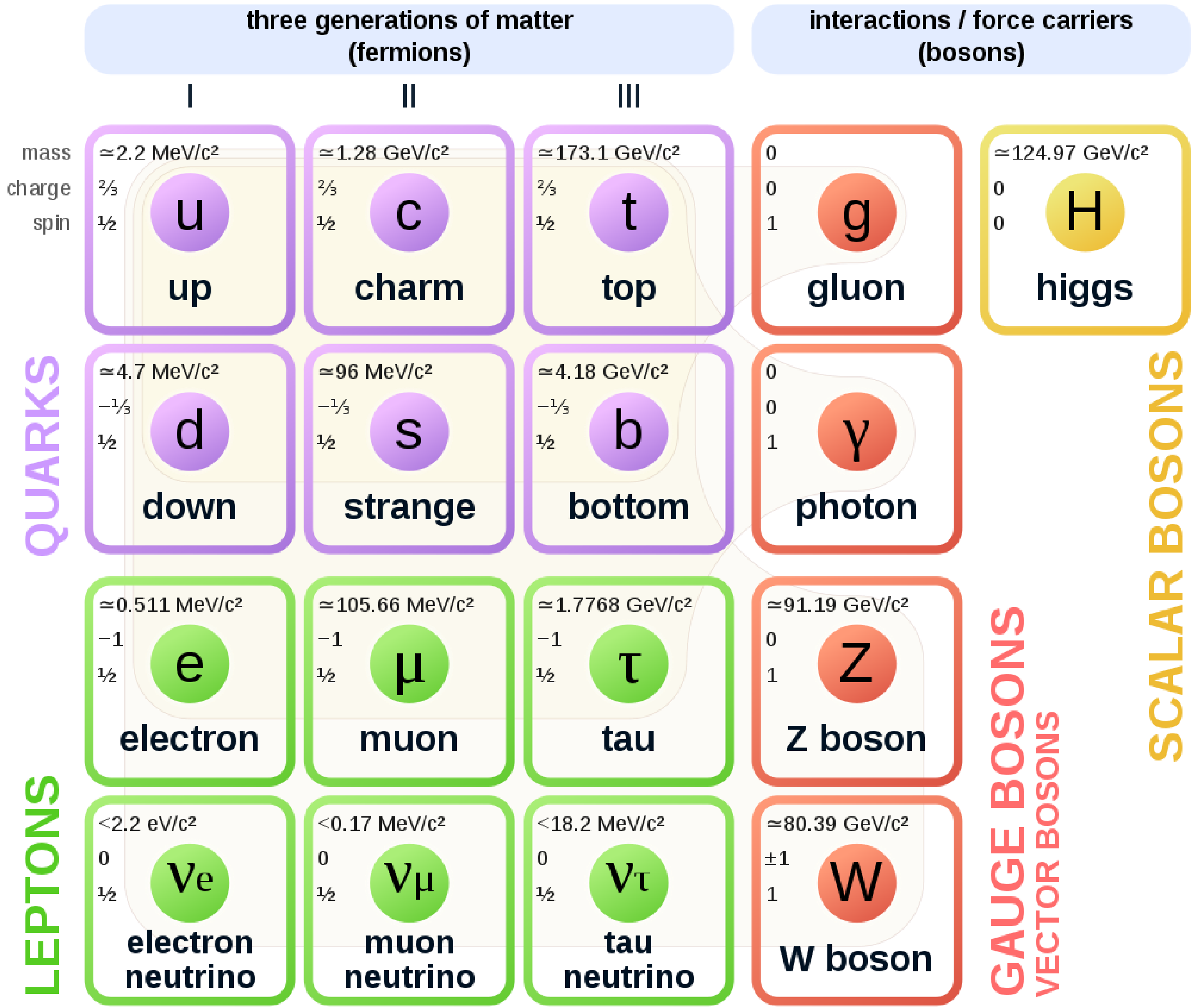

Standard Model of Elementary Particles

	three generations of matter (elementary fermions)			three generations of antimatter (elementary antifermions)			interactions / force carriers (elementary bosons)	
	I	II	III	I	II	III		
mass charge spin	≃ 2.2 MeV/c^2 ⅔ ½ u **up**	≃ 1.28 GeV/c^2 ⅔ ½ c **charm**	≃ 173.1 GeV/c^2 ⅔ ½ t **top**	≃ 2.2 MeV/c^2 −⅔ ½ $\bar{u}$ **antiup**	≃ 1.28 GeV/c^2 −⅔ ½ $\bar{c}$ **anticharm**	≃ 173.1 GeV/c^2 −⅔ ½ $\bar{t}$ **antitop**	0 0 1 g **gluon**	≃ 124.97 GeV/c^2 0 0 H **higgs**
QUARKS	≃ 4.7 MeV/c^2 −⅓ ½ d **down**	≃ 96 MeV/c^2 −⅓ ½ s **strange**	≃ 4.18 GeV/c^2 −⅓ ½ b **bottom**	≃ 4.7 MeV/c^2 ⅓ ½ $\bar{d}$ **antidown**	≃ 96 MeV/c^2 ⅓ ½ $\bar{s}$ **antistrange**	≃ 4.18 GeV/c^2 ⅓ ½ $\bar{b}$ **antibottom**	0 0 1 γ **photon**	
	≃ 0.511 MeV/c^2 −1 ½ e **electron**	≃ 105.66 MeV/c^2 −1 ½ μ **muon**	≃ 1.7768 GeV/c^2 −1 ½ τ **tau**	≃ 0.511 MeV/c^2 1 ½ e^+ **positron**	≃ 105.66 MeV/c^2 1 ½ $\bar{\mu}$ **antimuon**	≃ 1.7768 GeV/c^2 1 ½ $\bar{\tau}$ **antitau**	≃ 91.19 GeV/c^2 0 1 Z **Z^0 boson**	
LEPTONS	<2.2 eV/c^2 0 ½ ν_e **electron neutrino**	<0.17 MeV/c^2 0 ½ ν_μ **muon neutrino**	<18.2 MeV/c^2 0 ½ ν_τ **tau neutrino**	~~<2.2 eV/c^2~~ 0 ½ $\bar{\nu}_e$ **electron antineutrino**	<0.17 MeV/c^2 0 ½ $\bar{\nu}_\mu$ **muon antineutrino**	<18.2 MeV/c^2 0 ½ $\bar{\nu}_\tau$ **tau antineutrino**	≃ 80.39 GeV/c^2 1 1 W^+ **W^+ boson**	≃ 80.39 GeV/c^2 −1 1 W^- **W^- boson**

GAUGE BOSONS
VECTOR BOSONS
SCALAR BOSONS

now <0.8 eV/c^2, see Nature Physics **18**,160–166 (2022)

So why do we think there is physics beyond the Standard Model?

Baryon asymmetry of the Universe:
Why is there not more anti-matter?
Why are we even here?

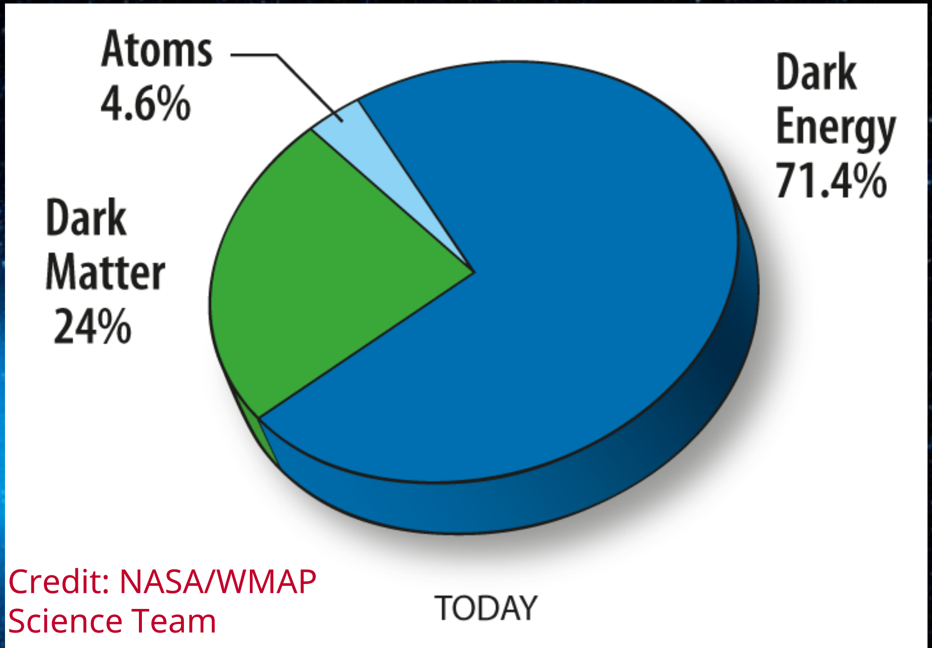

Credit: NASA/WMAP Science Team

Dark energy:
What is it?

Dark matter:
What is it?

Neutrinos do have mass!
How heavy are they?
How do they obtain mass?

Gravity is completely absent in the Standard Model but dominates this picture and is key to DM!

The Standard Model of Particle Physics is incomplete!

Three frontiers of particle physics

Beyond Standard Model Physics

High energy

Direct production of BSM particles @ LHC

CP violation in s-, b- and c- quark sector

This Workshow

Cosmology

Astroparticle physics and astronomy

CMB, galaxies, large scale structure, gravitationa waves

CvB

Highest intensity / exposure

Detection Experiments

Charged lepton flavor violation
$0\nu\beta\beta$ decay searches
$\mu \rightarrow eee$, $\mu \rightarrow e\gamma$

New particles / interactions:

Highest precision

Electron & muon g-2
Absolute ν mass scale
N flavor oscillation experiments
Electric dipole moments
Particle livetimes
Decay correlations

This Talk

High precision measurements in relative units
ppm = 10^{-6}
ppb = 10^{-9}
ppt = 10^{-12}

Interplay
Energy-frontier ↔ Precision-frontier ↔ Theory

Overlapping areas of high-energy and high-precision physics and complementary approaches

- Particle mass measurements: M_Z, M_W, M_H, m_b, m_t, m_e, m_μ, m_ν, …
- Gauge coupling constants: α_{QCD}, α_{QED}, G_F, G_{grav}, …
- Gauge structure of the interactions: $SU(3)_C \times SU(2)_L \times U(1)_Y$
- Overarching and wide-ranging questions:
  - How many generations are there?
  - Mixing angles of quarks and neutrinos?
  - Lepton number and flavor violation?
    - Majorana or Dirac neutrinos
    - Charged Lepton Flavor Violation
  - CP violation:
    - Electric dipole moments?
    - K and B sector at accelerators

Extremely successful exploration of the SM at the energy and precision frontier paired with exquisite theory!

The electron and the muon

In the context of this lecture we well mostly concentrate on electrons and muons …

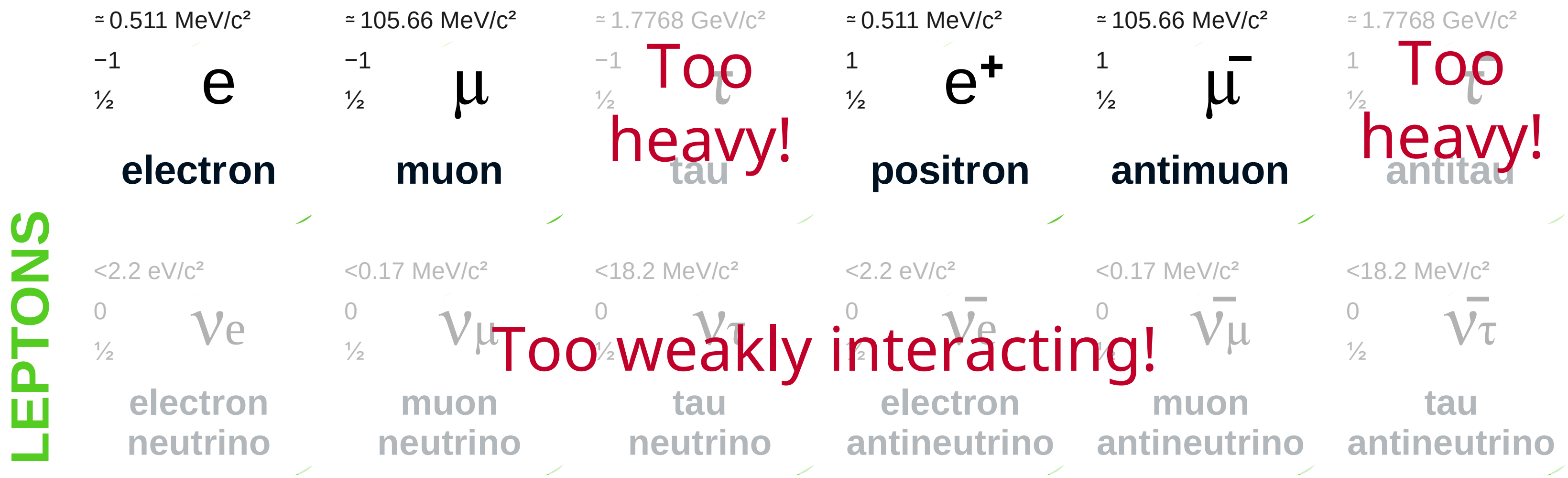

… and their anti-particles, because they provide an ideal test ground!

Discovery of muons
First experimental evidence

A high-energy experiment in 1933: Study of atmospheric rays (Today’s signal is tomorrows background!)
„Untersuchung der Ultrastrahlung in der Wilsonkammer.“, Paul Kunze, Zeitschrift für Physik, Vol. 83, 1933

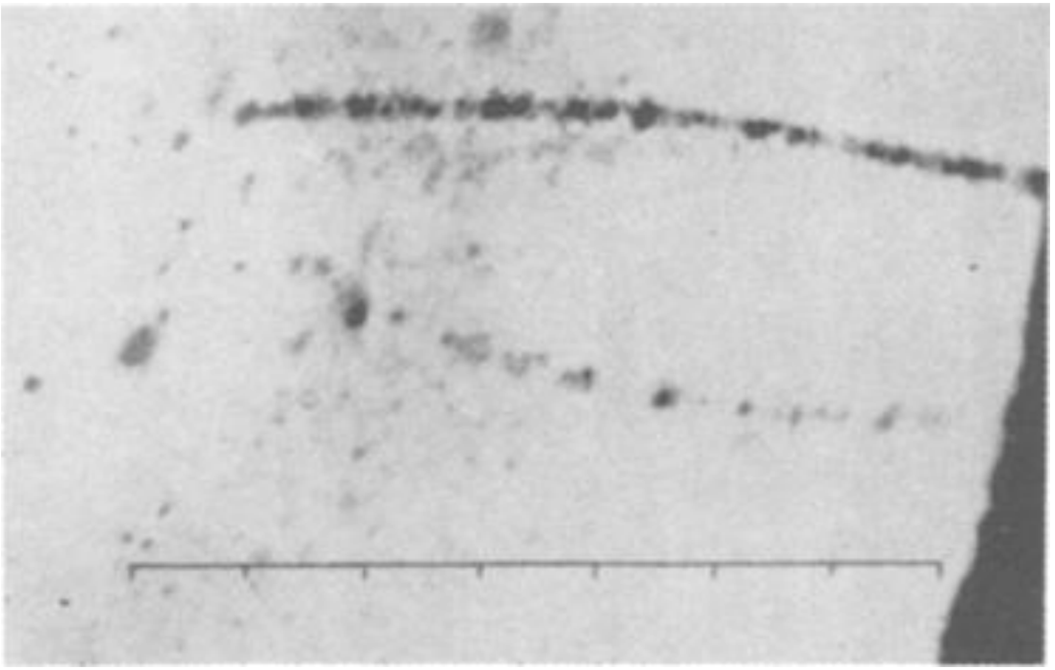

Fig. 5.
Doppelspur als Resultat einer vermutlichen Kernexplosion. 7-fache Vergrößerung. Untere Spur = Elektron von 37 000 000 V. Natur der oberen positiven Korpuskel nicht sicher bekannt.

Die andere Doppelspur des gleichen Typus (Fig. 5) zeigt dicht nebeneinander die dünne Spur eines Elektrons von 37 Millionen Volt, und eine wesentlich stärker ionisierende positive Partikel kleinerer Krümmung. Die Natur dieser Partikel ist unbekannt; für ein Proton ionisiert sie wohl zu wenig, und für ein positives Elektron[1]) zu viel. Vorliegende Doppelspur ist vermutlich ein Ausschnitt aus einem „Schauer“ von Partikeln, wie sie von Blackett und Occhialini beobachtet wurden, also das Resultat einer Kernexplosion.

The other double track of the same type (Fig.5) shows in close proximity the thin track of an electron of 37 million volts, and a track from a significantly stronger ionizing positive particle with smaller radius of curvature. The nature of this particle is unknown; for a proton it is seemingly ionizing too little, and for a positive electron too much.(…)

… followed by more evidence …

Cloud Chamber Observations of Cosmic Rays at 4300 Meters Elevation and Near Sea-Level

CARL D. ANDERSON AND SETH H. NEDDERMEYER, *Norman Bridge Laboratory of Physics, California Institute of Technology*
(Received June 9, 1936)

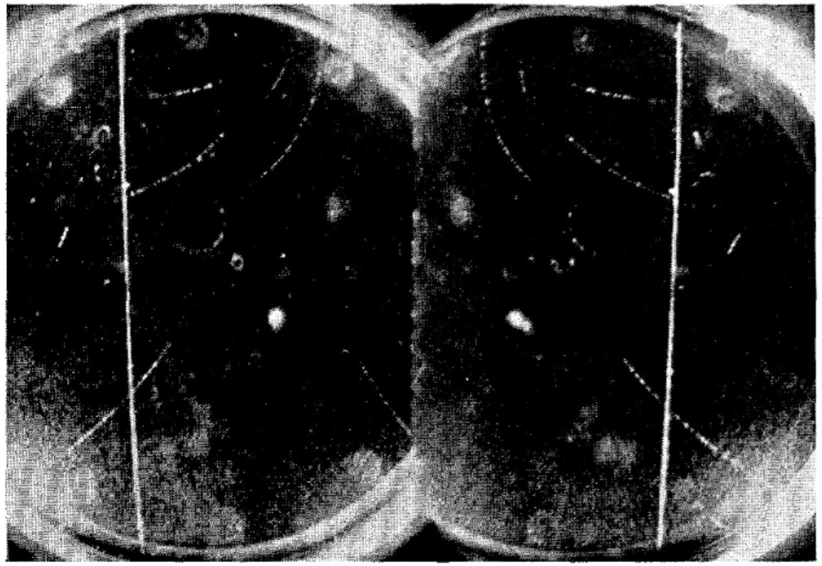

FIG. 8. Pike's Peak, 7900 gauss. A strongly ionizing particle traversing nearly vertically the full diameter of the chamber. It is probably coincident in time with the electron shower which also appears. If traveling downward it has a positive charge and an $H\rho = 1.8 \times 10^6$ gauss cm. If it is assumed to be a proton its energy is 150 MEV and its velocity 0.5 c. The density of ionization exhibited by this track is therefore not inconsistent with the view that it represents a proton. Only a very few examples of strongly ionizing particles traversing the chamber vertically are observed.

New Evidence for the Existence of a Particle of Mass Intermediate Between the Proton and Electron

J. C. STREET
E. C. STEVENSON

Research Laboratory of Physics,
Harvard University,
Cambridge, Massachusetts,
October 6, 1937.

On the Nature of Cosmic-Ray Particles

Y. NISHINA, M. TAKEUCHI, AND T. ICHIMIYA
Institute of Physical and Chemical Research, Tokyo
(Received August 28, 1937)

loss of about a half of the energy. The loss of energy by ionization and the range in lead calculated from the thickness of the lead bar and the final $H\rho$ are consistent, if we assume the mass in question of the particle to be 1/7 to 1/10 that of the proton. The above values of $H\rho$ and the specific ionization shown by the corresponding tracks are in accordance with the assumed mass. This value must necessarily be provisional and subject to a possible alteration. For accurate determination we need more tracks of appropriate energies.

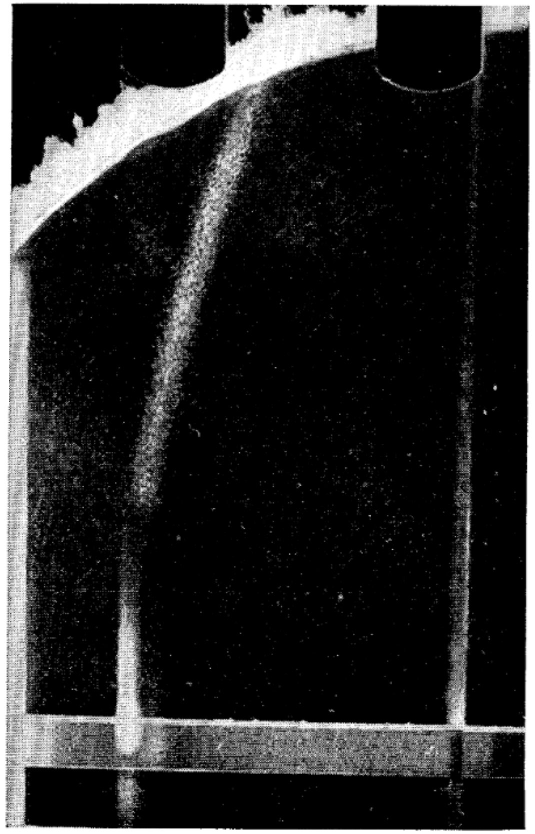

FIG. 3. Track *B*.

Basic properties of muon

particlezoo.com

Charged lepton generation	2^{nd}	
Charge	$q_\mu = \pm (1\text{-}1.1(2.1) \times 10^{-9})\ e$	[1 ppb]
Spin	$s = \hbar/2$	
Mass	$m_\mu = 0.1134289257(25)\ u$ $= 105.6583745(24)\ \text{MeV}/c^2$	[22 ppb]
Lifetime	$\tau_\mu = 2.1969811(22)\ \mu s$	[1 ppm] Most precise lifetime of all particles
Muon/proton magnetic moment ratio	$\mu_\mu / \mu_p = 3.183345142(71)$	[22 ppb]
Spin g-factor	$g_\mu = 2.0023318414(12)$	[0.6 ppb]
Anomalous magnetic moment	$a_\mu = (g_\mu-2)/2 = 0.0011659209(6)$	[540 ppb]

FNAL E989 goal 140 ppb

- Allowed μ^- - decays

$$\mu^- \to e^- + \bar{\nu}_e + \nu_\mu \quad \sim 100\%\ \text{BR}$$
$$\mu^- \to e^- + \bar{\nu}_e + \nu_\mu + \gamma \quad (6.0\pm0.5) \times 10^{-8}\ \text{BR}$$
$$\mu^- \to e^- + \bar{\nu}_e + \nu_\mu + e^+ + e^- \quad (3.4\pm0.4) \times 10^{-5}\ \text{BR}$$

M. Tanabashi *et al.* (Particle Data Group), Phys. Rev. D **98**, 030001 (2018)

"A heavy cousin of the electron"

- Limits on charged lepton flavor violating decay branches:
  - <1.3% BR $\mu^- \rightarrow e^- + \bar{\nu}_\mu + \nu_e$
  - < 4.2 x 10^{-13} BR: $\mu^- \rightarrow e^- + \gamma$
  - < 1.0 x 10^{-12} BR: $\mu^- \rightarrow e^- + e^+ + e^-$
  - < 7.2 x 10^{-11} BR: $\mu^- \rightarrow e^- + \gamma + \gamma$
- Limits on LFV μ^- to e^- conversion:
  - < 7 x 10^{-13} BR: $\sigma\left(\mu^- \mathrm{Au} \rightarrow e^- \mathrm{Au}\right) / \sigma\left(\mu^- \mathrm{Au} \rightarrow \mathrm{capture}\right)$

- Muons are also used to probe other systems:
  - Proton charge radius puzzle (new Lamb shift measurement in H confirms it)
  - Tomography (e.g. Egyptian pyramids, …)
  - …

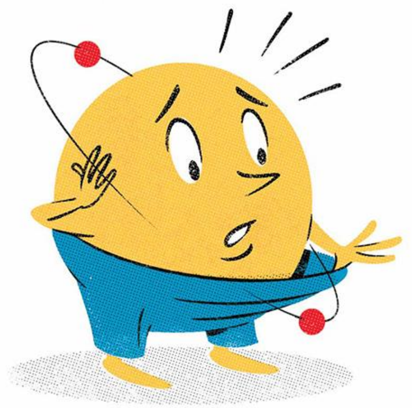

Chris Gash, in NYT

M. Tanabashi *et al.* (Particle Data Group), Phys. Rev. D **98**, 030001 (2018)

"Why are muons such a good probe?"

From an experimentalist's point of view the muon is

- substructure-less charged lepton $\rightarrow$ electromagnetic manipulation of external d.o.f.
- spin with magnetic moment $\rightarrow$ electromagnetic manipulation of intrinsic d.o.f
- 206 times heavier than the electron
  - light enough to be produced in large numbers $\rightarrow$ high statistics
  - heavy enough to (potentially) couple to new physics $\rightarrow$ high sensitivity
- long-lived enough to be efficiently transported $\rightarrow$ "clean" environment
- short-lived enough to observe its exponential decay with high rate $\rightarrow$ high statistics
- a self-analyzing polarimeter
  - Parity violating production (EW)
  - Parity violating decay (EW)

“They allow for high precision tests!”

From a theoretician’s point of view the muon is a very clean system
in which highest precision predictions are achievable!

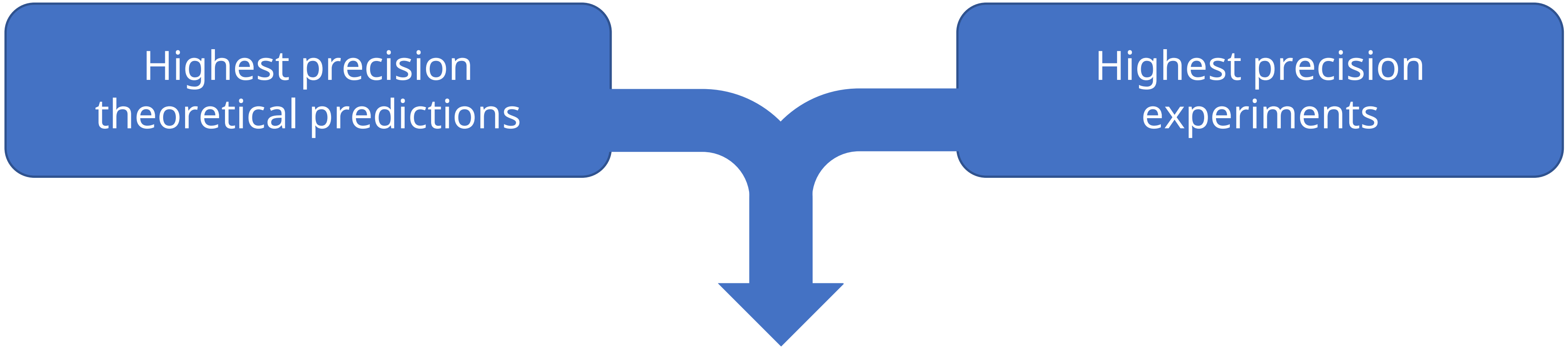

Highest precision test

Classical magnetic dipole moment

Classical Electrodynamic

Any object that creates a vector potential of the form

$$\vec{A}\left(\vec{x}\right) = \frac{\mu_0}{4\pi}\frac{\vec{\mu}\times\vec{x}}{\left|\vec{x}\right|^3}$$

is a $\vec{\mu}$ magnetic dipole moment

e.g. localized current distribution

$$\vec{\mu} = \frac{1}{2}\int \vec{x'} \times \vec{J}\left(\vec{x'}\right) d^3x'$$

Relation to angular momentum

E.g. a sphere with homogenous mass and charge distribution

$$\vec{\mu} = \frac{Q}{2M}\vec{L}$$

$\vec{L}$	total angular momentum
Q	total electric charge
M	total mass

Point-like charge on circular orbit

$$\vec{L} = 2\pi r^2 f m\,\hat{e}_z$$

$$\vec{\mu} = r^2 e\pi f\,\hat{e}_z$$

Classical magnetic dipole moment

Potential energy of a magnetic dipole

$$U = -\vec{\mu} \cdot \vec{B}$$

A magnetic dipole moments tend to align along the magnetic field direction to lower their potential energy.

Torque

$$\vec{M} = \vec{\mu} \times \vec{B}$$

Magnetic dipole moments not aligned with the magnetic field feel a torque and start to precess!

Classic electromotor

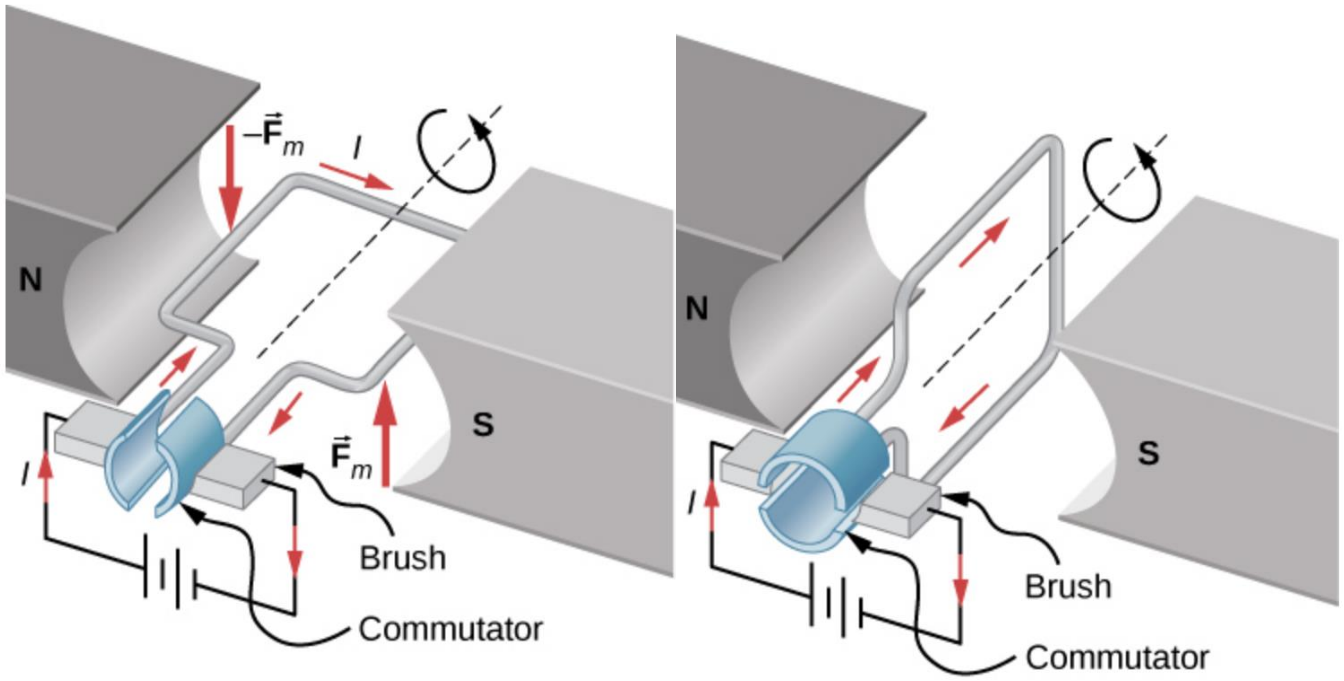

Spin – A new degree of freedom!

Stern and Gerlach (1924): quantization of the spin of the unpaired 5 s^1 electron in silver atoms

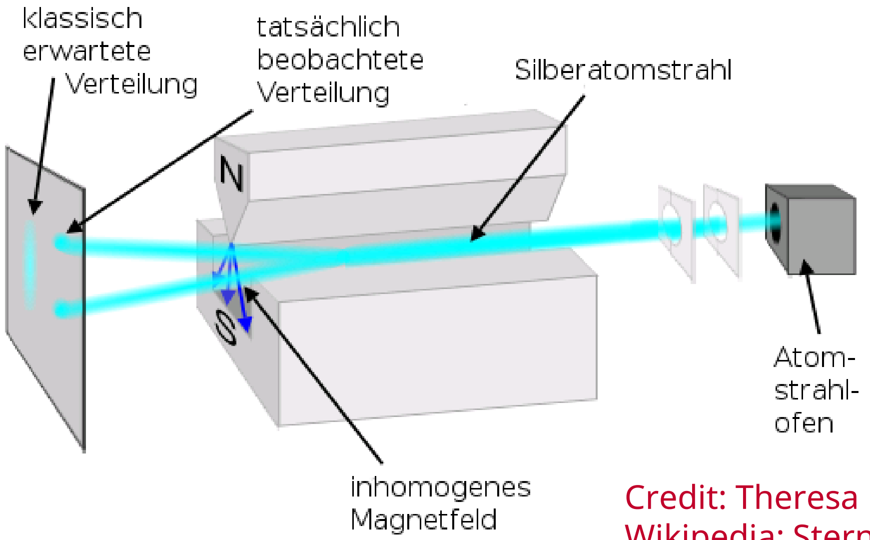

$$\vec{F} = -\vec{\nabla}\left(\vec{\mu}\cdot\vec{B}\right)$$

Credit: Theresa Knott
Wikipedia: Stern-Gerlach-Versuch

Goudsmith and Uhlenbeck (1925): fine-structure in the anomalous Zeeman effect of hydrogen!
G. und U. found that the magnetic moment of this state was compatible with an electron magnetic moment of one (!) Bohr magneton with spin ½!

Magnetic dipole moment twice as large as expected

The g-factor of a particle with spin

Most general definition $\vec{\mu} = g\mu_X \vec{I}$ with spin $\vec{S} = \hbar \vec{I}$

- Bohr magneton $\mu_B = \frac{e\hbar}{2m_{\mathrm{e}}}$ typical for leptons
- Nuclear magneton $\mu_N = \frac{e\hbar}{2m_{\mathrm{p}}}$ typical for hadrons

g factor dimensionless scale parameter to express the measured magnetic moment in terms of natural units

First measurement of g for electrons using atoms found $g_e \cong 2$
but an explanation was lacking at that time!

Dirac to the rescue

We assume EDM=0
for the rest of the lecture

This differs from (1) by the two extra terms

$$\frac{eh}{c}(\boldsymbol{\sigma}, \mathbf{H}) + \frac{ieh}{c}\rho_1(\boldsymbol{\sigma}, \mathbf{E})$$

in F. These two terms, when divided by the factor $2m$, can be regarded as the additional potential energy of the electron due to its new degree of freedom. The electron will therefore behave as though it has a magnetic moment $eh/2mc \cdot \boldsymbol{\sigma}$ and an electric moment $ieh/2mc \cdot \rho_1 \boldsymbol{\sigma}$. This magnetic moment is just that assumed in the spinning electron model. The electric moment, being a pure imaginary, we should not expect to appear in the model. It is doubtful whether the electric moment has any physical meaning, since the Hamiltonian in (14) that we started from is real, and the imaginary part only appeared when we multiplied it up in an artificial way in order to make it resemble the Hamiltonian of previous theories.

: 0

eld

Dipole moments in general

- The prediction of the Dirac equation is applicable to any point-like charged particle with spin S=1/2
- The muon and the tau had not been discovered by 1928! Neither the positron!
- Initial interpretation of the negative energy states as protons were also rejected on the discovery of $g_p \cong 5.59$ [today's value: 5.5856946893(16)]

g_e isn’t quite 2

Sensitive atomic spectroscopy by Kusch and Foley revealed in 1947 that $g_e \neq 2$!

Precision Measurement of the Ratio of the Atomic ‘*g* Values’ in the $^2P_{3/2}$ and $^2P_{1/2}$ States of Gallium*

P. Kusch and H. M. Foley
Columbia University, New York, New York
November 3, 1947

If the electronic configuration in these states is accurately described by Russell-Saunders coupling the above discrepancy must be assigned to a change in the *g* value of the intrinsic moment of the electron or of the orbital moment from their accepted values. If the electron spin *g* value $g_S = 2 + \delta_S$ and the orbital *g* value $g_L = 1 + \delta_L$, then $\Delta = \frac{3}{2}\delta_S - 3\delta_L$. Our present experiments, even assuming Russell-Saunders coupling, do not permit any evaluation of δ_S and δ_L. However, the discrepancy could be accounted for by taking $g_S = 2.00229 \pm 0.00008$ and $g_L = 1$, or alternatively $g_S = 2$ and $g_L = 0.99886 \pm 0.00004$.

Interestingly Kusch and Foley considered both possibilities, also the $g_L \neq 1$.

→ Reflects the amount of uncertainty in the interpretation

Schwinger to the rescue

Schwinger explains the deviation only about 2 month later!

In today's pictorial language:

Dirac (1928) + Schwinger (1947/8)

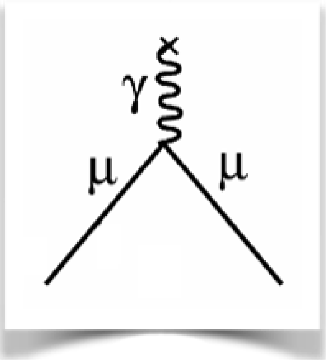

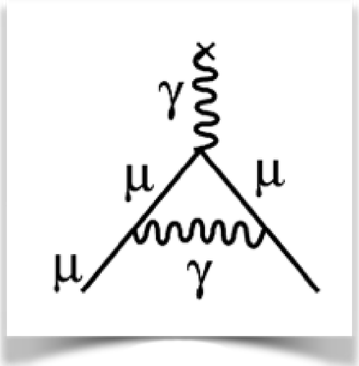

The deviation of g from the simple Dirac value is called the **anomalous magnetic moment**

$$a_\mu = \frac{g_\mu - 2}{2}$$

On Quantum-Electrodynamics and the Magnetic Moment of the Electron

JULIAN SCHWINGER
Harvard University, Cambridge, Massachusetts
December 30, 1947

The detailed application of the theory shows that the radiative correction to the magnetic interaction energy corresponds to an additional magnetic moment associated with the electron spin, of magnitude $\delta\mu/\mu = (\frac{1}{2}\pi)e^2/\hbar c = 0.001162$. It is indeed gratifying that recently acquired experimental data confirm this prediction. Measurements

Recalling that the nuclear moments have been calibrated in terms of the electron moment, we find the additional moment necessary to account for the measured hydrogen and deuterium hyperfine structures to be $\delta\mu/\mu = 0.00126 \pm 0.00019$ and $\delta\mu/\mu = 0.00131 \pm 0.00025$, respectively. These values are not in disagreement with the theoretical prediction. More precise conformation is provided by measurement of the g values for the $^2S_{\frac{1}{2}}$, $^2P_{\frac{1}{2}}$, and $^2P_{3/2}$ states of sodium and gallium.[3] To account for these results, it is necessary to ascribe the following additional spin magnetic moment to the electron, $\delta\mu/\mu = 0.00118 \pm 0.00003$.

Schwinger to the rescue

Schwinger explains the deviation only about 2 month later!

In today's pictorial language

Dirac (1928) + Schw

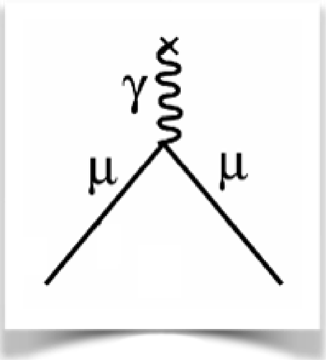

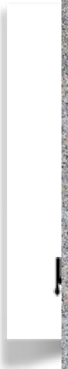

The deviation of g from the
called the **anomalous magnetic moment**

$$a_\mu = \frac{g_\mu - 2}{2}$$

On Quantum-Electrodynamics and the Magnetic Moment of the Electron

Julian Schwinger
Harvard University, Cambridge, Massachusetts
December 30, 1947

The detailed application of the theory shows that the radiative correction to the magnetic interaction energy
litional magnetic moment associated
pin, of magnitude $\delta\mu/\mu = (\frac{1}{2}\pi)e^2/\hbar c$
ed gratifying that recently acquired
nfirm this prediction. Measurements
clear moments have been calibrated
on moment, we find the additional
account for the measured hydrogen
fine structures to be $\delta\mu/\mu = 0.00126$
.00131±0.00025, respectively. These
reement with the theoretical predic-
nformation is provided by measure-
for the $^2S_{\frac{1}{2}}$, $^2P_{\frac{1}{2}}$, and $^2P_{3/2}$ states of
To account for these results, it is necessary to ascribe the following additional spin magnetic moment to the electron, $\delta\mu/\mu = 0.00118 \pm 0.00003$.

Todays calculation of a_μ

Theorists have collaborations as well

Muon g-2 Theory Initiative

Goal: Arrive at consensus for SM prediction

- 135 theorists
- 8-year program
- evaluating 824 publications
- White Paper published in 2020
- arXiv 2006.08443

$$a_\mu^{SM} = 116591810(43) \times 10^{-11}\ (0.37ppm)$$

Muon g-2 in SM

			a_μ^{SM} portion	δa_μ^{SM} portion
QED	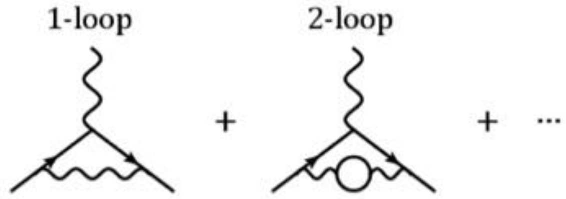	Perturbative (Known to five-loop)	$\sim$ 99.99%	~0.001%
EW	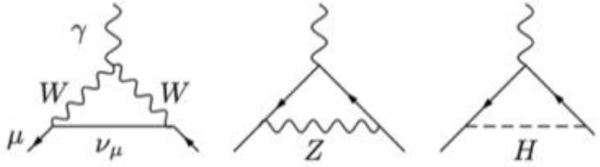	Perturbative (Known to two-loop)	$\sim$ 1 ppm	~0.2%
HVP	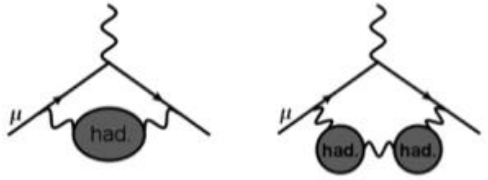	Non-perturbative (Data-driven & lattice)	$\sim$ 59 ppm	~84%
HLbL	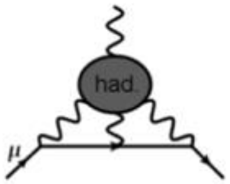	Non-perturbative (Data-driven & lattice)	$\sim$ 1 ppm	~16%

Muon g-2 in SM

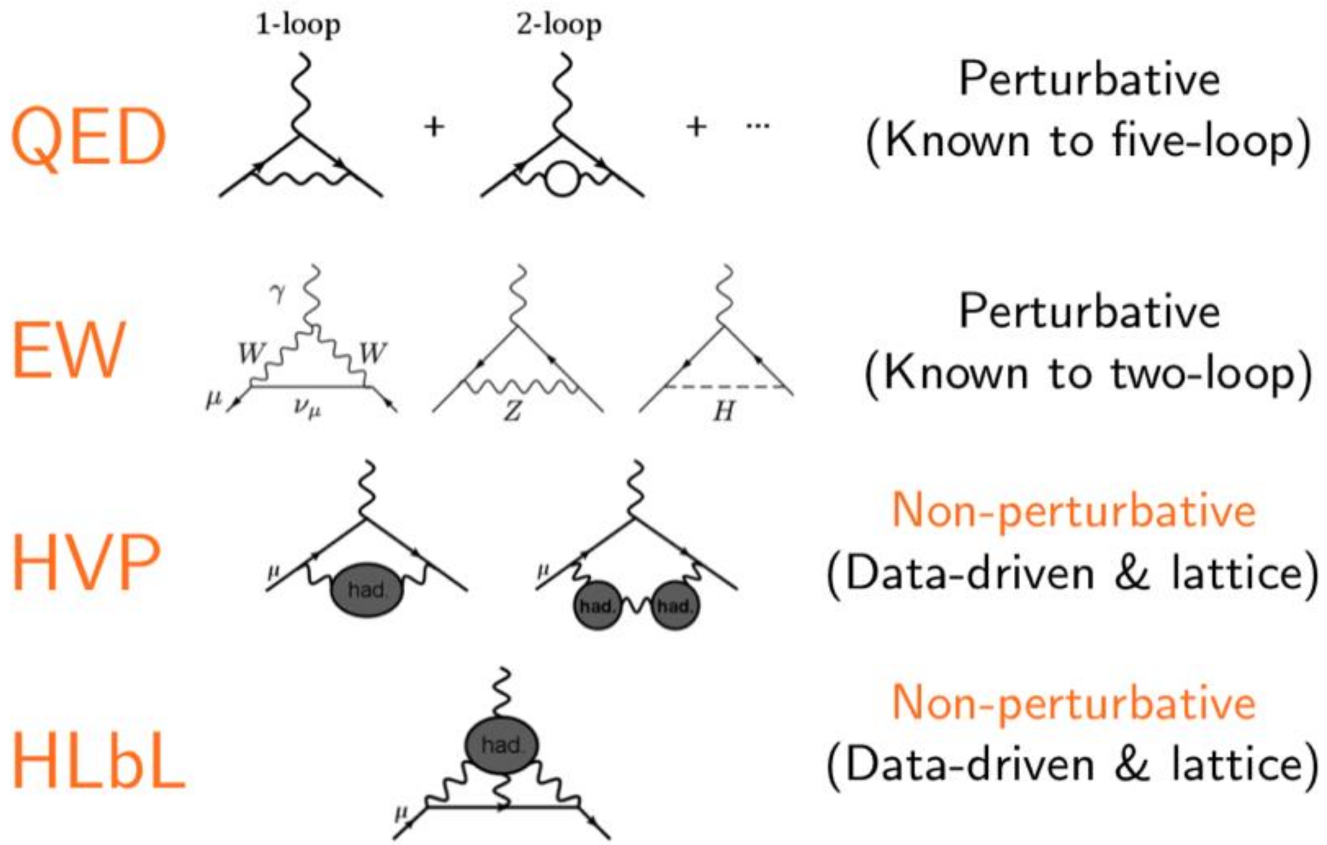

1-loop
2-loop
QED
Perturbative
(Known to five-loop)
EW
Perturbative
(Known to two-loop)
HVP
Non-perturbative
(Data-driven & lattice)
HLbL
Non-perturbative
(Data-driven & lattice)

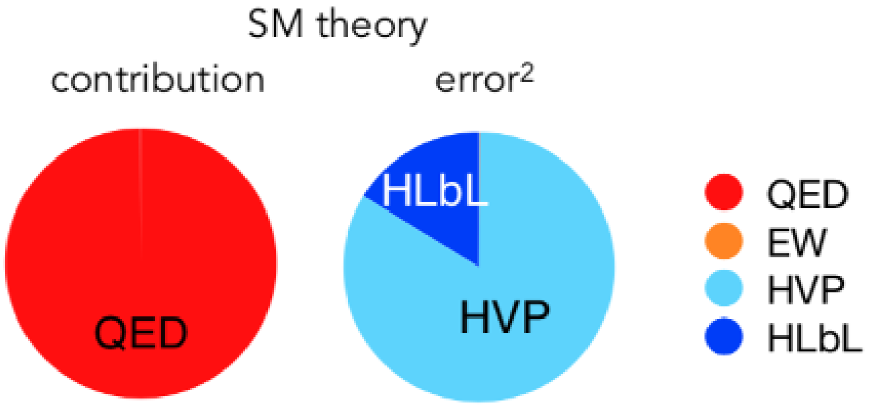

SM theory
contribution
error²
QED
HLbL
HVP
QED
EW
HVP
HLbL

Why Muon g-2?

Status before 2021

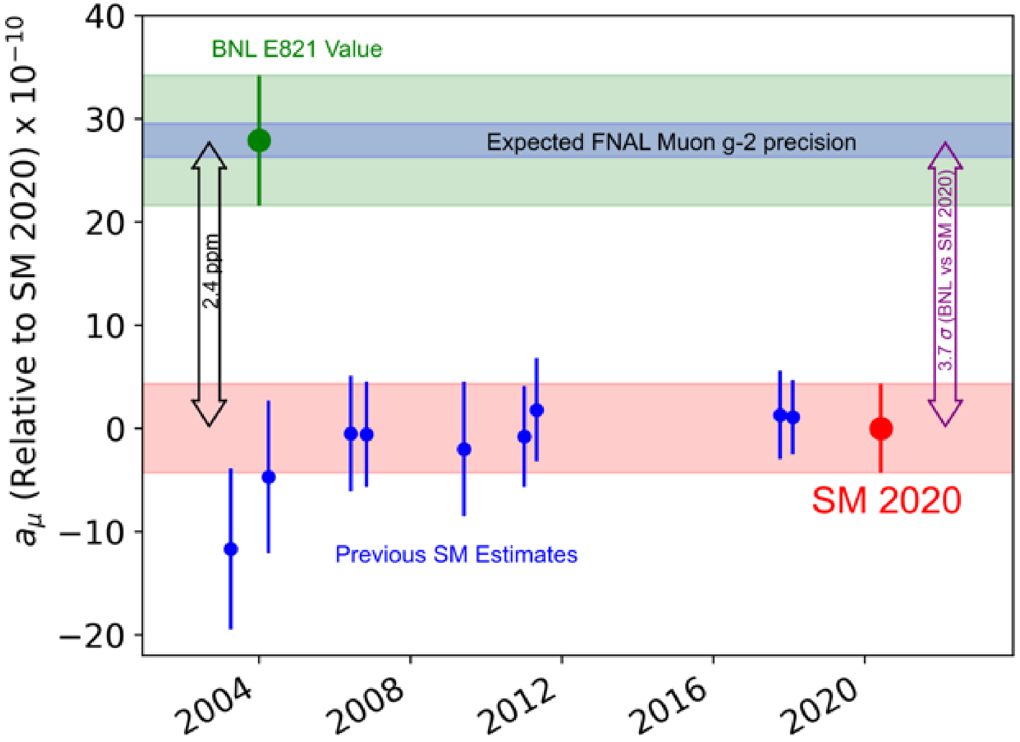

Most precise SM measurements

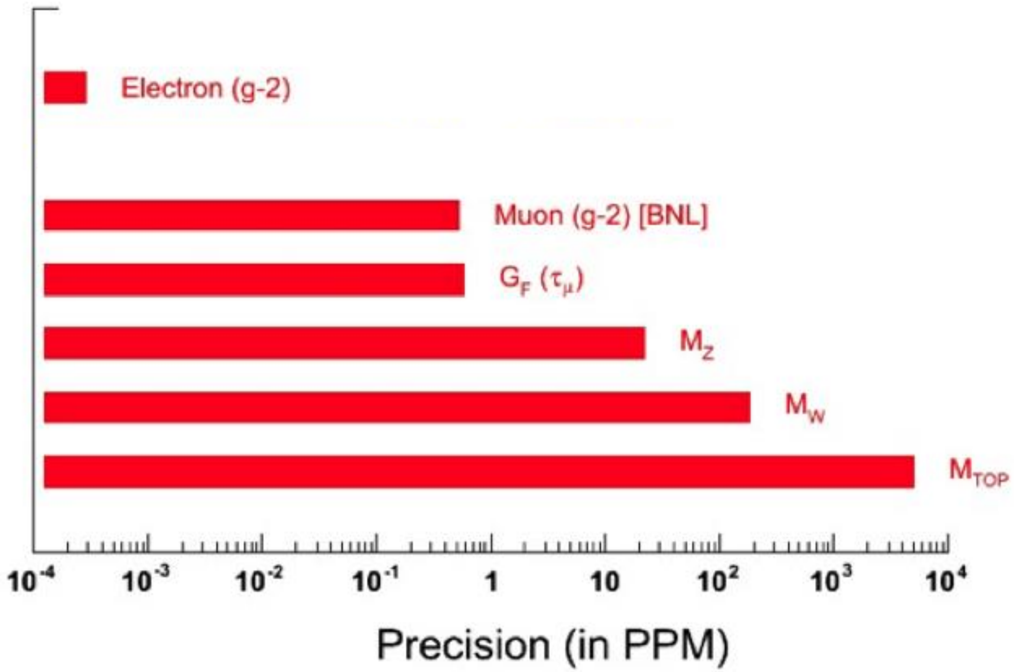

Beyond Standard Model Physics

- Extra contribution to anomalous magnetic moment

$$a_\mu = a_{\mathrm{QED}} + a_{\mathrm{weak}} + a_{\mathrm{hadron}} + a_{\mathrm{BSM}}$$

- Naïve scaling

$$\Delta a_{\mathrm{l}}^{\mathrm{BSM}} \propto \frac{g_{\mathrm{BSM}}}{16\pi^2} \frac{(\text{lepton mass})^2}{(\text{new particle mass})^2}$$

- Comparison with electron g-2

$$\left(\frac{m_\mu}{m_{\mathrm{e}}}\right)^2 = \left(\frac{105\,\mathrm{MeV}}{0.5\,\mathrm{MeV}}\right)^2 \approx 43000$$

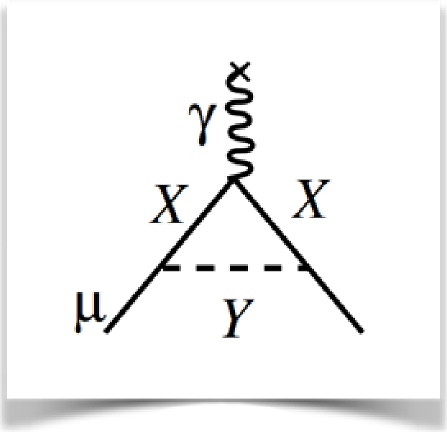

- Muon g-2 is ~43000 more sensitive to new physics compared to electron g-2

Precision Physics

- "Never measure anything, but frequency" (A. Schawlow)
- Time or inverse time is what we can measure best!

• 1s-2s transition in H	$\sigma = 4.2 \times 10^{-15}$	Hänsch et al., 2011
• Electron g factor	$\sigma = 2.8 \times 10^{-13}$	Gabrielse et al., 2008
• Electron mass in u	$\sigma = 2.9 \times 10^{-11}$	Sturm et al., 2014

- These are all frequency-based measurements in pristinely controlled experimental environments!

Non-relativistic muon in homogeneous field

Cyclotron motion

Equilibrium between centrifugal force and Lorentz force

$$\frac{m_\mu v^2}{R} = evB$$

The magnetic field is a momentum filter

$$p_\mu = eBR$$

The cyclotron frequency is a constant

$$\omega_c = \frac{eB}{m_\mu}$$

Spin precession

Spin introduces magnetic moment

$$\vec{\mu} = g\frac{q}{2m}\vec{S}$$

Magnetic moment non parallel to magnetic field induces torque

$$\vec{M} = \vec{\mu} \times \vec{B}$$

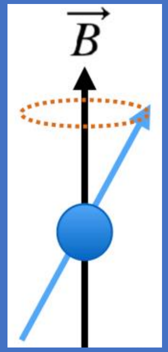

Spin precesses around external magnetic field axis with Lamor frequency

$$\omega_L = g\frac{eB}{2m_\mu}$$

Comparing two clocks

Difference in spin precession and cyclotron frequency proportional to a_μ

$$\vec{\omega}_a = \vec{\omega}_s - \vec{\omega}_c = \left(\frac{g-2}{2}\right)\frac{e}{m}\vec{B}$$

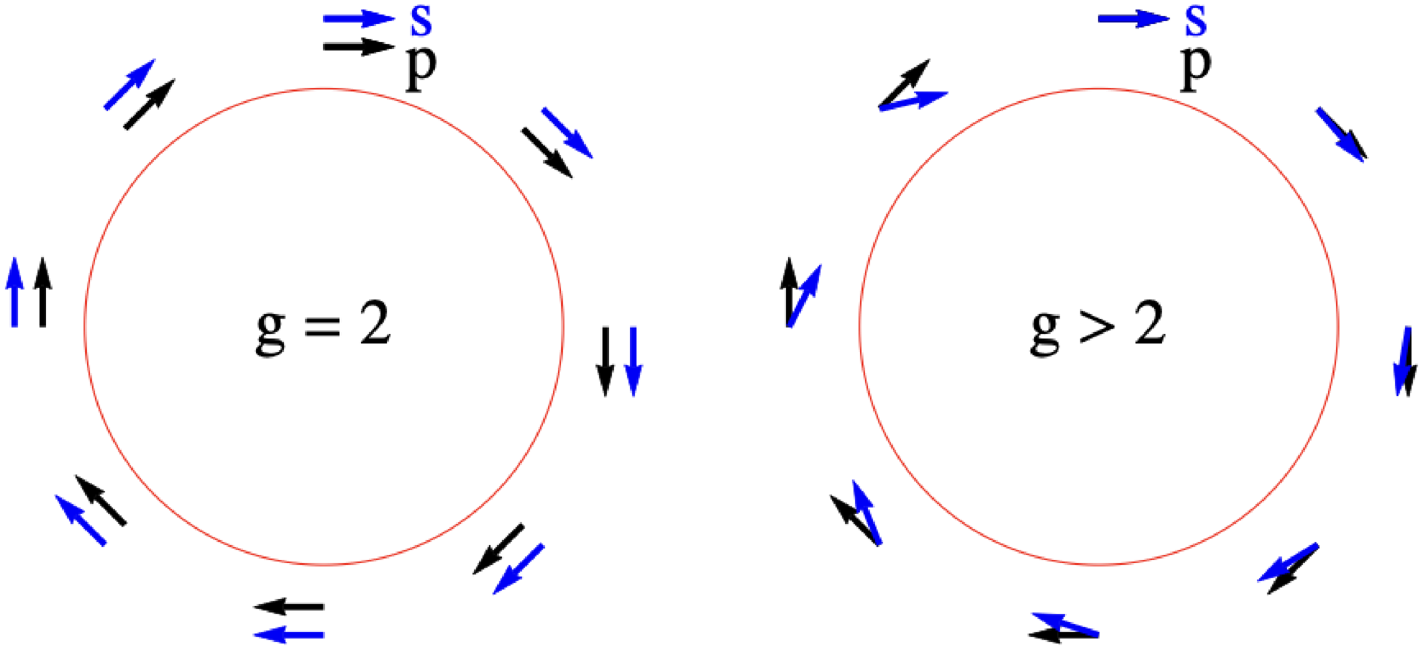

For g>2 the spin vector precesses faster than the momentum vector and gets out of phase!

Relativistic muon in homogeneous field

	Non-relativistic	Relativistic
Cyclotron frequency	$\vec{\omega}_c = \frac{e}{m_\mu}\vec{B}$	$\vec{\omega}_\text{c} = \frac{e}{\gamma m_\mu}\vec{B}$
Spin precession frequency	$\vec{\omega}_s = g\frac{e}{2m_\mu}\vec{B}$	$\vec{\omega}_\text{s} = -\left(\frac{g}{2} + \frac{(1-\gamma)}{\gamma}\right)\frac{e}{m_\mu}\vec{B}$

Thomas precession
Constant rotation of the spin's frame of reference!
Fully relativistic effect, vanishes as $\gamma \rightarrow 1$

Independent of kinematics!

	Non-relativistic	Relativistic
Anomalous precession frequency	$\vec{\omega}_a = \left(\frac{g-2}{2}\right)\frac{e}{m_\mu}\vec{B}$	$\vec{\omega}_a = \left(\frac{g-2}{2}\right)\frac{e}{m_\mu}\vec{B}$

Relativistic muon in magnetic & electric fields

$$\vec{\omega}_{\mathrm{a}} = \vec{\omega}_{\mathrm{s}} - \vec{\omega}_{\mathrm{c}} = \frac{e}{m}\left[a_\mu \vec{B} - a_\mu \left(\frac{\gamma}{\gamma+1}\right)\left(\vec{\beta}\cdot\vec{B}\right)\vec{\beta} - \left(a_\mu - \frac{1}{\gamma^2-1}\right)\frac{\vec{\beta}\times\vec{E}}{c}\right]$$

Non-relativistic limit

Electron motion non-perpendicular to magnetic field

Cyclotron motion assumed motion perpendicular to magnetic field

Pitch of electron

Relativistically generated motional magnetic field

Proportional to electric field

$a_\mu^{SM} = 116591810(43) \times 10^{-11}$

Disappears for $\gamma \approx 29.3$

Magic momentum

p_μ=3.094 GeV/c

Principle of muon g-2 experiments

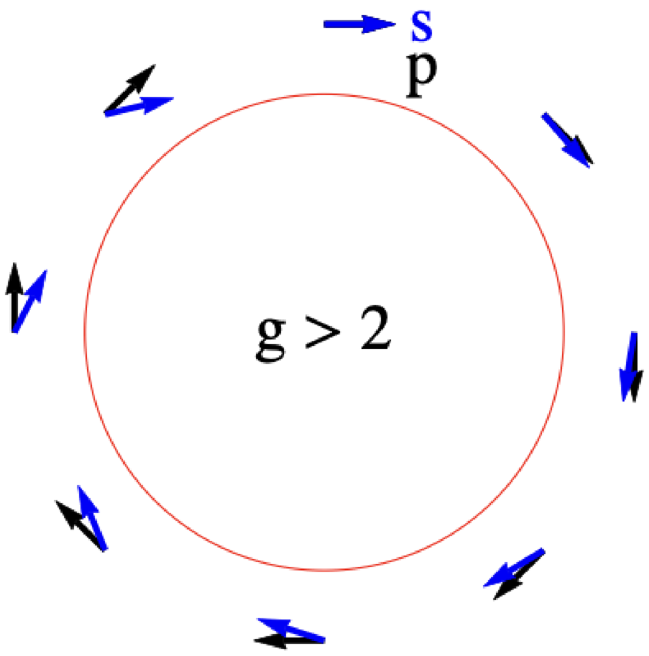

Store polarized muons at magic momentum in magnetic field

Measure spin polarization as function of time

$$\vec{\omega}_{\mathrm{a}} = \frac{e}{m}\left[a_\mu \vec{B} - a_\mu \left(\frac{\gamma}{\gamma+1}\right)\left(\vec{\beta}\cdot\vec{B}\right)\vec{\beta} - \left(a_\mu - \frac{1}{\gamma^2-1}\right)\frac{\vec{\beta}\times\vec{E}}{c}\right]$$

Precisely measure magnetic field

Complex beam dynamics

Muon decay in rest frame

S = 1/2
right-handed

S = 1/2
left-handed

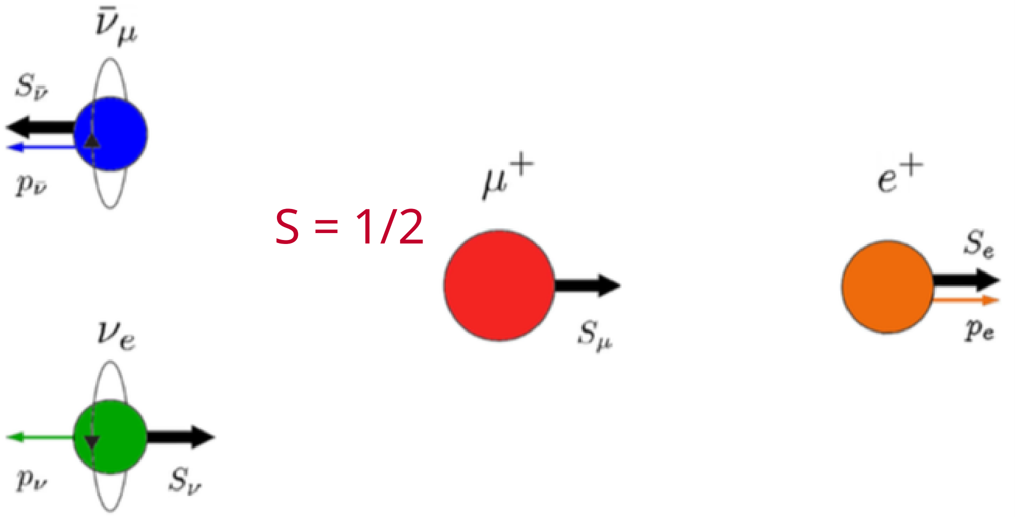

S = 1/2

S = 1/2
right-handed

Maximum positron energy ≅ 52.8 MeV

Positron emitted preferably in direction of muon spin!

Figure credit: K.S. Khaw, PhD thesis, ETHZ, 2015

Muon decay in rest frame

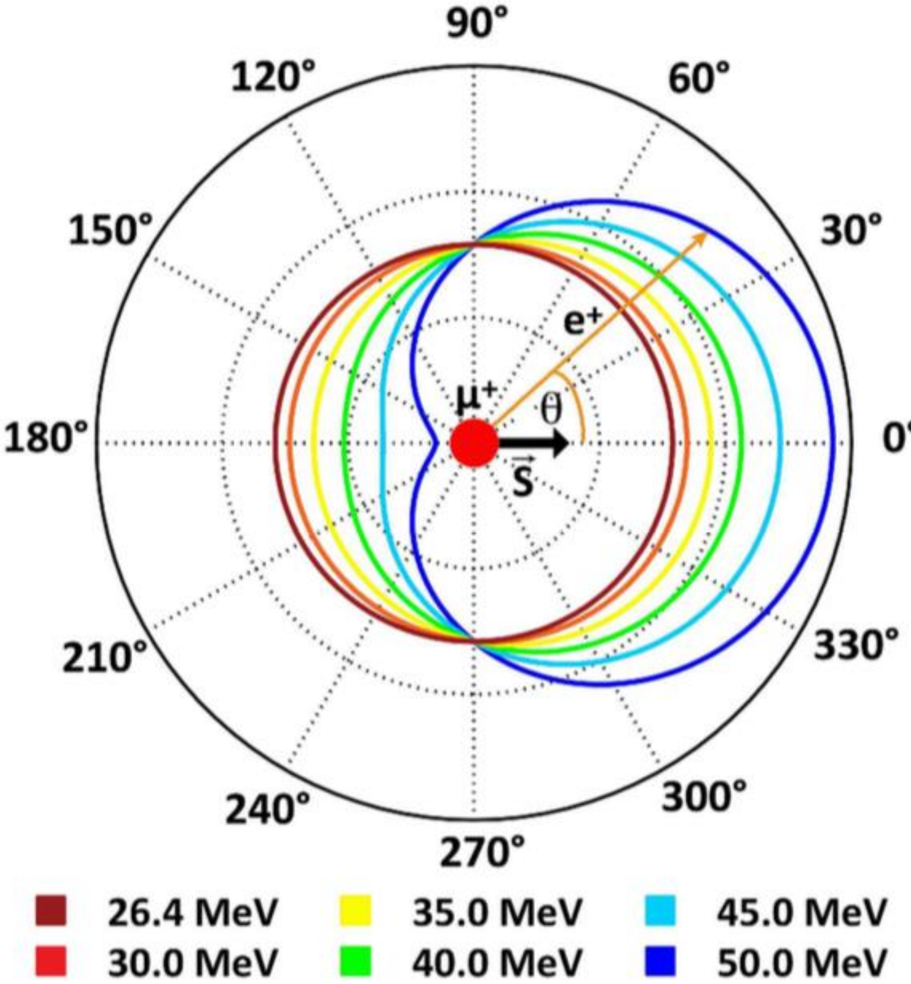

Figure credit: K.S. Khaw, PhD thesis, ETHZ, 2015

Angular differential decay distribution is energy dependent

$$N_e(\theta, E_e) \propto 1 - A(E_e)\cos\theta$$

$$A(E_e) = \frac{E_e^{max} - 2E_e}{3E_e^{max} - 2E_e}$$

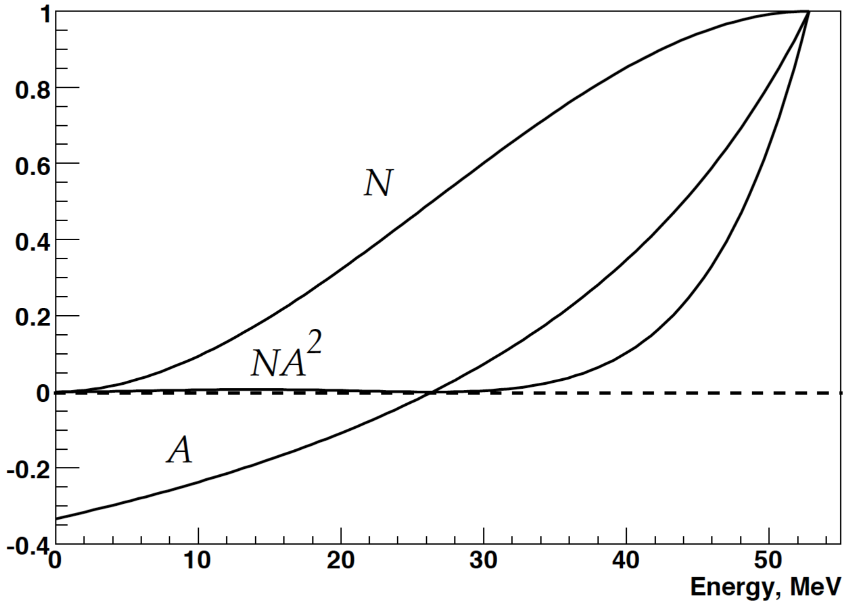

Figure: L. Roberts and W. Marciano, Lepton Dipole Moments

g-2 experiment with muon at rest

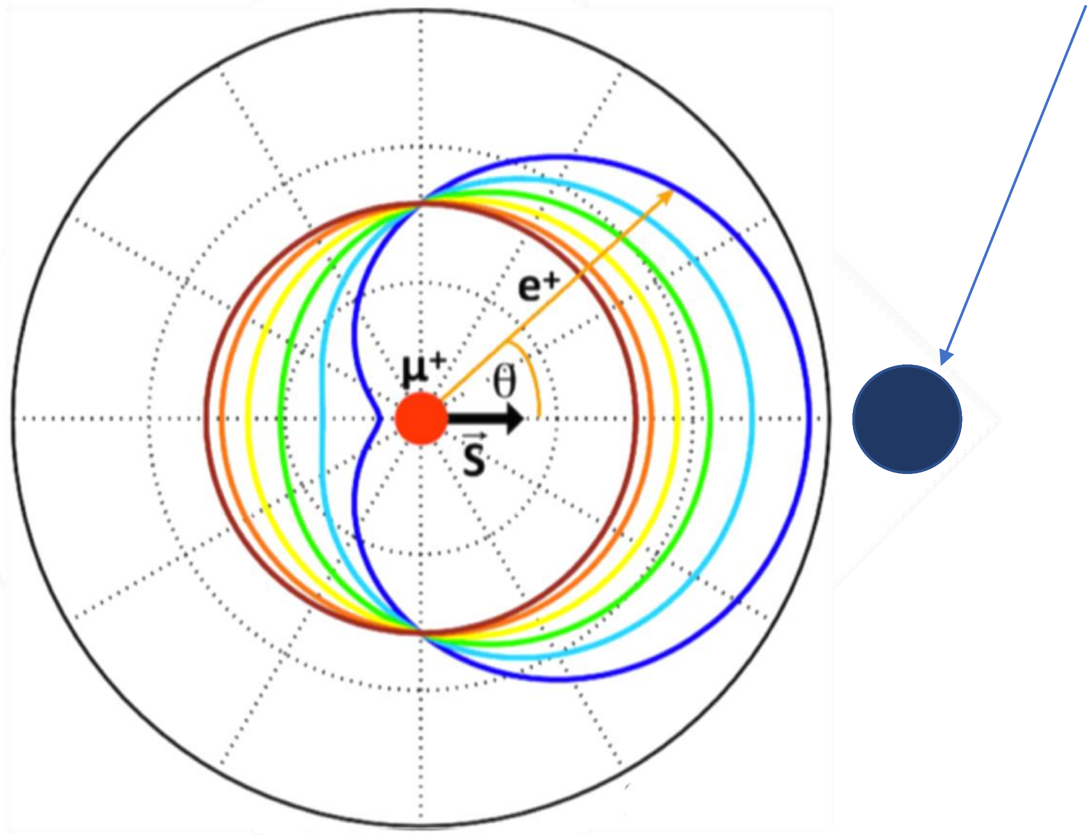

Decay positron detectors

- energy resolving
- segmented

Arrival time histogram at each detector will be modulated at:

$$\omega_{\mathrm{L}} = g\frac{eB}{2m_\mu}$$

Measure magnetic field

Only determines g not (g-2)/2

g-2 experiment in storage ring

Rest Frame

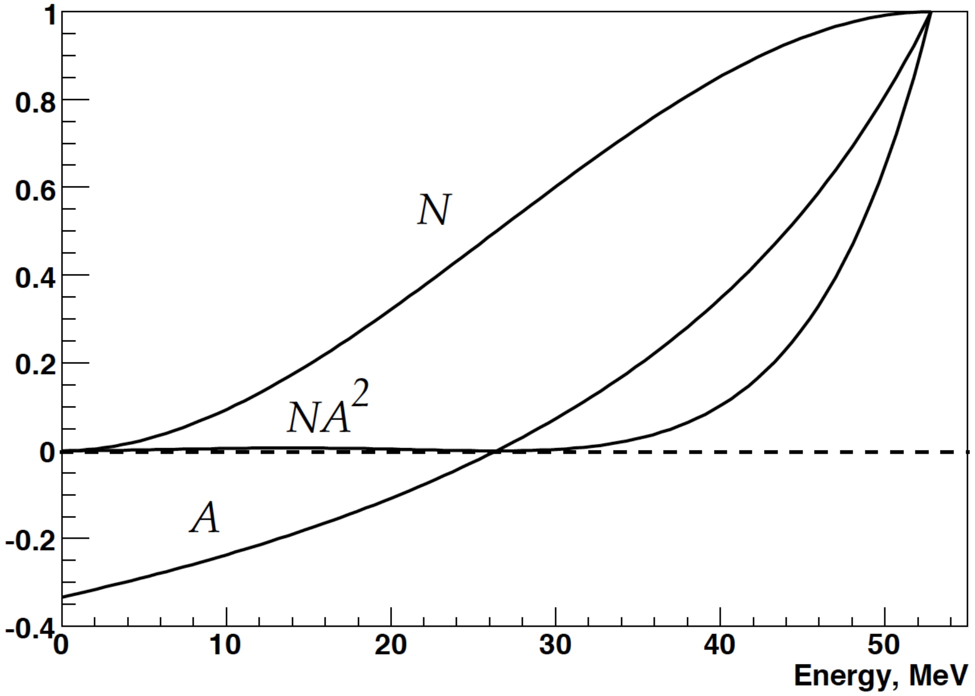

Boost
p_μ = 3.094 GeV/c

Laboratory Frame

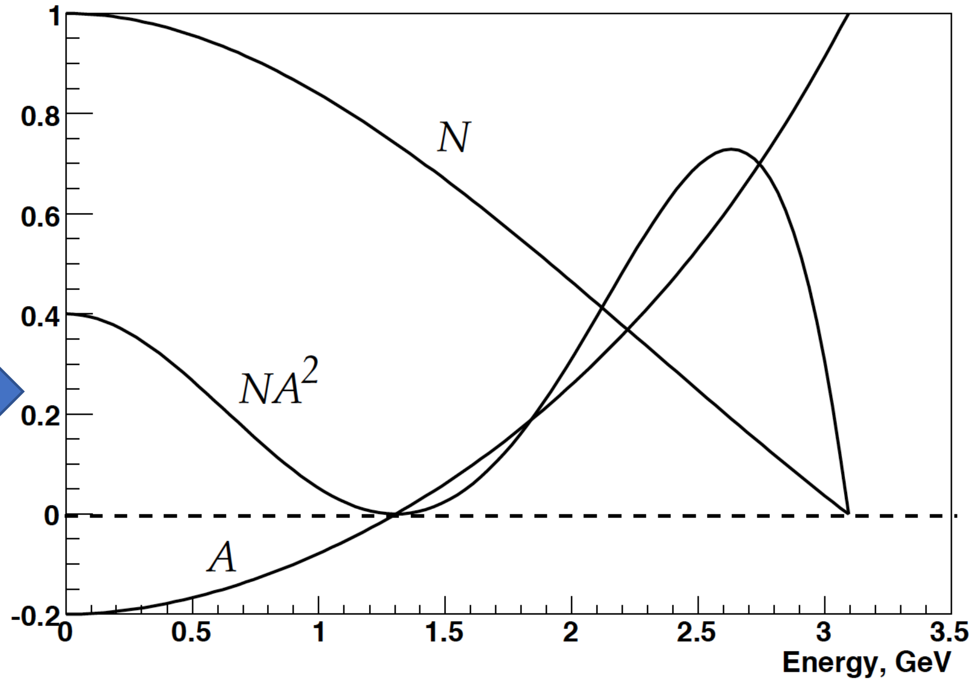

Figure: L. Roberts and W. Marciano, Lepton Dipole Moments

g-2 experiment in storage ring

Store polarized muons in storage ring

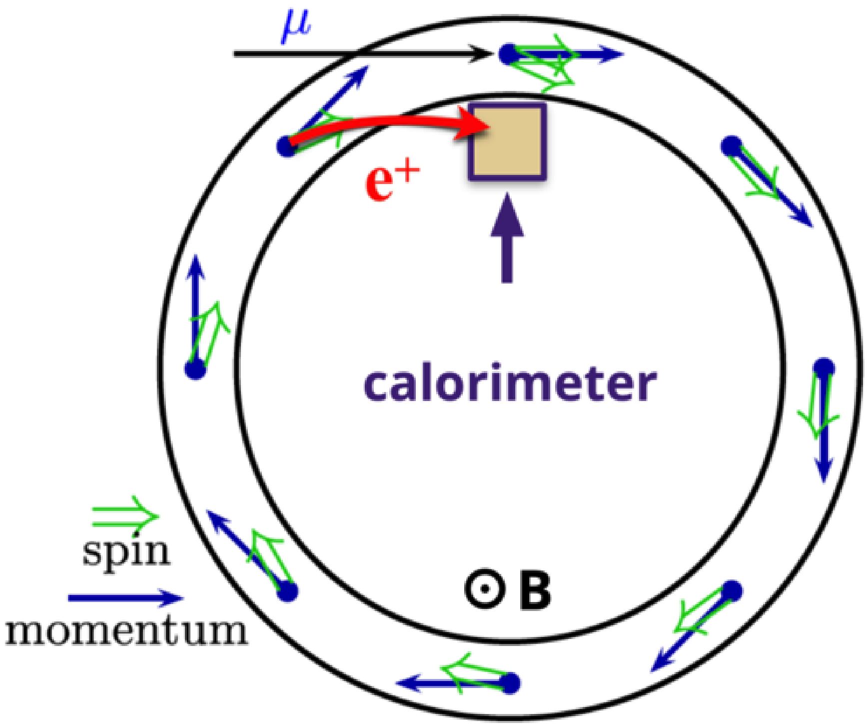

Decay positrons spiral in

Detect positrons above energy threshold

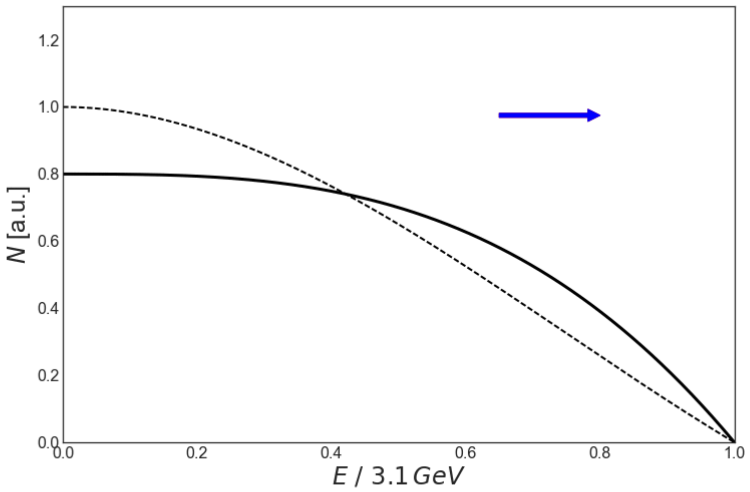

Observable: precession of muon polarization

$$\frac{d}{dt}(\hat{\boldsymbol{\beta}} \cdot \boldsymbol{s}) = -\frac{e}{mc}\boldsymbol{s}_{\perp} \cdot \left[a_\mu \hat{\boldsymbol{\beta}}\ \boldsymbol{x}\ \boldsymbol{B} + \left(\frac{g\beta}{2} - \frac{1}{\beta}\right)\boldsymbol{E} \right]$$

Measures (g-2)/2

The “wiggle” plot

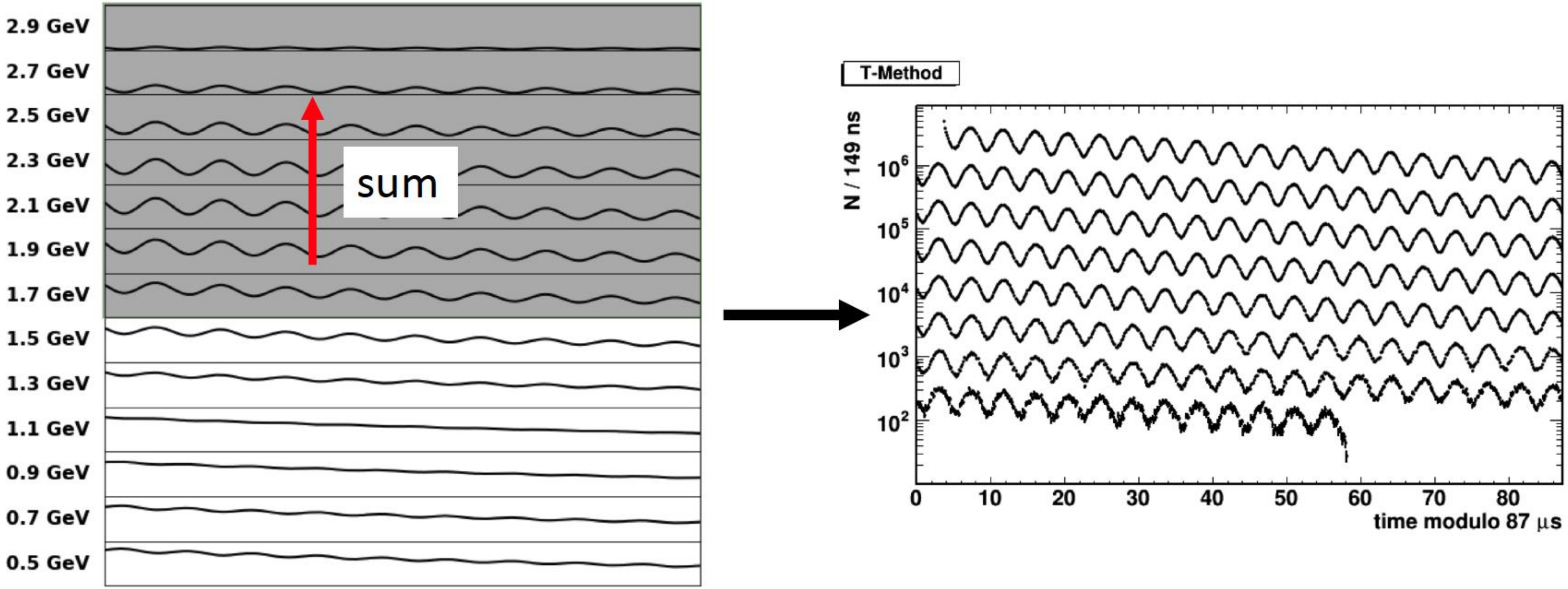

$$N(t) = N_0(E)\, e^{-\frac{t}{\gamma\tau}} \left[1 + A(E)\cos\left(\omega_a t - \phi(E)\right)\right]$$

Exponential decay from muon lifetime modulated with $\omega_a = a_\mu \frac{e}{m_\mu} B$

Calorimeter requirements

Fraction of positrons above a threshold energy in a calorimeter is given by

$$f(t) \propto \int_{E_{\text{thresh}}}^{E_{\text{max}}} N_0 e^{-\frac{t}{\gamma\tau}} N(E)\left[1 + A(E)\cos\left(\omega_{\text{a}} t - \phi(E)\right)\right] dE$$

But can be written as an effective function

$$f(t) \propto N_0 e^{-\frac{t}{\gamma\tau}} \left[\langle N \rangle_{\text{thresh}} + \langle A \rangle_{\text{thresh}} \cos\left(\omega_{\text{a}} t - \langle \phi \rangle_{\text{thresh}}\right)\right]$$

Any remaining time dependence of $\langle \phi \rangle_{\text{thresh}}$ will bias ω_a!

$$\cos\left(\omega_{\text{a}} t - \langle \phi \rangle_{\text{thresh}}(t)\right) \approx \cos\left[\left(\omega_{\text{a}} - \frac{d\langle \phi \rangle_{\text{thresh}}}{dt}\right) t - \langle \phi \rangle_{\text{thresh}}(0)\right]$$

Early to late effect

Calorimeter requirements

Assume two energy bins

$$N(t) = N_{1,0}(E_1)\, e^{-\frac{t}{\gamma_1 \tau_1}} \left[1 + A_1(E_1)\cos\left(\omega_\mathrm{a} t - \phi(E_1)\right)\right] + N_{2,0}(E_2)\, e^{-\frac{t}{\gamma_2 \tau_2}} \left[1 + A_2(E_2)\cos\left(\omega_\mathrm{a} t - \phi(E_2)\right)\right]$$

Phase of summed signal

$$\tan\left(\phi_\mathrm{sum}\right) = \frac{N_{1,0}(E_1)\, e^{-\frac{t}{\gamma_1 \tau_1}} A_1(E_1)\sin\left(\phi(E_1)\right) + N_{2,0}(E_2)\, e^{-\frac{t}{\gamma_2 \tau_2}} A_2(E_2)\sin\left(\phi(E_2)\right)}{N_{1,0}(E_1)\, e^{-\frac{t}{\gamma_1 \tau_1}} A_1(E_1)\cos\left(\phi(E_1)\right) + N_{2,0}(E_2)\, e^{-\frac{t}{\gamma_2 \tau_2}} A_2(E_2)\cos\left(\phi(E_2)\right)}$$

Any differential change between both energy groups will bias the frequency if it is time dependent!

- different storage times for different muon energies, phase-space dependent loss rates
- Detector gain change: $A_{1,2}$ are energy-dependent
- Detector pile up: wrong energy reconstruction

What needs to be measured?

Anchor *B*, *e* and m_μ to other high-precision measurements and calculations

$$\frac{\mu'_p(T_r)}{\mu_e(H)}$$

10.5 ppb uncertainty at T_r = 34.7°C
Metrologia 13, 179 (1977)

$$\frac{m_\mu}{m_e}$$

Muonium hyperfine splitting
22 ppb uncertainty
Phys.Rev.Lett. 82, 11 (1999)

$$a_\mu = \frac{\omega_a}{\tilde{B}}\frac{m_\mu}{e} = \frac{\omega_a}{\tilde{\omega}'_p(T_r)}\frac{\mu'_p(T_r)}{\mu_e(H)}\frac{\mu_e(H)}{\mu_e}\frac{m_\mu}{m_e}\frac{g_e}{2}$$

$$\tilde{B} = \frac{\hbar\tilde{\omega}'_p}{2\mu'_p}$$

proton spin-precession

Using nuclear magnetic resonance (NMR) technique

$$\frac{\mu_e(H)}{\mu_e}$$

Bound state QED calculation
Exact
Rev. Mod. Phys. 88, 035009 (2016)

$$\frac{g_e}{2}$$

Measurement
0.28 ppt uncertainty
Phys. Rev. A 83, 052122 (2011)

Technique developed over 40 years

Goal: 100ppb statistical ⊕ 100ppb systematic uncertainty

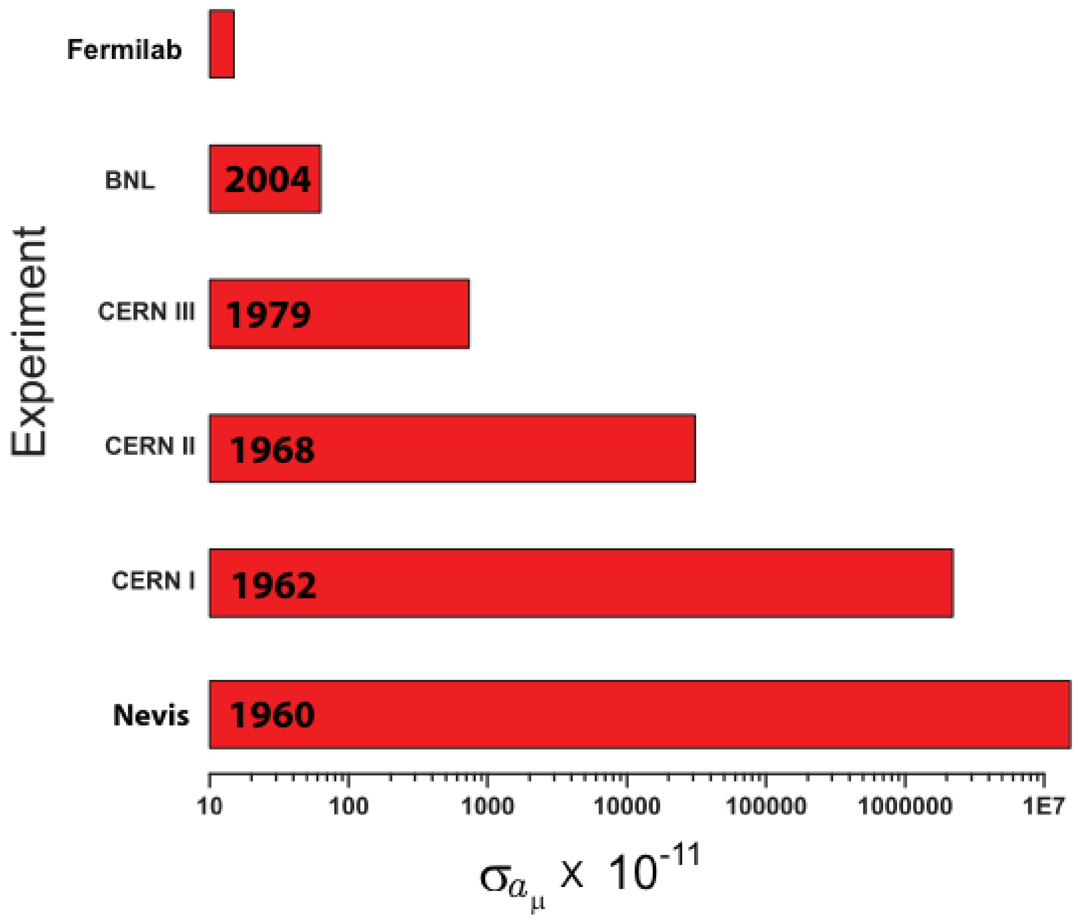

Superconducting storage ring magnet
Muon Injection and magnetic kicker
Superconducting inflector magnet

NMR technique

Magic momentum technique

Storage ring technique to measure g-2

Measured g_μ from muon at rest

What needs to be done?

- Production of a polarized muon beam
- Preparation of the muon beam for the experiment
- Storage of the muon beam
- Detection of the decay positrons
  → determination of ω_a
- Measurement of the magnetic field
- Measurement of the muon beam distribution

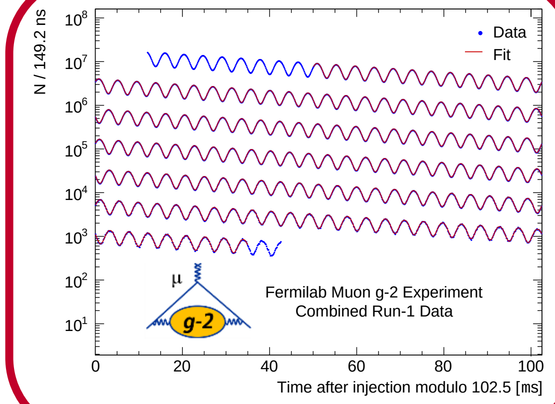

100 ppb statistic
70 ppb systematic

external measurements

$$a_\mu = \frac{\omega_a}{\tilde{B}}\frac{m_\mu}{e} = \frac{\omega_a}{\tilde{\omega}'_p(T_r)}\frac{\mu'_p(T_r)}{\mu_e(H)}\frac{\mu_e(H)}{\mu_e}\frac{m_\mu}{m_e}\frac{g_e}{2}$$

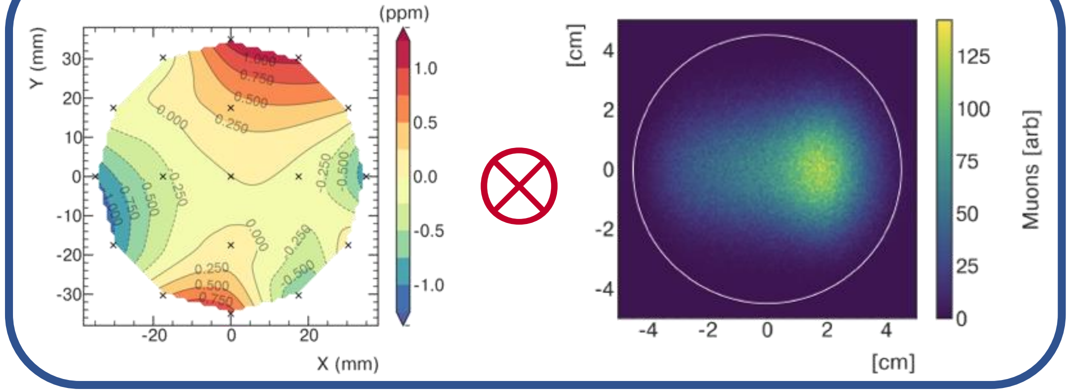

70 ppb systematic

Extracting a_μ

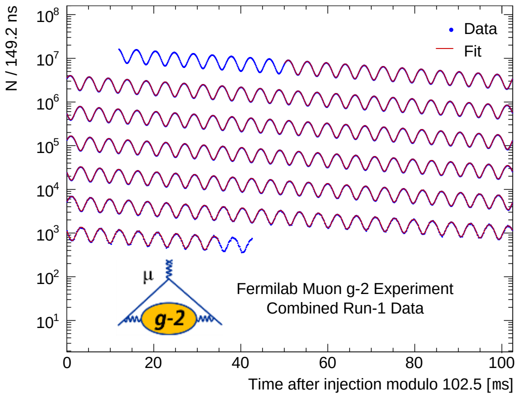

Anomalous spin precession frequency

Clock blinding

Muon beam dynamics corrections

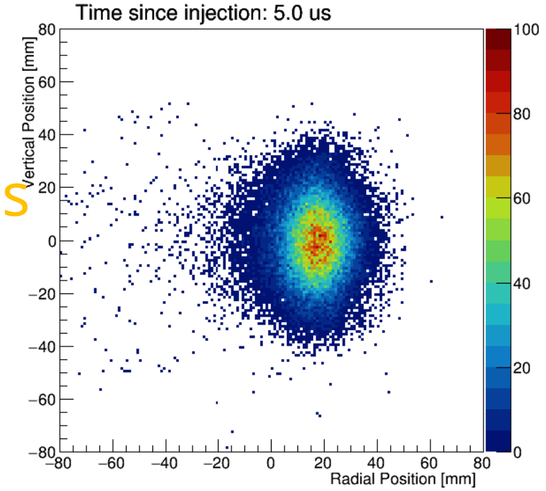

$$\frac{\omega_a}{\tilde{\omega}'_p} = \frac{f_{\text{clock}}\,\omega_a^{\text{meas}}\left(1 + C_e + C_p + C_{ml} + C_{pa}\right)}{f_{\text{calib}}\left\langle M(x,y,\phi)\,\omega'_p(x,y,\phi)\right\rangle\left(1 + B_k + B_q\right)}$$

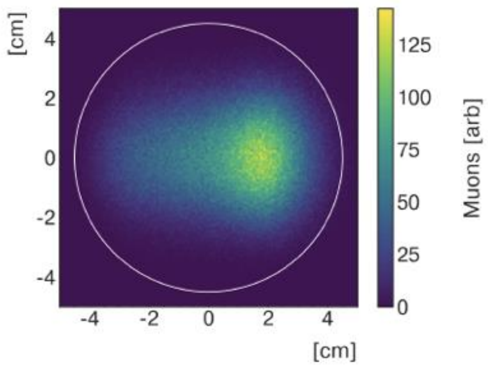

Spatial muon distribution

Spatial distribution of magnetic field

Transient magnetic fields

Calibration

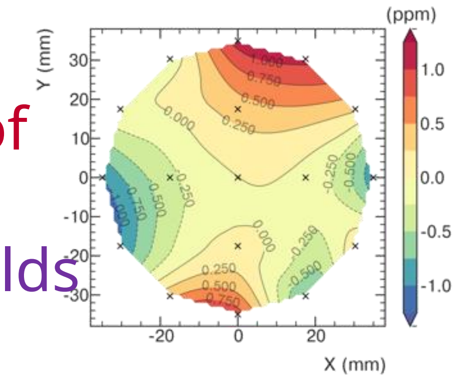

Muon beam production

- 8 GeV protons on Be/Ni target, $p^+ + p^+ \rightarrow p^+ + \mathrm{n} + \pi^+$
- Pion decay, $\pi^+ \rightarrow \mu^+ + \nu_\mu$

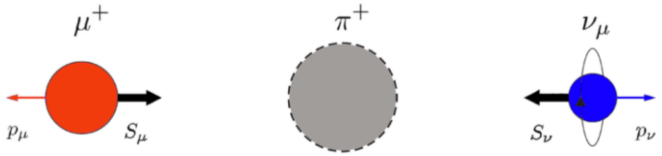

ν_μ must be left-handed → μ^+ also left-handed!
→Polarized muon beam (95%)

- Momentum selective beam line

$$p = 3.094 \frac{GeV}{c} \pm 2\%$$

- Beam purification in energy-dispersive delivery ring
  μ^+ outrun p^+, π^+ decay away
- ~10,000 μ^+ (from 10^{12} p) at 3.1 GeV every 10 ms
- Bunch length of 120 ns

Fermilab muon campus

- Linac/Booster: Start with 4 x 10^{12} p^+/pulse
- Split p^+ into 8 bunches in recycler ring
- 8 GeV p^+ energy, 120 ns long bunch impinging onto Be/Ni target

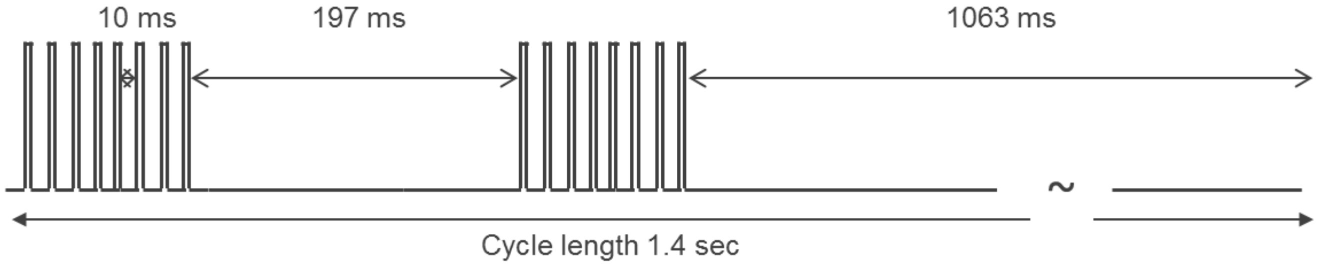

- Beam preparation to avoid pile-up

Muon Production

- Proton on target produce pions $p^+ + p^+ \to p^+ + n + \pi^+$

- Pions decay via weak interaction (parity violation)

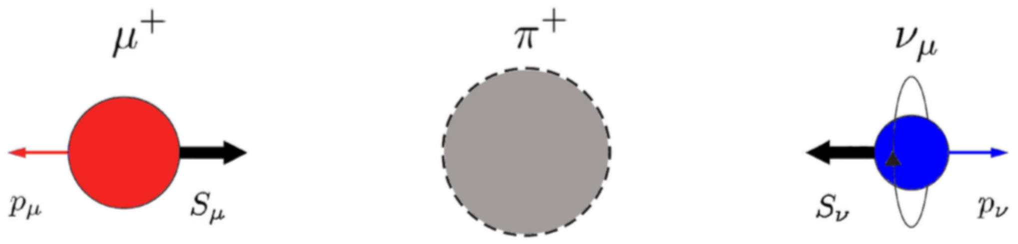

- Close to 100% muon spin-polarization
  - μ^+: muon spin *anti-aligned* with momentum (because of the left-handed ν_μ!)
  - μ^-: muon spin *aligned* with muon momentum

- Very small contamination with e^+/e^- !

Fermilab muon campus

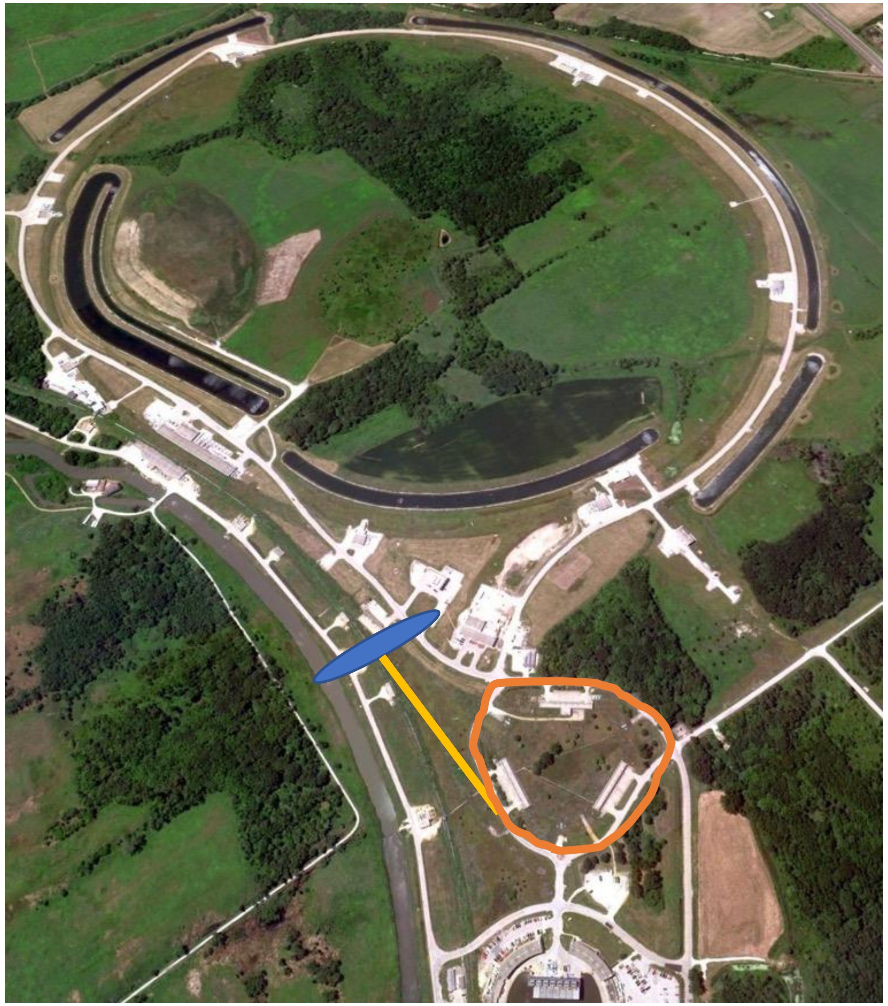

- Beam fragments focused on beam line
- Beamline is 280 m long
- p_π = 3.11 GeV/c ± 10% (or any other charged particle)
- Pion decay length ~ 170 m (20% left at end)
- 80% of pions have decayed to muons
- Beamline optimized for muons with p_μ = 3.094 GeV/c ± 2%
- 500m delivery ring used to purify the muon beam
- All particles arrive with same momentum
- Different particles have different speed $\beta = p/E$
  p^+ (3.094 GeV/c): 0.9569 c μ^+ (3.094 GeV/c): 0.9994 c
- After 4 turns muons and protons are separated
- 1/10 of muon lifetime but 11.5 times pion lifetime

→ Pure lepton beam

Reused Magnet from BNL Experiment

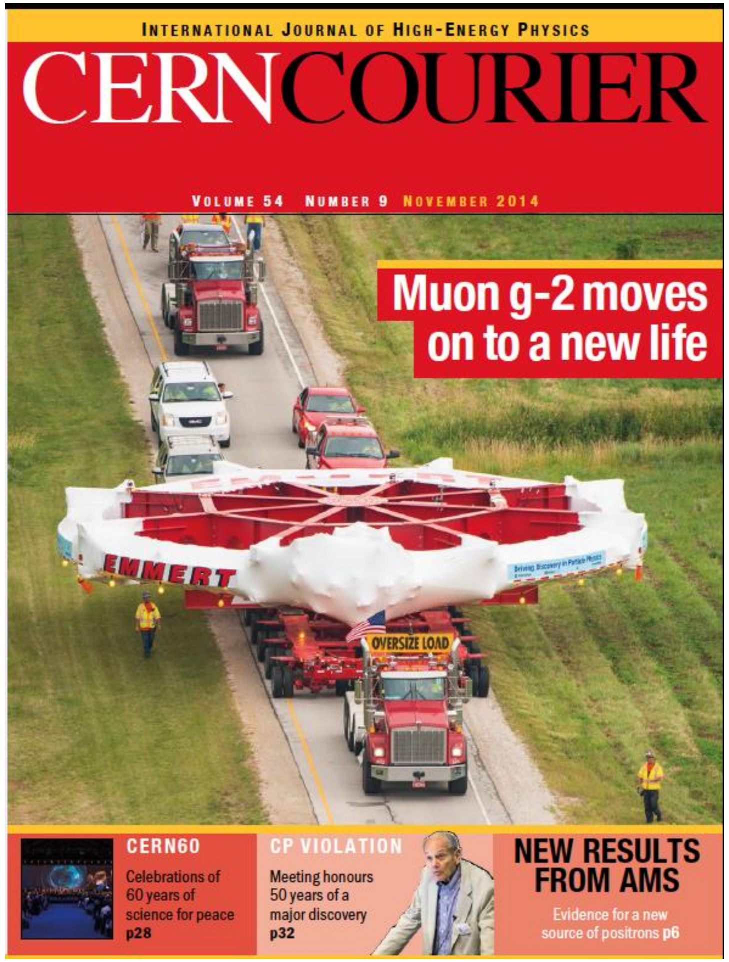

The superconducting magnet

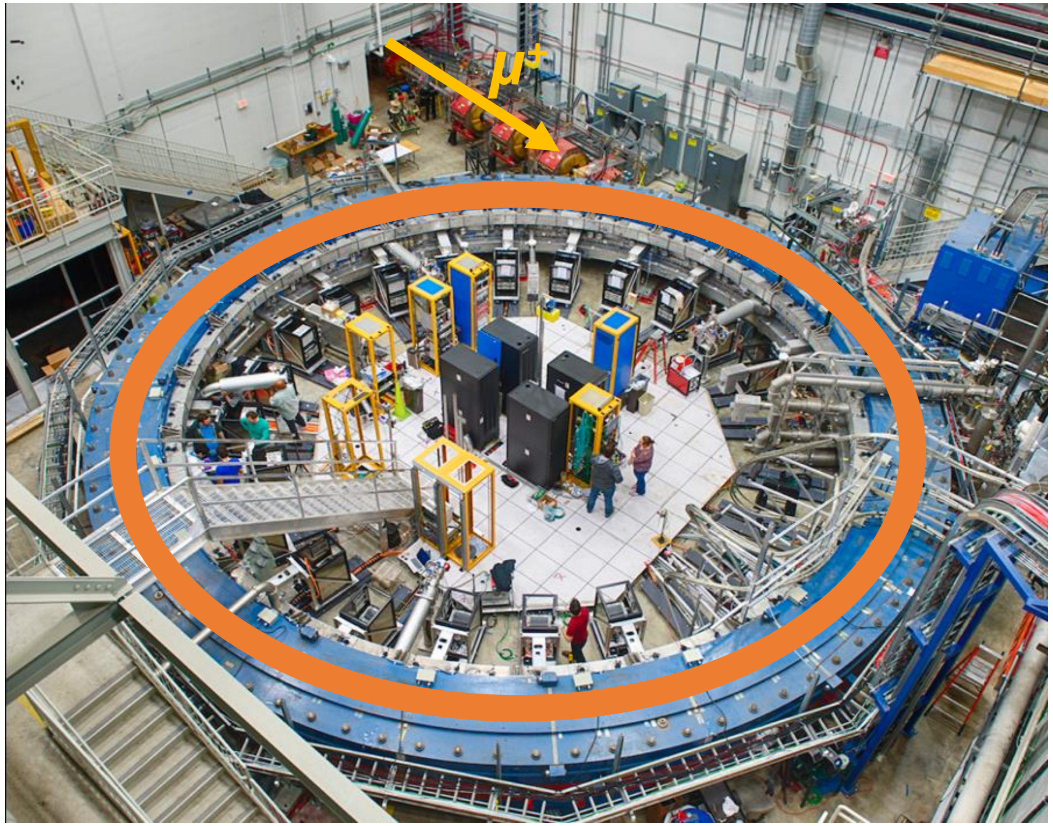

- $p_\mu^{magic} = 3.094 \frac{GeV}{c} \pm 0.5\%$
- 3 cryostats with 4 superconducting coils (5300 A)
- 1.45 T vertical magnetic field
- 90 mm muon storage region
- 180 mm gap for vacuum chambers
- Muon cyclotron period 149 ns (~6.7 MHz)
- Beam pulse length: 120 ns

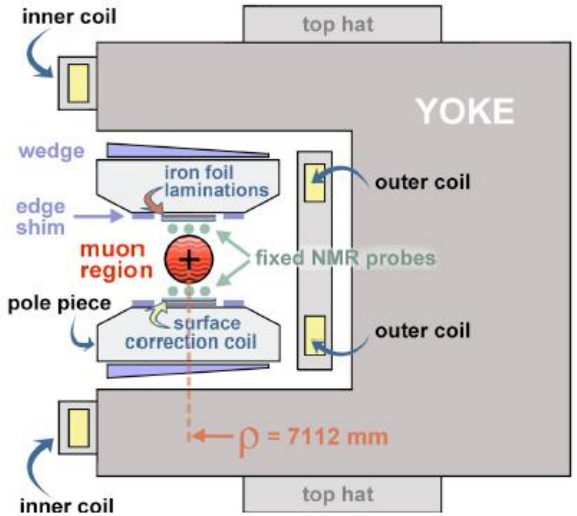

How do muons get into the ring?

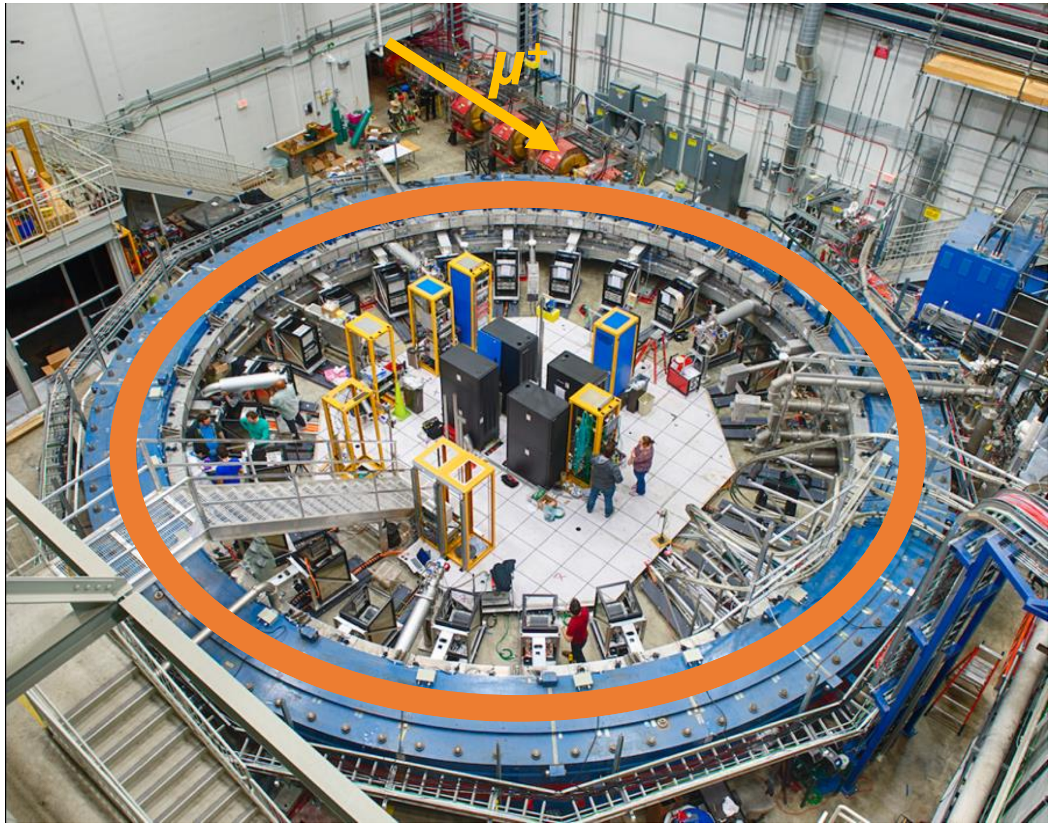

Muon are deflected in magnetic field due to Lorentz force

Need muons to travel straight into magnet

Need superposition of magnetic fields

Need material free region

Inflector magnet

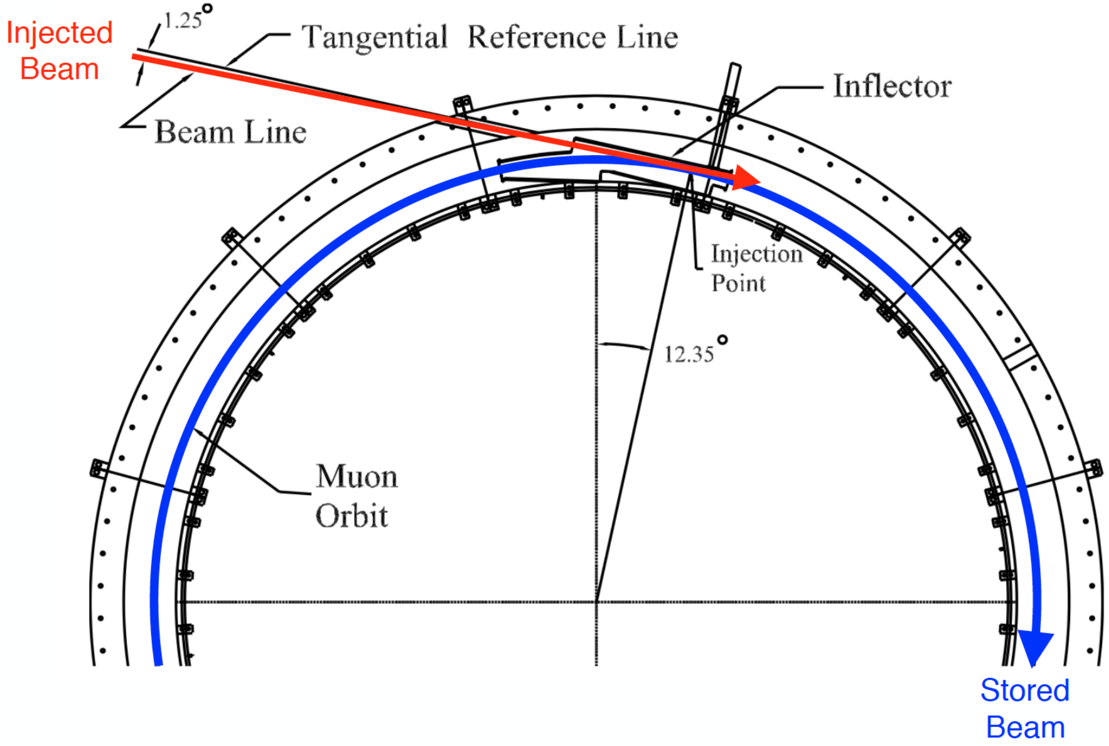

Horizontal cut through the magnet yoke

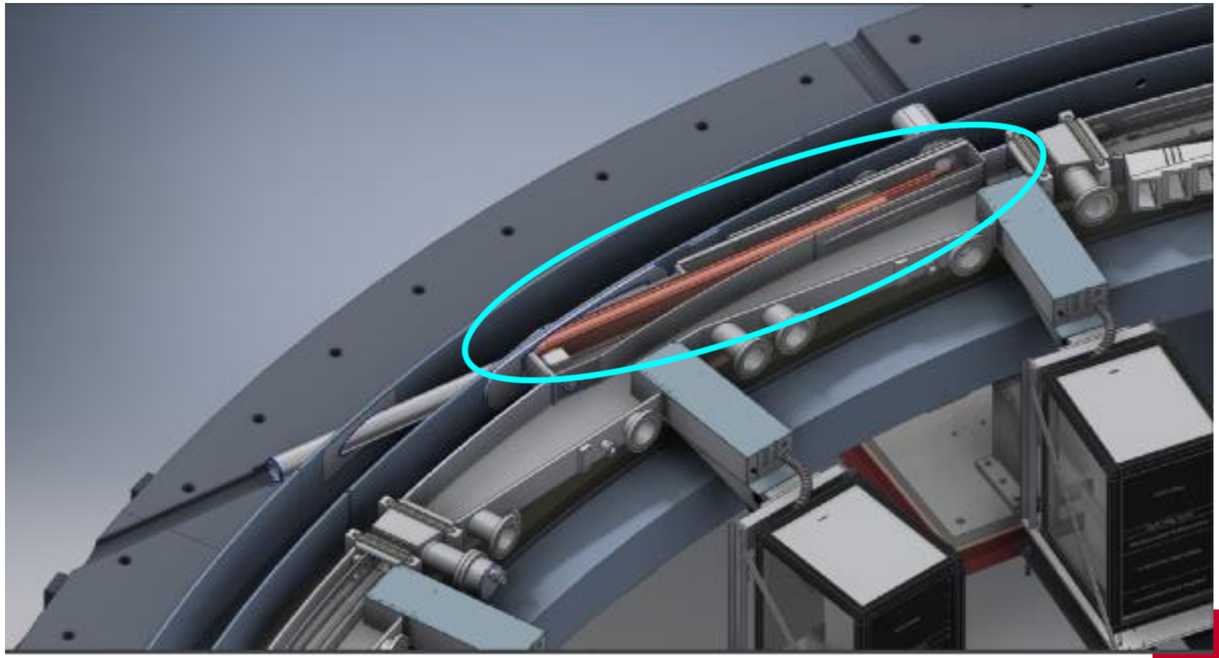

Figure credit: Nathan Froemming, PhD thesis, UW, 2018

Inflector magnet

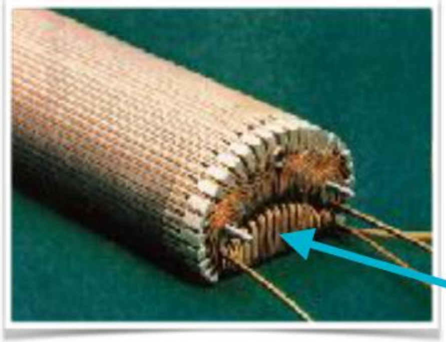

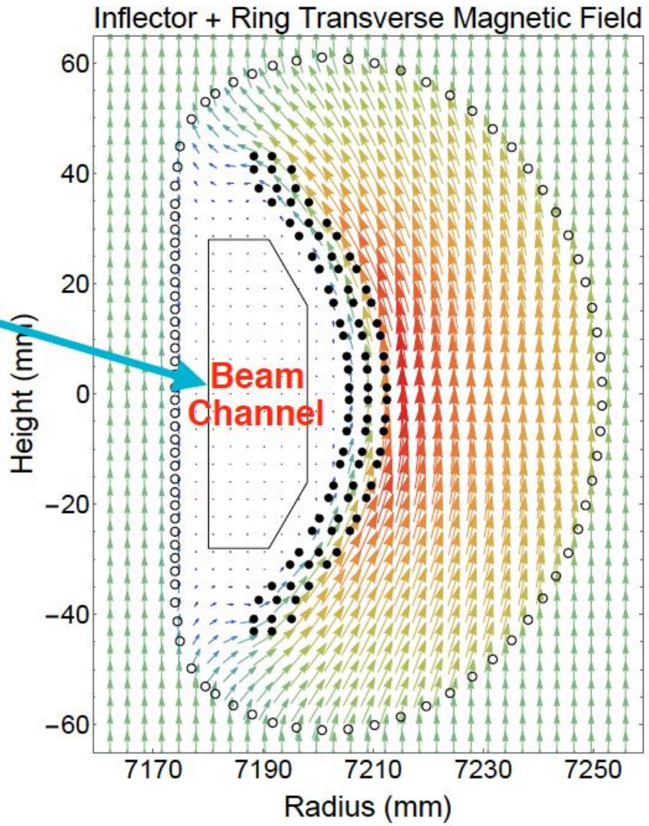

Superconducting magnet coil to cancel magnetic field in yoke

Superconducting shield to confine return flux of the inflector magnet without disturbing magnetic field in muon storage region

How to get the beam onto storage orbit?

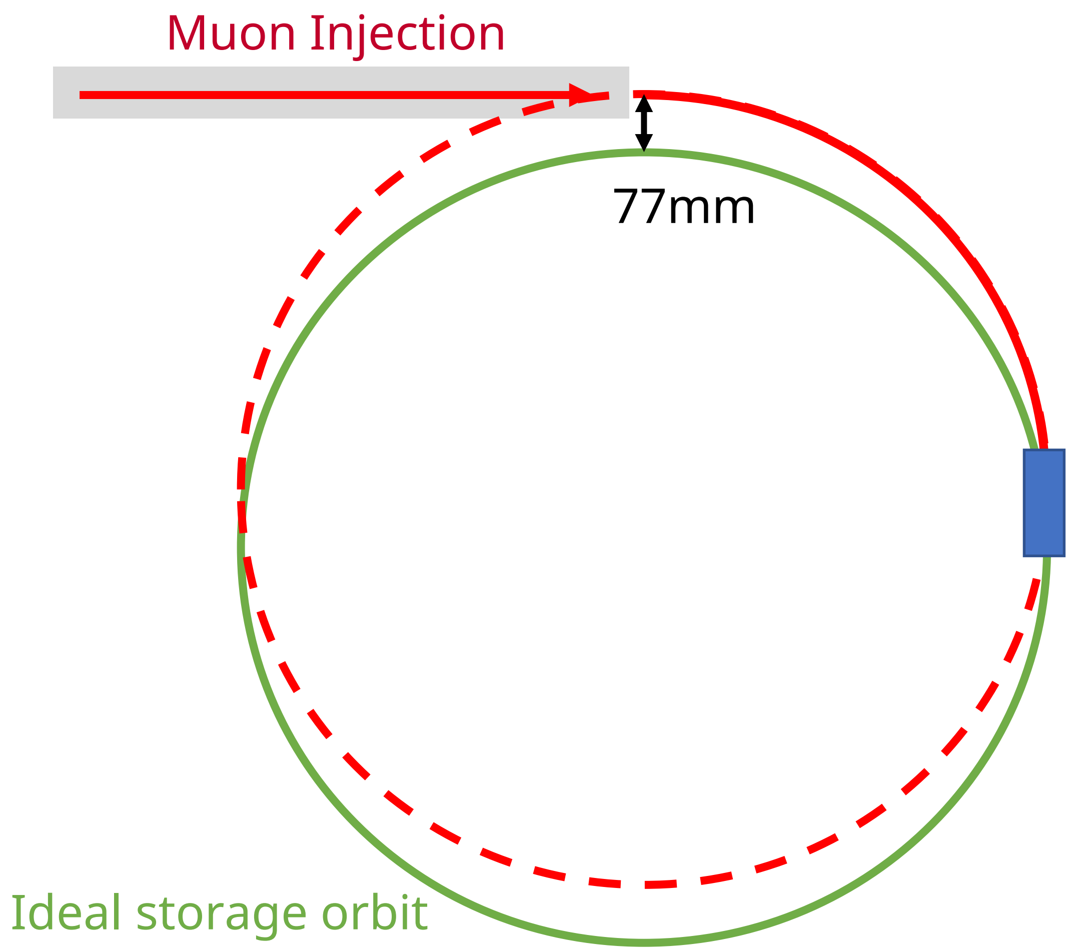

- After inflector muon see homogeneous magnetic field
  →Muons travel on a circle
- After one revolution muons would hit the inflector magnet
- Muon injection and ideal storage orbit displaced by 77mm
- Beam needs to be deflected on ideal storage orbit
- Apply 10.8mrad kick in first revolution
  - Field must be changed by ~2%
- Kicker should not be present after one revolution
  - Revolution time 149 ns
  - Bunch length 120 ns

The kicker system

- Change field locally by 2% within ~150 ns
- 3 pairs of plates at roughly 90°
- Apply HV pulse at 4700 A into ~12.5 Ω in 150 ns
- Very challenging to the materials

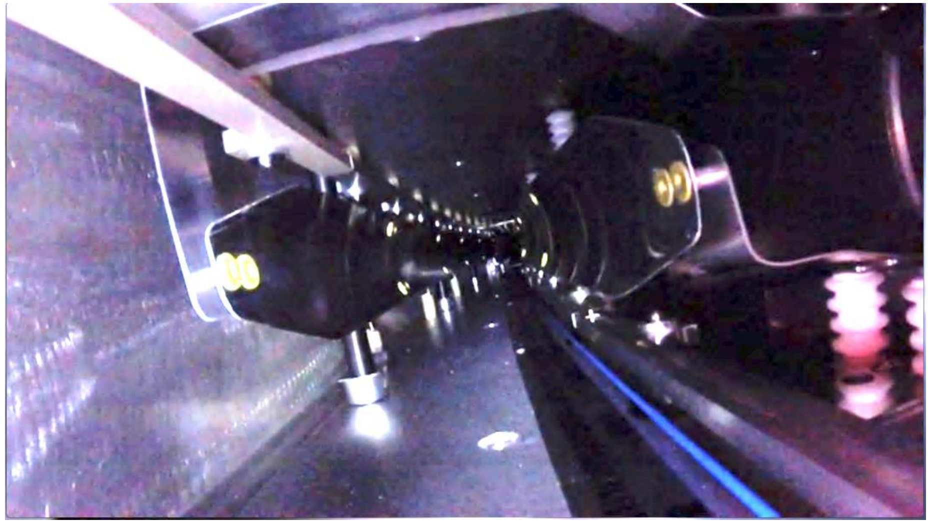

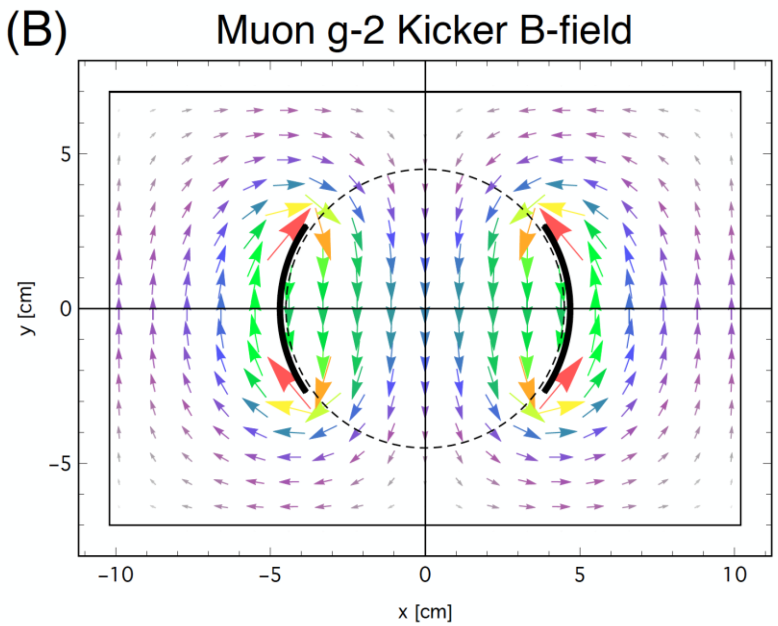

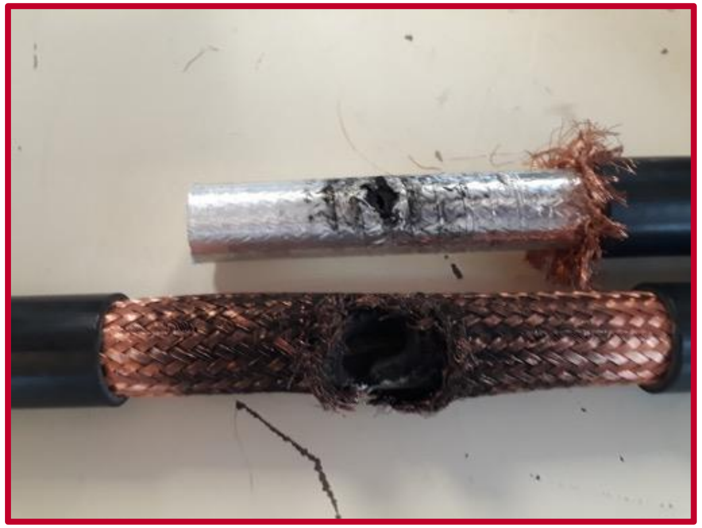

Keeping the muons stored

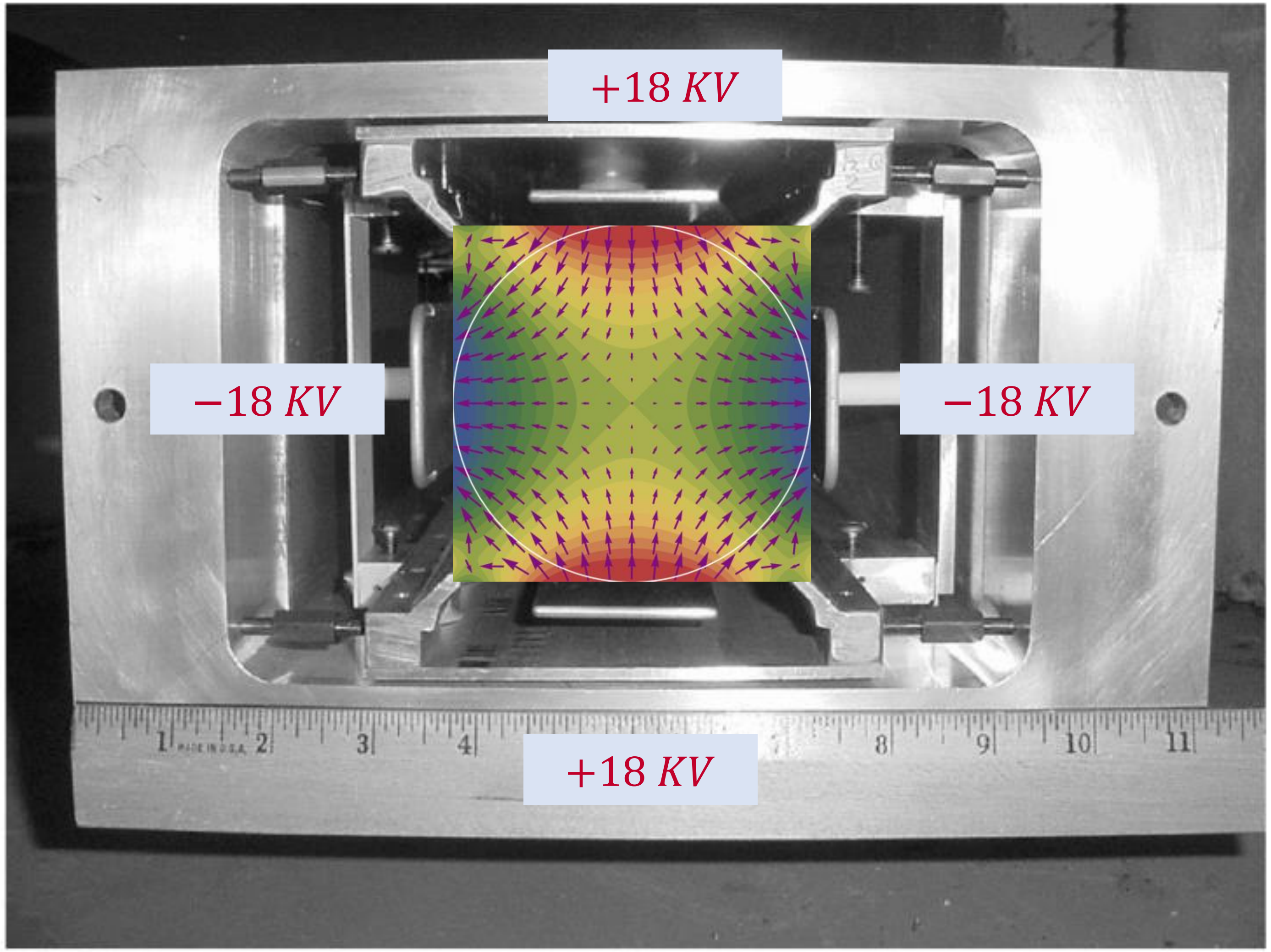

- At magic momentum electric fields have a very small impact on ω_a
- Electrostatic quadrupoles focus beam vertically
- Electrostatic quadrupoles defocus beam radially
- Magnetic field focus beam radially
- Complex beam dynamics

Beam focusing

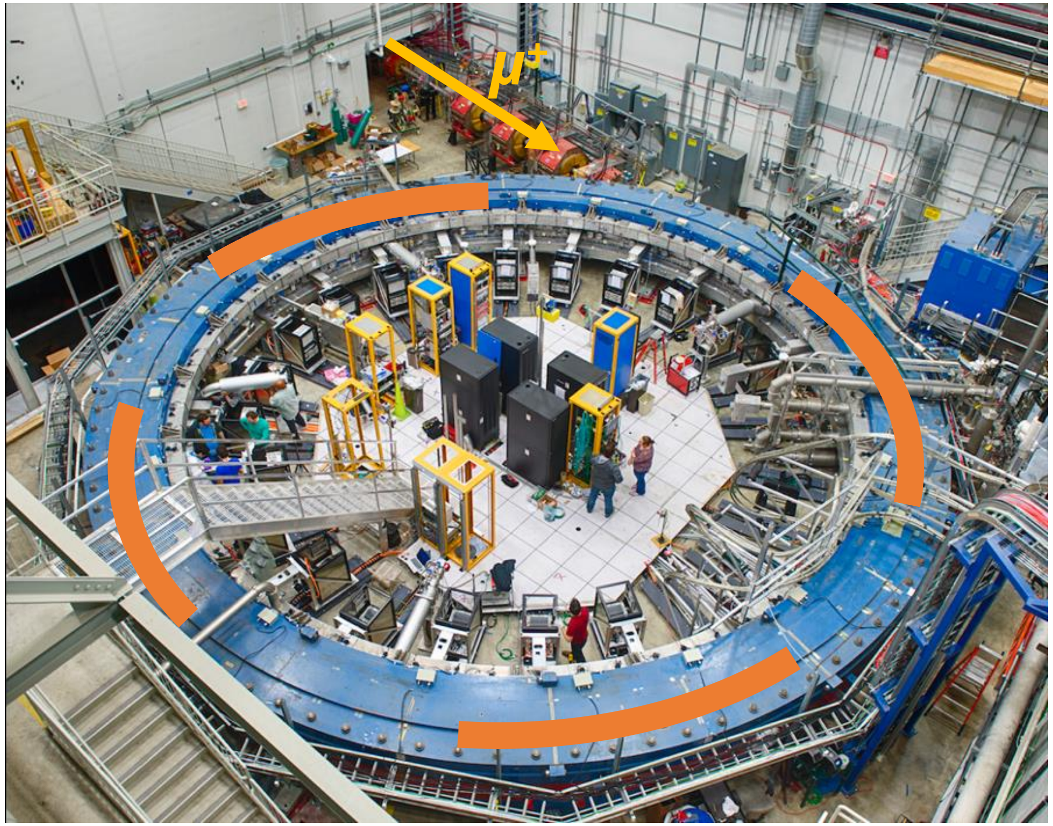

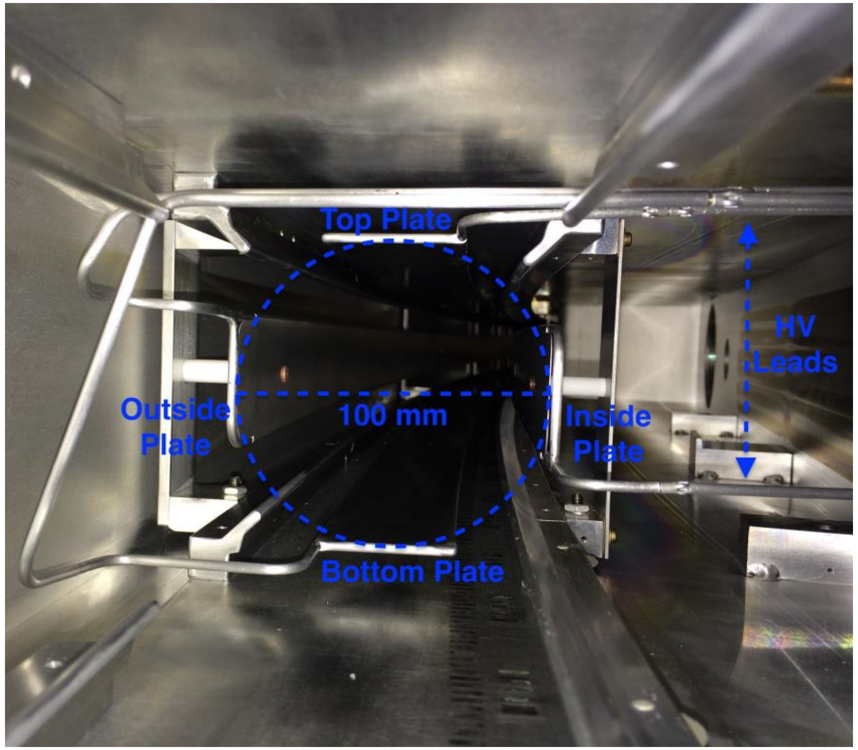

Pulsed “electrostatic” quadrupoles
Vertical focusing and confinement of muon beam
Quasi-penning trap cover 43% of the ring

Muon beam dynamics in storage ring

- Electrostatic quadrupoles imprint harmonic potential around their central position
- Muon storage close to central position
  - Perturbative approach
- Newton's second law and Lorentz force

$$\frac{d\vec{p}}{dt} = e\left(\vec{E} + \frac{d\vec{v}}{dt} \times \vec{B}\right)$$

- Three differential equations
- Harmonic oscillator in vertical direction $\omega_{\mathrm{y}} = \sqrt{n}\omega_{\mathrm{c}}$
- Harmonic oscillator in horizontal direction $\omega_{\mathrm{x}} = \sqrt{1-n}\,\omega_{\mathrm{c}}$
- *n* depends on quadrupole HV settings
- Resonant condition for

$$M\nu_{\mathrm{x}} + N\nu_{\mathrm{y}} = P \quad \text{with}\,\mathrm{M,N} \in \mathbb{Z}\,\text{and}\,\mathrm{P} \in \mathbb{N}$$

- Avoid ω_a interference

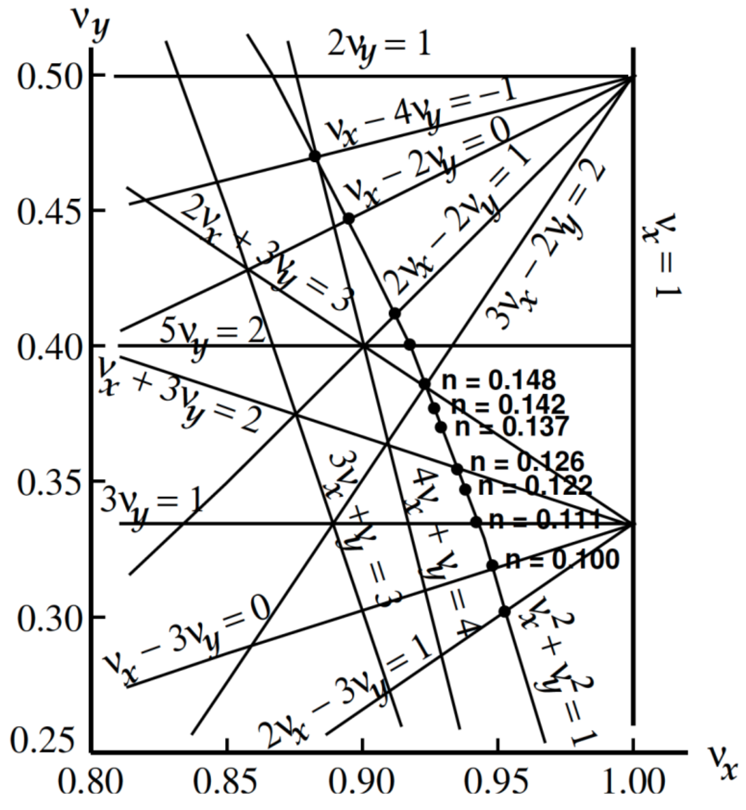

Pitch correction

- Muons have transversal momentum components

$$\Delta\vec{\omega}_{\mathrm{a,pitch}} = -a_{\mu}\frac{e}{m}\left(\frac{\gamma}{\gamma+1}\right)\left(\vec{\beta}\cdot\vec{B}\right)\vec{\beta}$$

- Transversal component oscillates with $\omega_{\mathrm{y}} = \sqrt{n}\omega_{\mathrm{c}}$

- Effect mainly averages out to first order, but second order effect is

$$\left\langle\frac{\Delta\omega_{\mathrm{a}}}{\omega_{\mathrm{a}}}\right\rangle_{\mathrm{pitch}} = -\frac{\langle\psi^2\rangle}{2} = -\frac{n\langle y^2\rangle}{2R_0^2}$$

- Introduces always a negative bias
- Correction can be derived from measurements of the muon beam distribution

Scaping of beam edges

- Beam dynamics could make muons oscillated into physical objects around the muon storage area
- potential early-to-late in muon loss factor

- First apply small vertical focusing
- Edge of stored muons collide with collimators

- Second apply higher vertical focusing
- Stored muons well separated from collimators

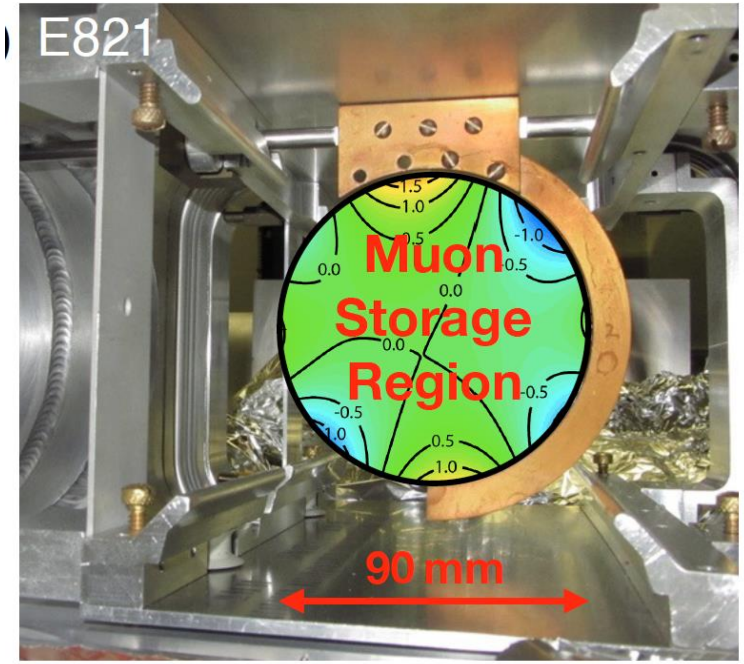

Positron detection

1/12 of the ring

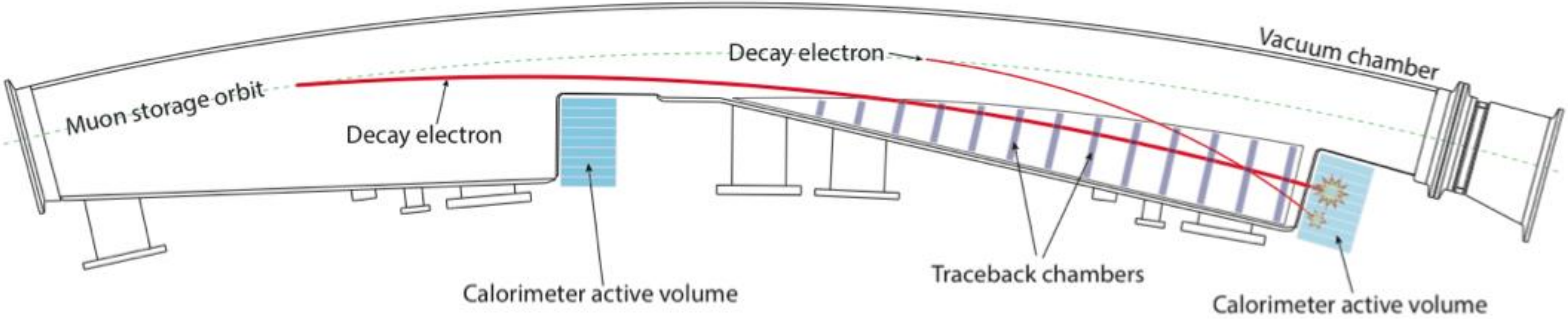

- Positron cyclotron radius small because $m_e << m_\mu$
- Positrons spiral inwards
- Measure positron arrival time and energy with 24 calorimeters

- In front of two calorimeters straw trackers are placed to reconstruct positron trajectory
- Allows reconstruction of beam profile

Tracking Detectors

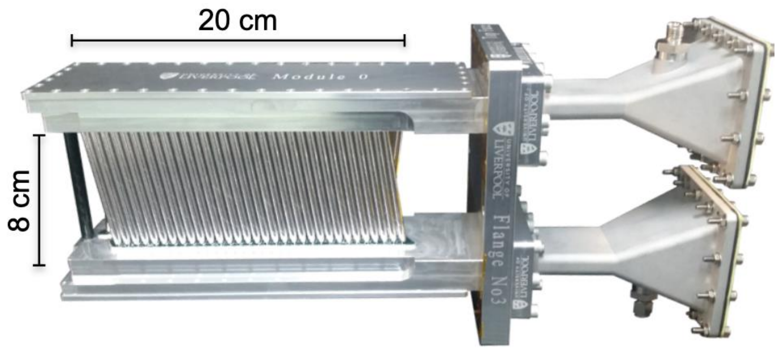

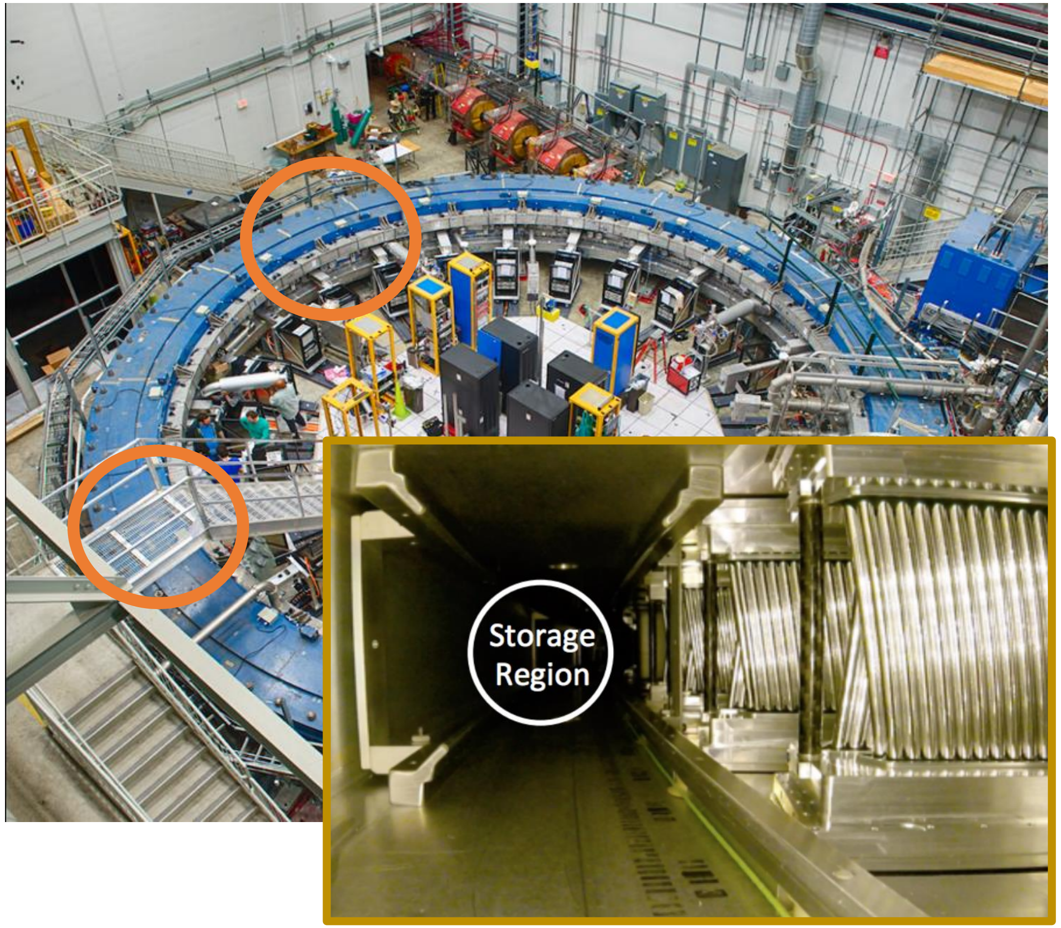

- Two tracking stations, each with 8 modules
- 128 gas-filled straws per module
- Determine e+ trajectory to decay position and extrapolate to find muon beam distribution!
- Input for beam dynamics simulations

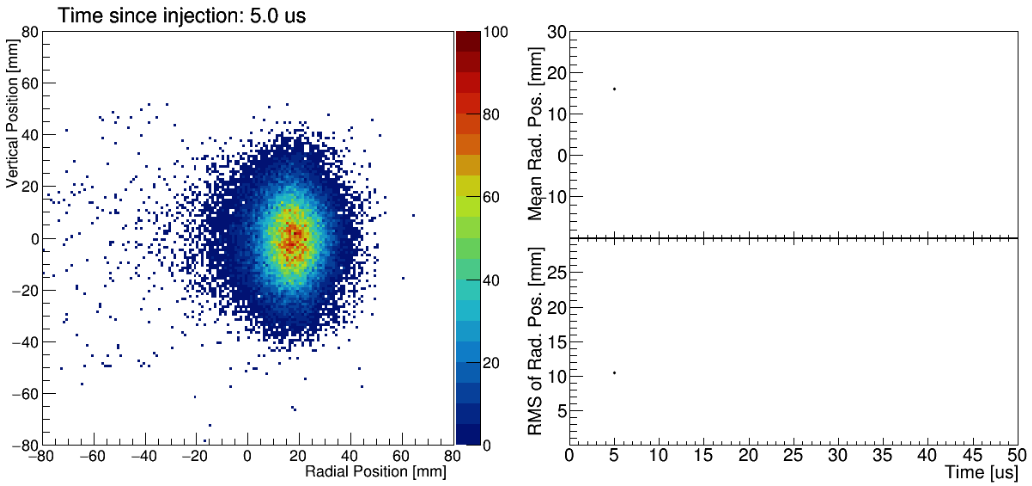

Positron detection

- Main detector for the inward curling decay positrons → carriers of the ω_a signal
- The two critical measured properties: positron energy and detection time
- **The most important requirement**
  An unbiased ω_a frequency determination if the detector characteristics are stable over 700 μs!
  Otherwise, early-to-late phase evolution!
- General requirements:
  - Fast signal generation → reduce pile-up
  - Segmentation → reduce pile-up
  - High dynamic range → "early-to-late" effect
  - Work in the magnetic stray field → solid angle coverage, low p^+ detection threshold
  - Do not disturb the precision magnetic field!

Positron detection

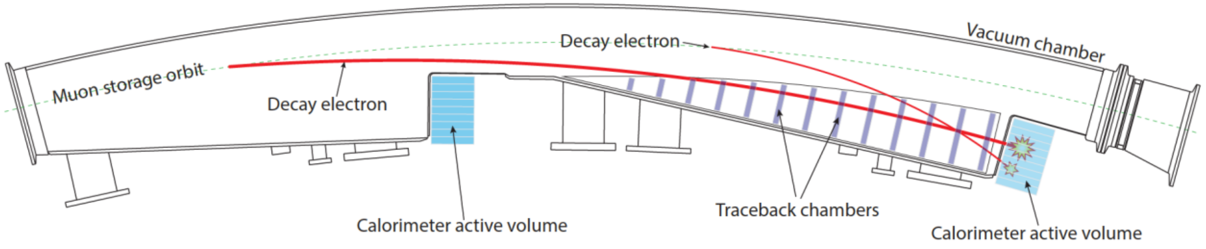

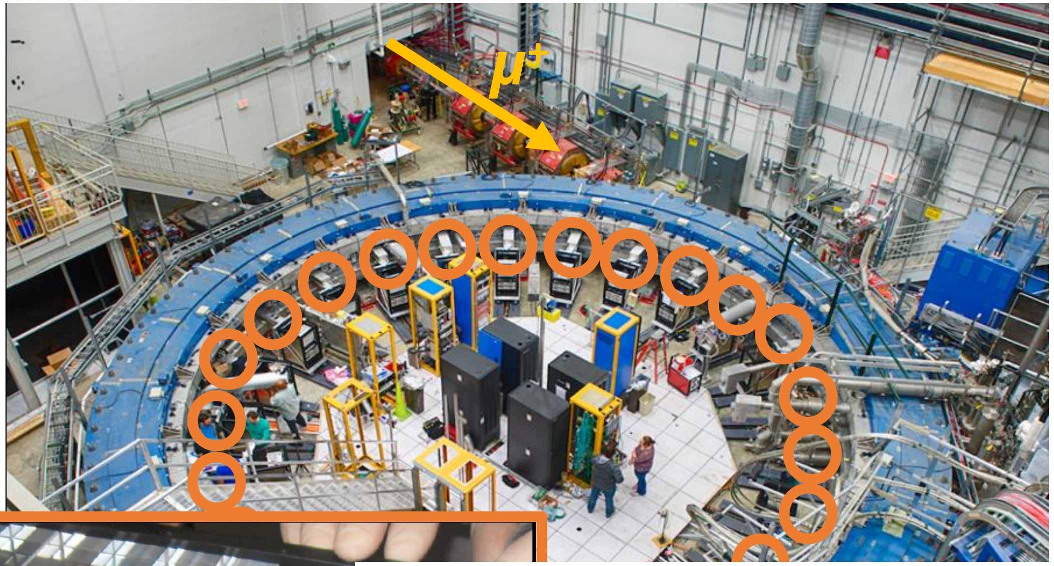

- 24 calorimeter stations
- 9 x 6 arrays of PbF2 crystals
- Using Cherenkov light
  - Only present while positron in crystal (fast signal, less pile up)
- Individual SiPM readout boards
  - Single photon sensitivity (up to 1000s)
  - Saturation at high light intensity
  - Very compact footprint
  - Very fast
  - Operate in high magnetic field
- 1296 channels
- 12-bit, 800 MS/s waveform digitizer

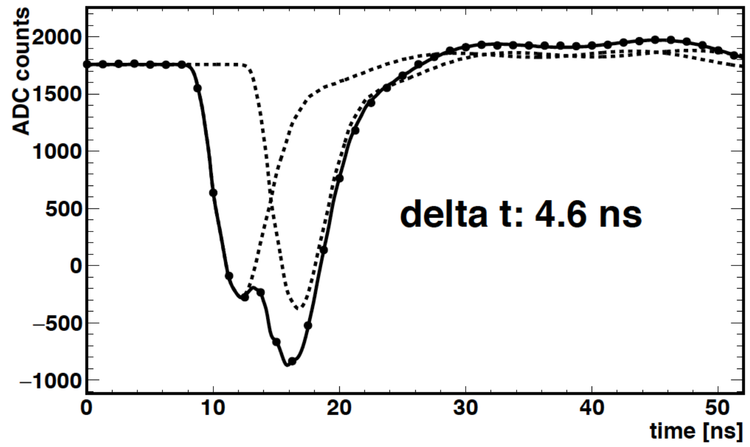

Laser Calibration System

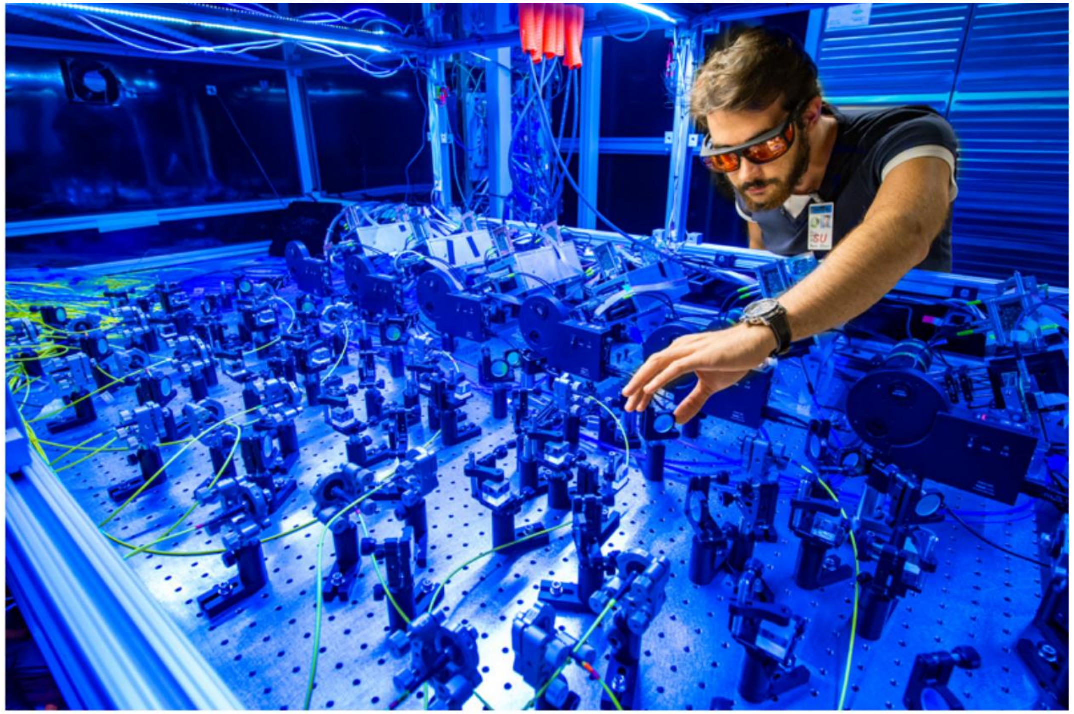

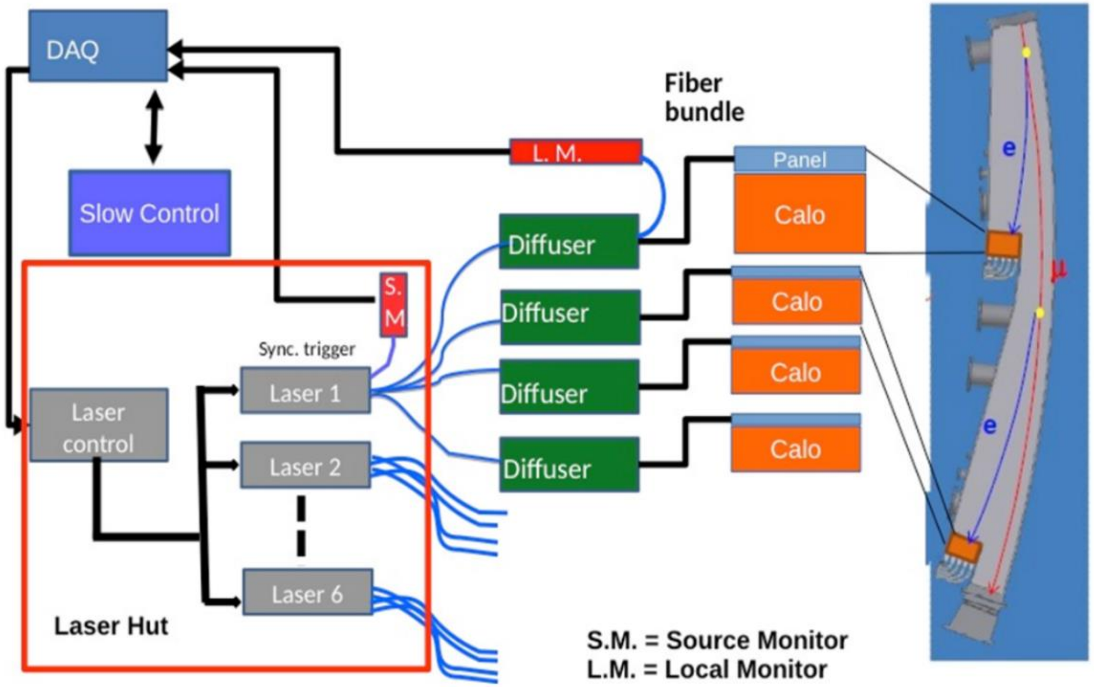

Figure credit: Andrea Fioretti

- Inject laser pulses systematically also during beam operation (about 10% of time)

Gain Stability

Long term gain changes due to temperature changes
Long term gain changes can be corrected

Short term gain drops
- Initial beam flash at injection
- Consecutive hits

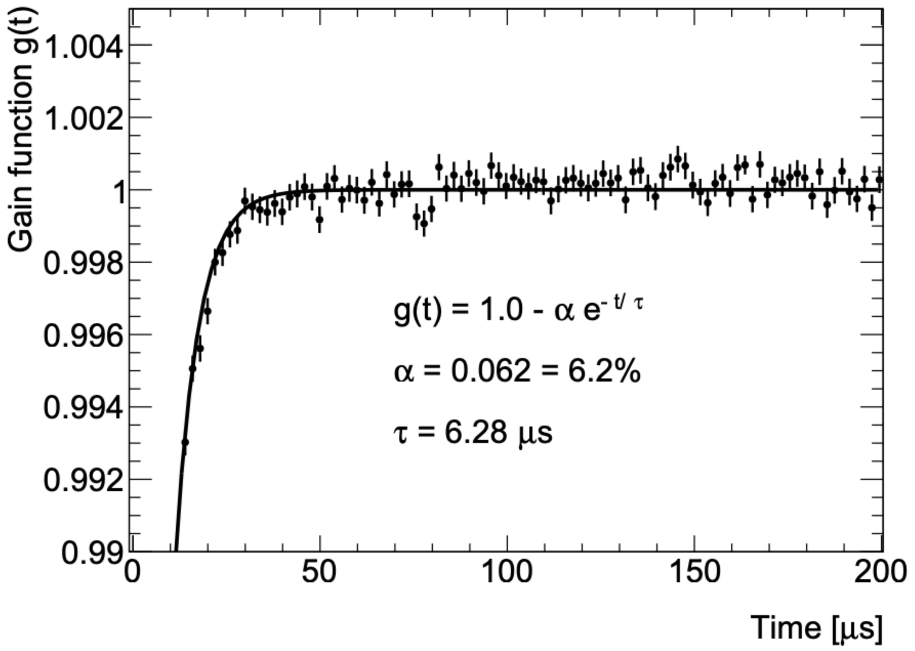

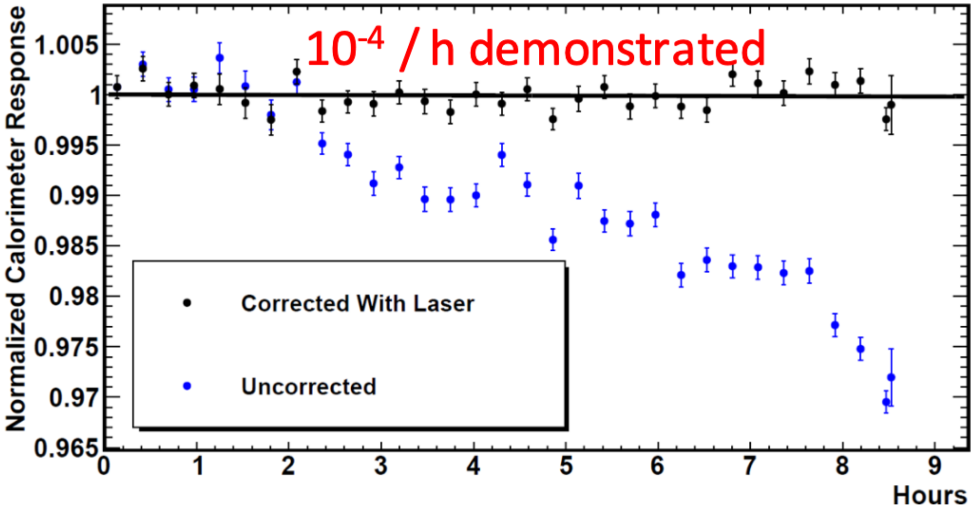

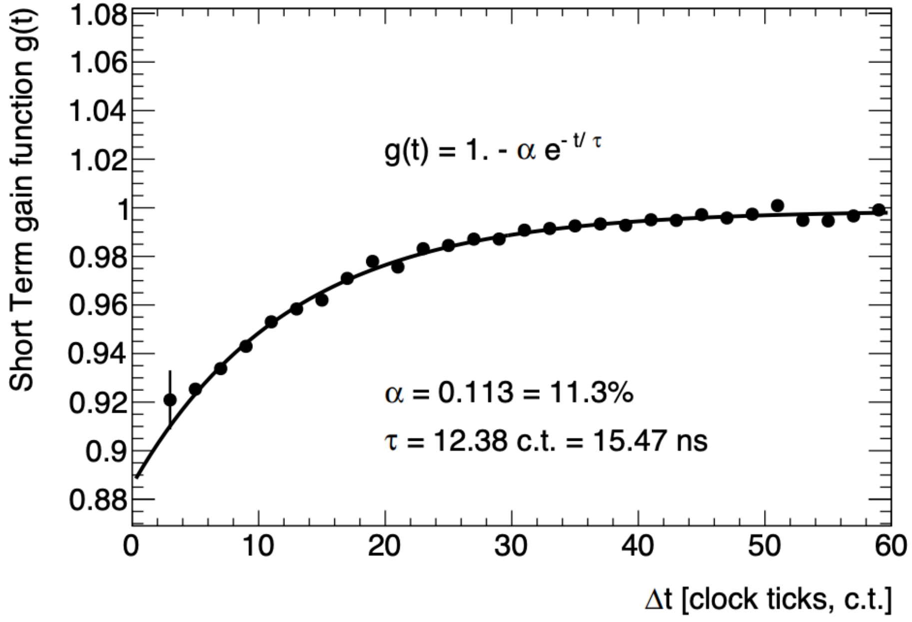

Positron detection

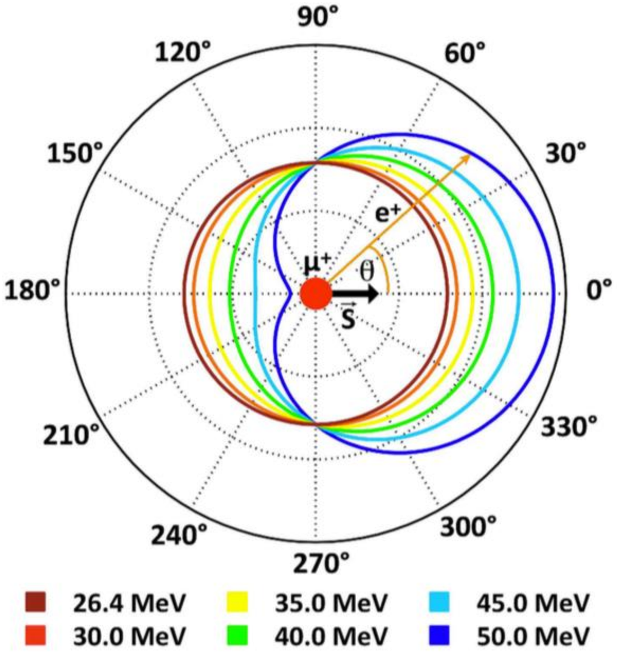

With detector acceptance

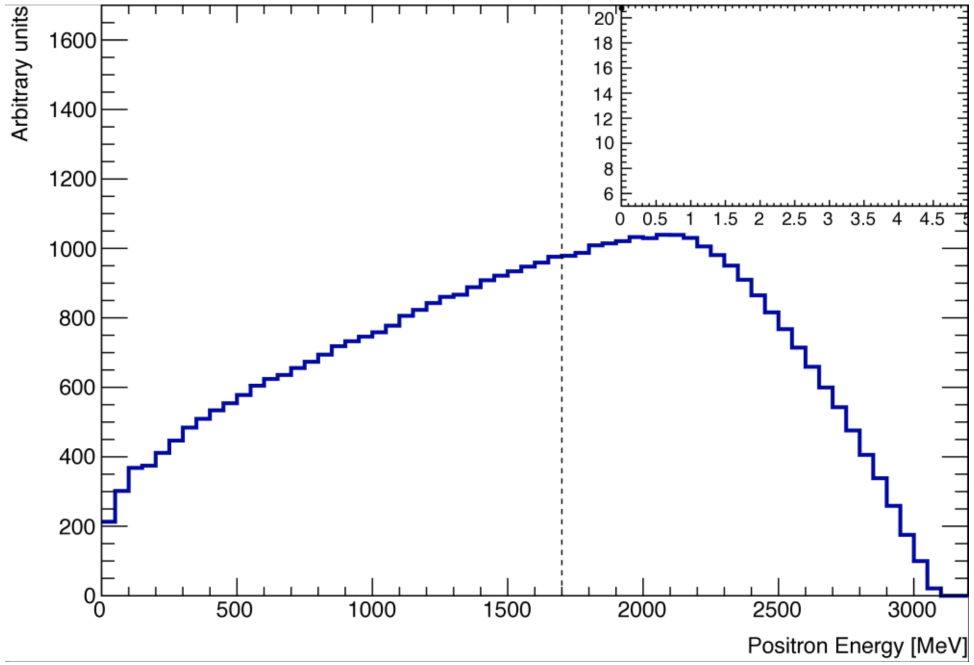

Spin precession in muon rest frame transforms to above-energy-threshold count rate modulation in laboratory frame

Five parameter fit

$$f(t) \propto N_0 e^{-\frac{t}{\gamma\tau}} \left[\langle N\rangle_{\mathrm{thresh}} + \langle A\rangle_{\mathrm{thresh}} \cos\left(\omega_{\mathrm{a}} t - \langle\phi\rangle_{\mathrm{thresh}}\right)\right]$$

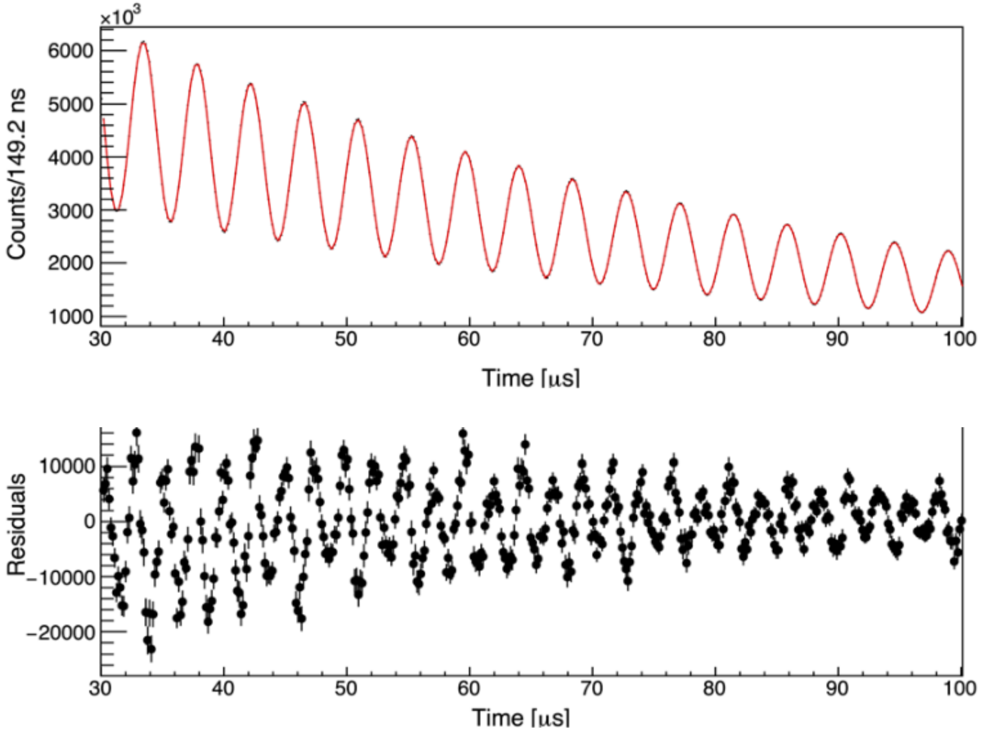

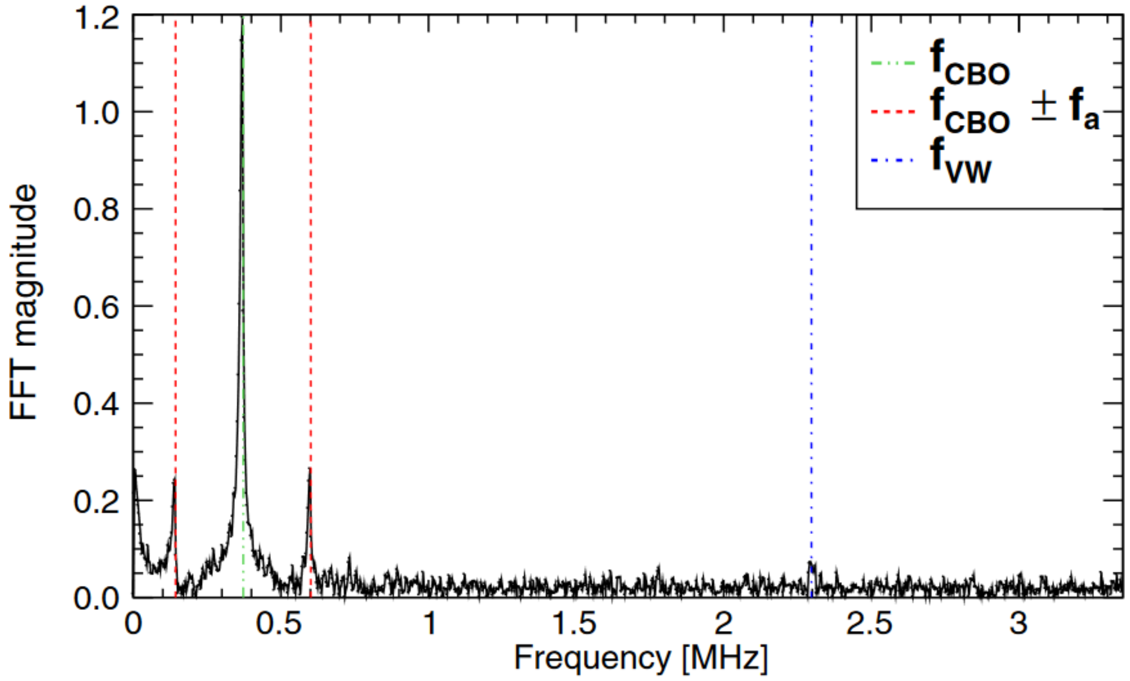

22 parameter fit

$$N_0\, e^{-\frac{t}{\gamma\tau}}\,(1\ +\ A\ \cdot A_{BO}(t)\cos(\omega_a\, t + \phi\ \cdot \phi_{BO}(t)\,)\,)\cdot N_{\text{CBO}}(t)\cdot N_{\text{VW}}(t)\cdot N_y(t)\cdot N_{\text{2CBO}}(t)\cdot J(t)$$

$$A_{\text{BO}}(t) = 1 + A_A\cos(\omega_{\text{CBO}}(t) + \phi_A)e^{-\frac{t}{\tau_{\text{CBO}}}}$$

$$\phi_{\text{BO}}(t) = 1 + A_\phi\cos(\omega_{\text{CBO}}(t) + \phi_\phi)e^{-\frac{t}{\tau_{\text{CBO}}}}$$

$$N_{\text{CBO}}(t) = 1 + A_{\text{CBO}}\cos(\omega_{\text{CBO}}(t) + \phi_{\text{CBO}})e^{-\frac{t}{\tau_{\text{CBO}}}}$$

$$N_{\text{2CBO}}(t) = 1 + A_{\text{2CBO}}\cos(2\omega_{\text{CBO}}(t) + \phi_{\text{2CBO}})e^{-\frac{t}{2\tau_{\text{CBO}}}}$$

$$N_{\text{VW}}(t) = 1 + A_{\text{VW}}\cos(\omega_{\text{VW}}(t)t + \phi_{\text{VW}})e^{-\frac{t}{\tau_{\text{VW}}}}$$

$$N_y(t) = 1 + A_y\cos(\omega_y(t)t + \phi_y)e^{-\frac{t}{\tau_y}}$$

$$J(t) = 1 - k_{LM}\int_{t_0}^{t}\Lambda(t)dt$$

$$\omega_{\text{CBO}}(t) = \omega_0 t + Ae^{-\frac{t}{\tau_A}} + Be^{-\frac{t}{\tau_B}}$$

$$\omega_y(t) = F\omega_{\text{CBO}(t)}\sqrt{2\omega_c/F\omega_{\text{CBO}}(t) - 1}$$

$$\omega_{\text{VW}}(t) = \omega_c - 2\omega_y(t)$$

Beam dynamics effects have to be considered

22 parameter fit

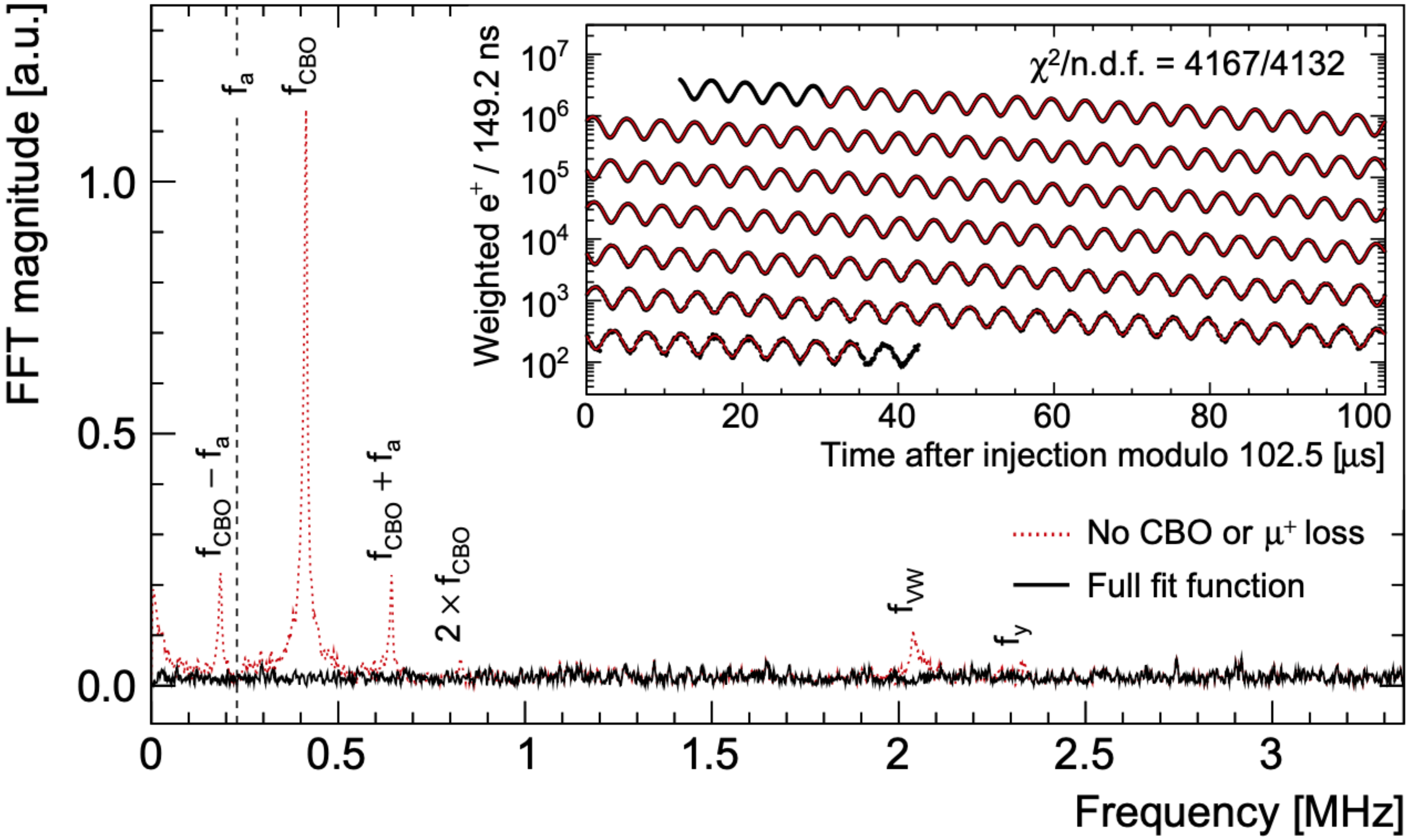

$t) \cdot N_{2CBO}(t) \cdot J(t)$

Beam dynamics effects have to be considered

Asymmetry weighted method

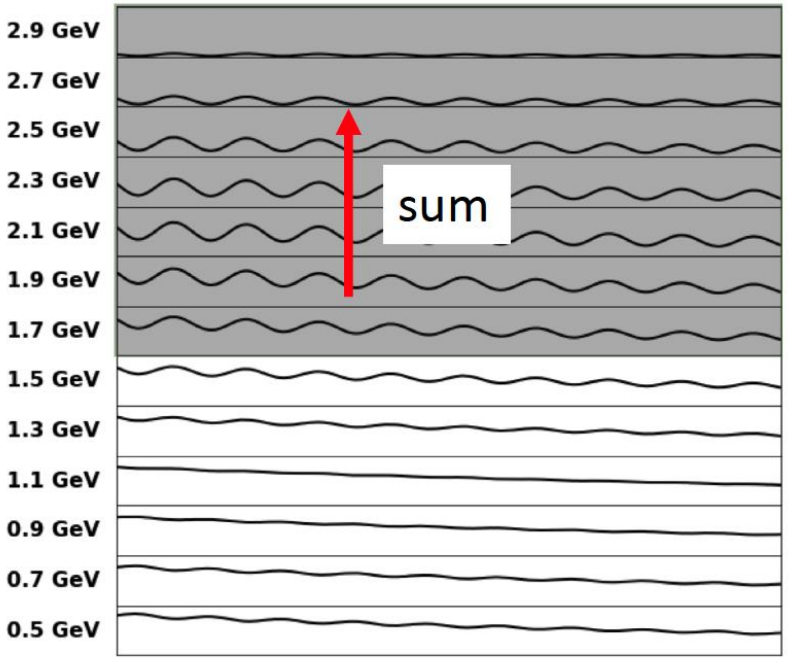

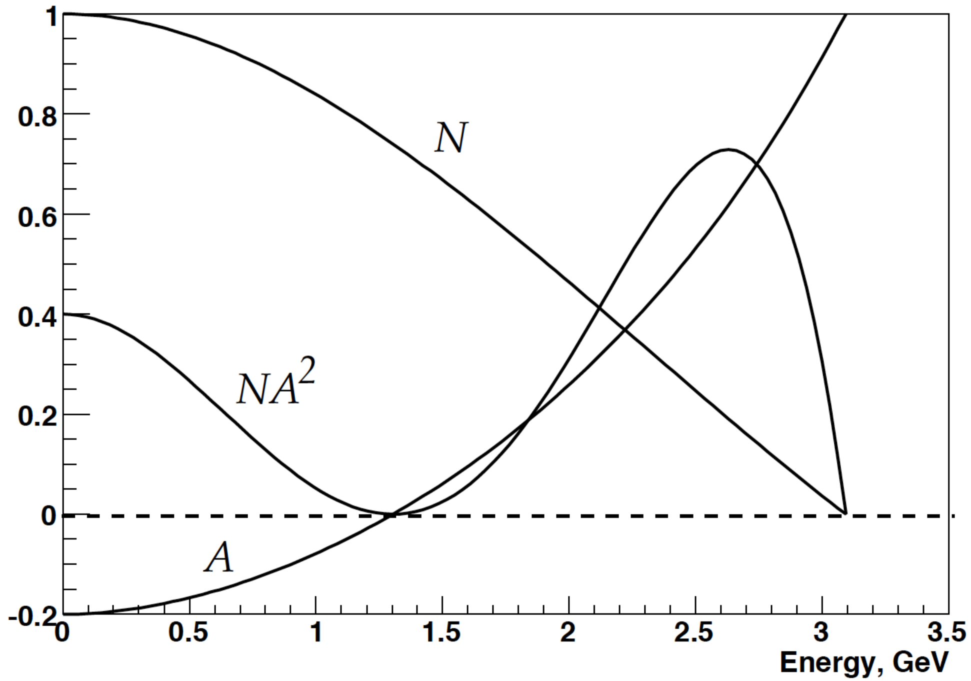

- Asymmetry is energy dependent
- High energy positrons have stronger asymmetry
- Introduce weight proportional to asymmetry

Ratio method

- Split positrons randomly in four sets
- Time shift one set by $+T_a/2$ and one by $-T_a/2$
- Build the ratio

$$r(t) = \frac{[u_+(t) - v_1(t)] + [u_-(t) - v_2(t)]}{[u_+(t) + v_1(t)] + [u_-(t) + v_2(t)]}$$

- Gets rid of exponential decay and any slow drift

$$r(t) = A\cos\left(\omega_a^m t + \phi\right) - \frac{1}{16}\left(\frac{T_a}{\gamma\tau_\mu}\right)^2 + \mathcal{O}((T_a/(4\gamma\tau_\mu))^4)$$

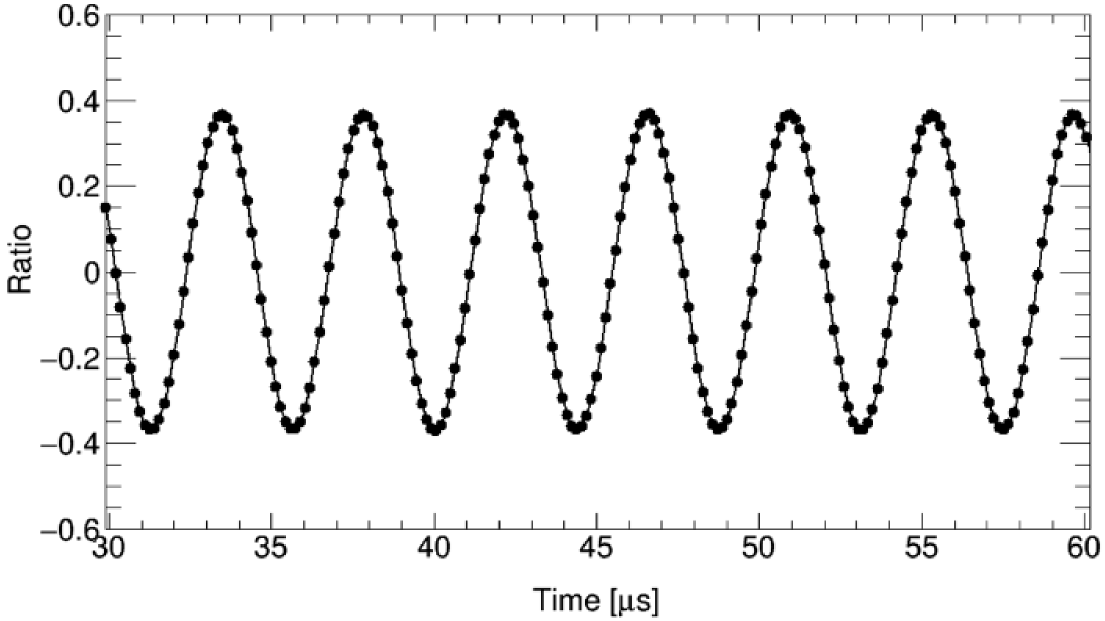

$$u_+(t) = \frac{1}{4}n(t + T_a/2),$$

$$u_-(t) = \frac{1}{4}n(t - T_a/2),$$

$$v_1(t) = \frac{1}{4}n(t),$$

$$v_2(t) = \frac{1}{4}n(t).$$

Finite beam length

- Individual calorimeters see has oscillation with frequency ω_c caused by bunch distribution
- Add time offset uniformly distributed between $-T_c/2$, $T_c/2$
- With time bunch decoheres because of momentum spread of initial beam
- Used to calculate momentum distribution → corresponds to equilibrium radius
- Used to calculate electric field correction

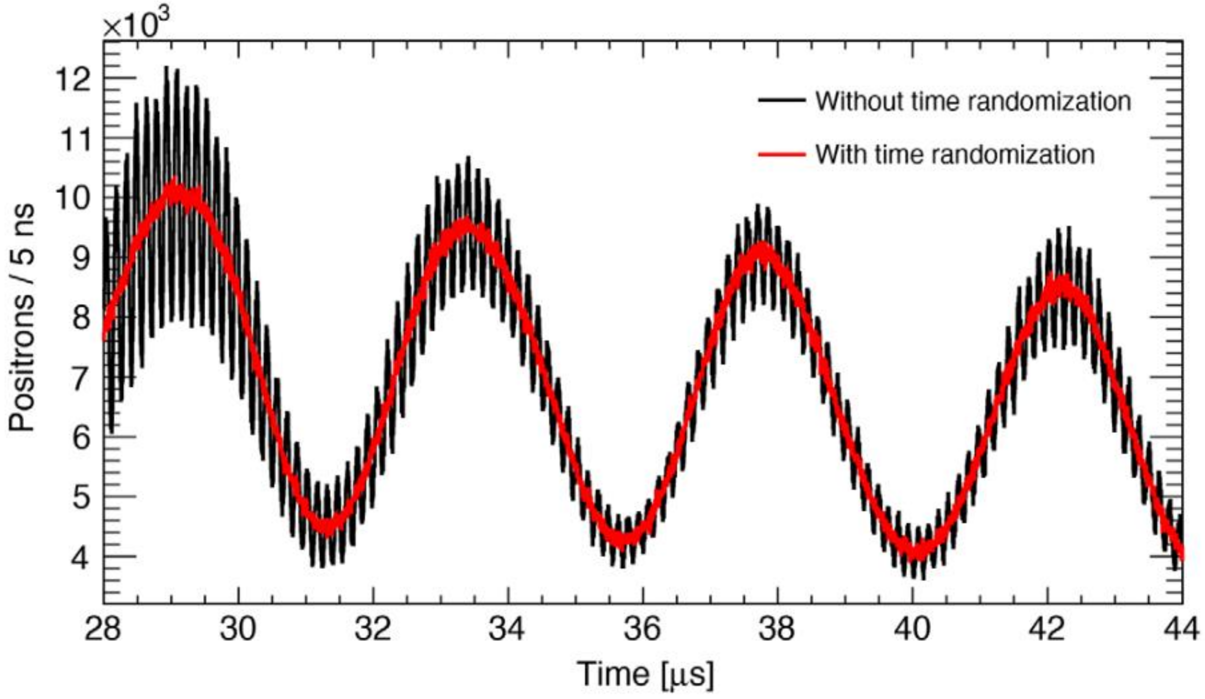

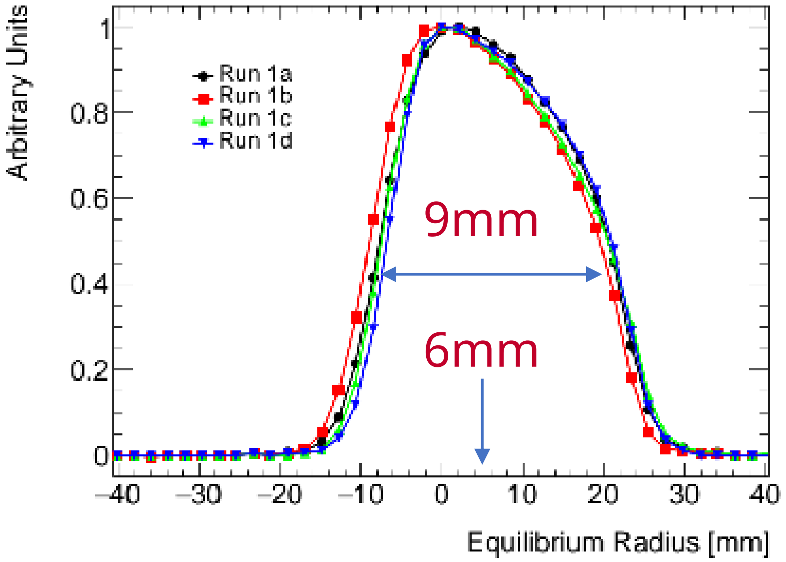

Electric field correction

$$\vec{\omega}_a = \frac{e}{m}\left[a_\mu \vec{B} - a_\mu \left(\frac{\gamma}{\gamma+1}\right)\left(\vec{\beta}\cdot\vec{B}\right)\vec{\beta} - \left(a_\mu - \frac{1}{\gamma^2-1}\right)\frac{\vec{\beta}\times\vec{E}}{c}\right]$$

- Off-center beam sees electric field
- Correction given by

$$C_e = -2n(1-n)\beta^2 \frac{\langle x_e^2 \rangle}{R_0^2}$$

  - *n* given by ESQ HV settings
  - *β* known from magic momentum
  - R_0 nominal orbit radius

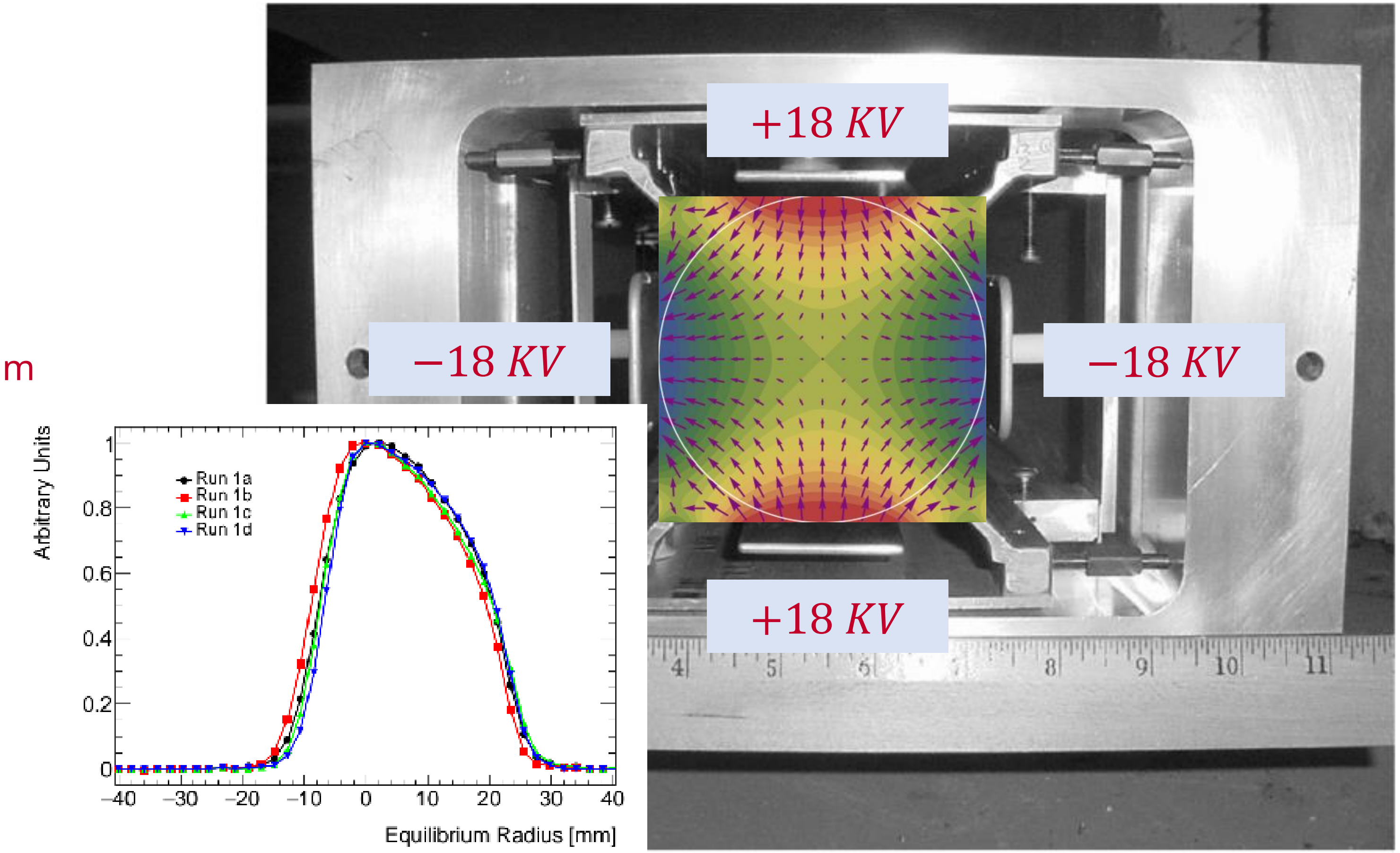

Pitch correction

- Muons have transversal momentum (pitch)

$$\frac{e}{m}\left[a_\mu \vec{B} - a_\mu \left(\frac{\gamma}{\gamma+1}\right)\left(\vec{\beta}\cdot\vec{B}\right)\vec{\beta} - \left(a_\mu - \frac{1}{\gamma^2-1}\right)\frac{\vec{\beta}\times\vec{E}}{c}\right]$$

- Vertical beam motion simulated by three different beam dynamics simulations

- Using tracker beam distribution as input and cross-check

- Correction given by mean acceptance-corrected vertical amplitude

$$C_p = \frac{n}{4R_0^2}\langle A^2\rangle$$

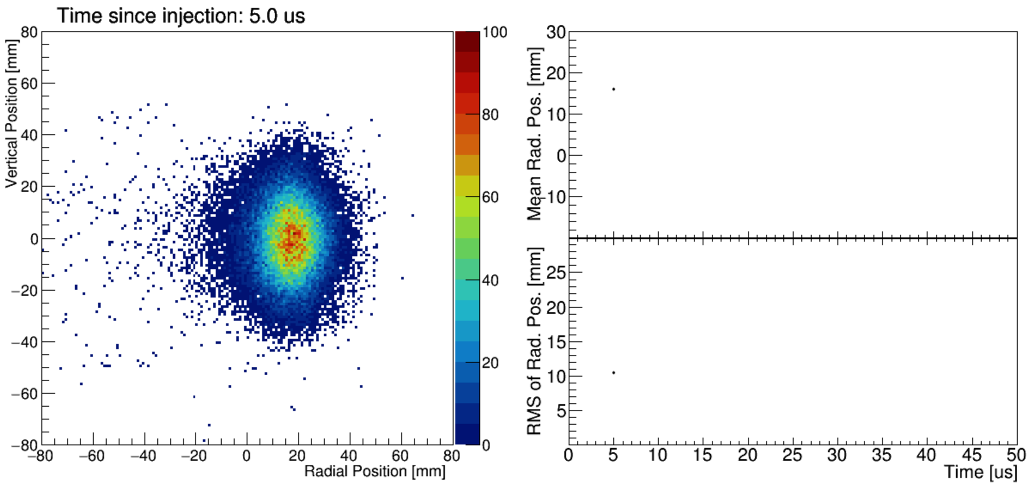

Lost muons

- Beside decay muons get lost by interaction with obstacles or collimators
- Lost muons pass through several calorimeters
- Deposited energy of a MiP with ~170MeV
- Successive calorimeter hits separated by 6.15ns
- Require measurement in three successive calorimeters to reduce random coincidences
- Monitors rate up to overall factor
- Low momentum muon lost faster
  → Early to late effect
- Needs to be corrected

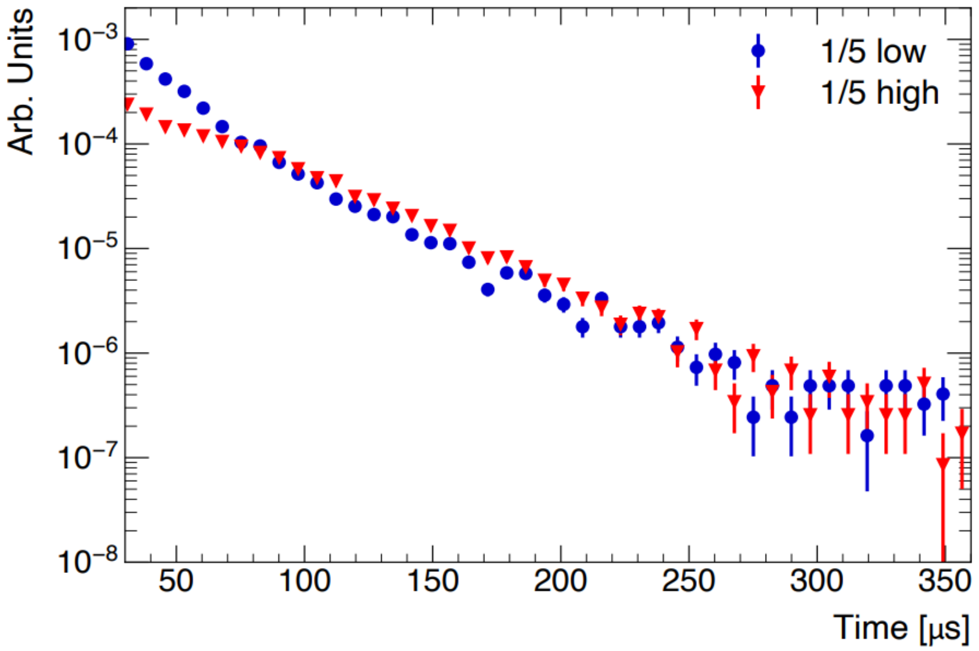

Finite Calorimeter Acceptance

- Since finite calorimeter acceptance we are sensitive to muon decay position

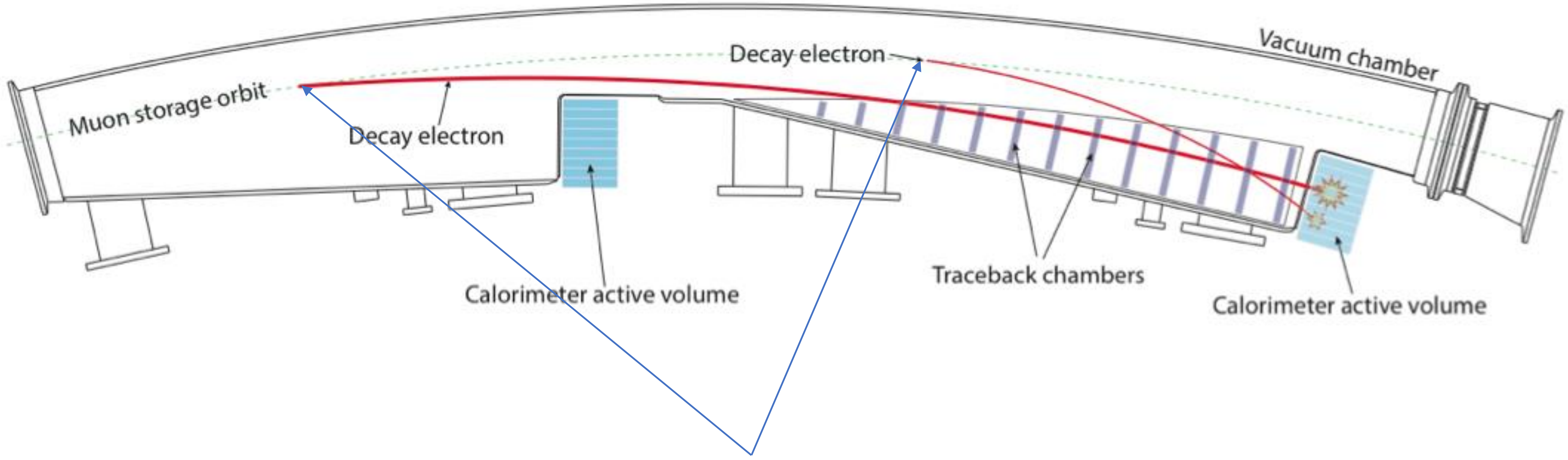

Muon spin has precessed a bit further

Phase acceptance

Muon distribution

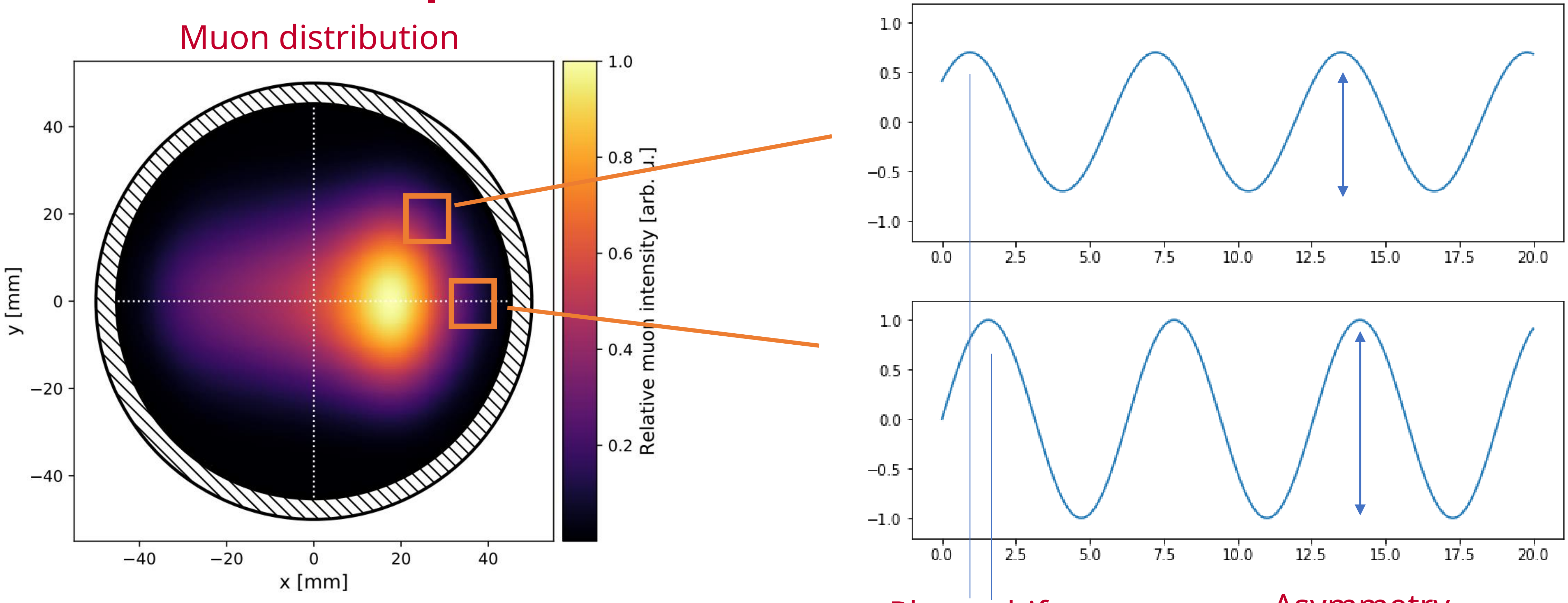

Phase shift

Asymmetry difference

Depends on energy and time

Beam profile must be well-understood during measurement period

Phase acceptance

Muon distribution

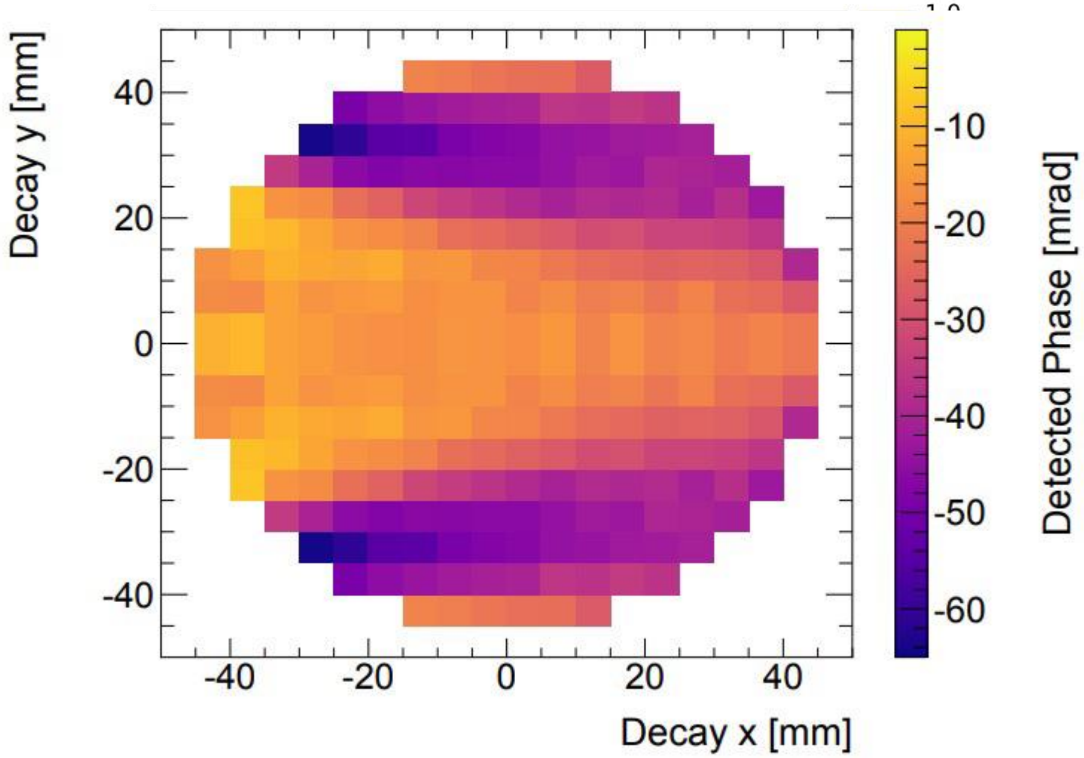

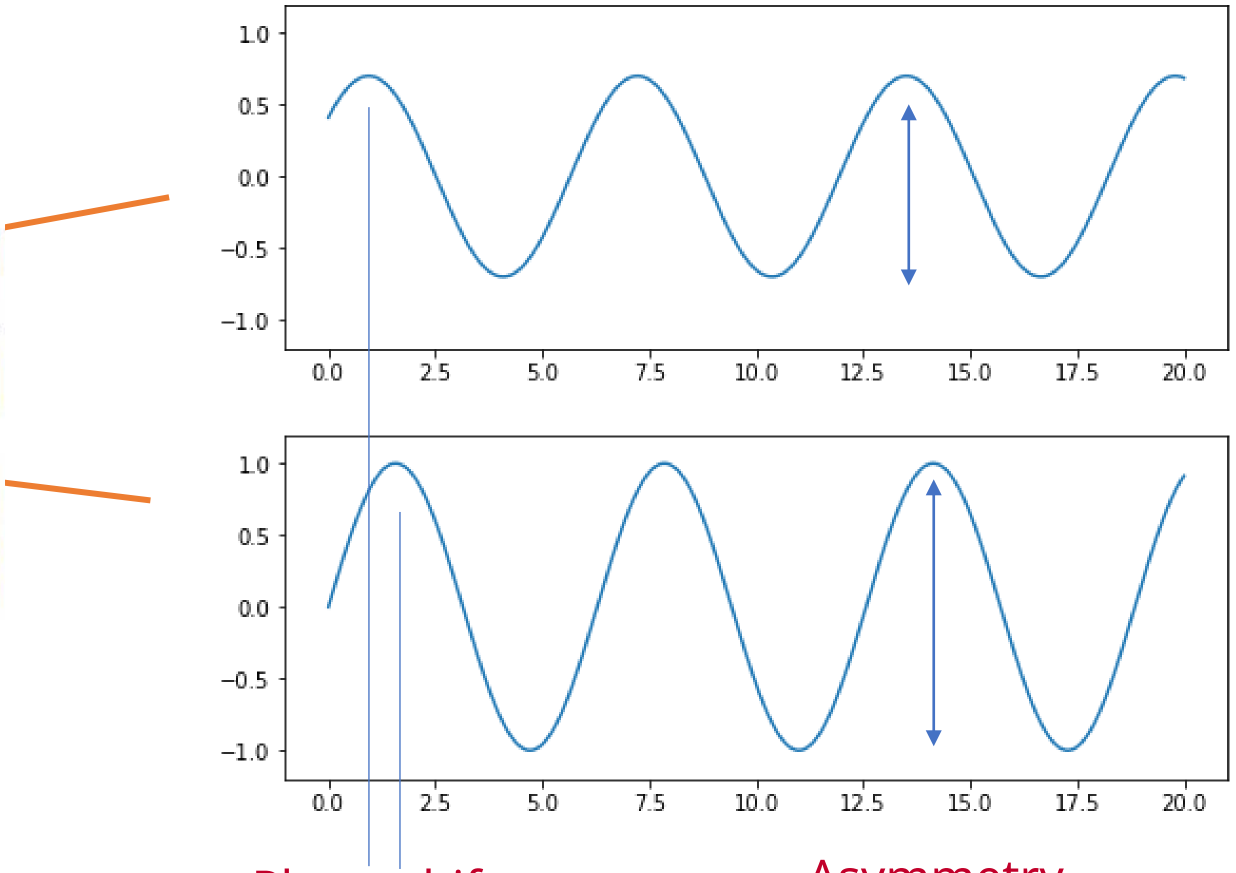

Phase shift

Asymmetry difference

Depends on energy and time

Beam profile must be well-understood during measurement period

Extracting a_μ

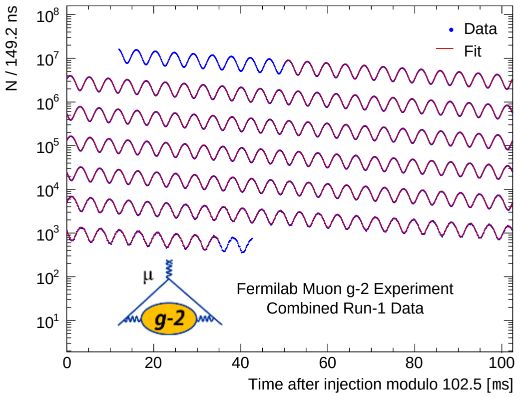

Anomalous spin precession frequency

Clock blinding

Muon beam dynamics corrections

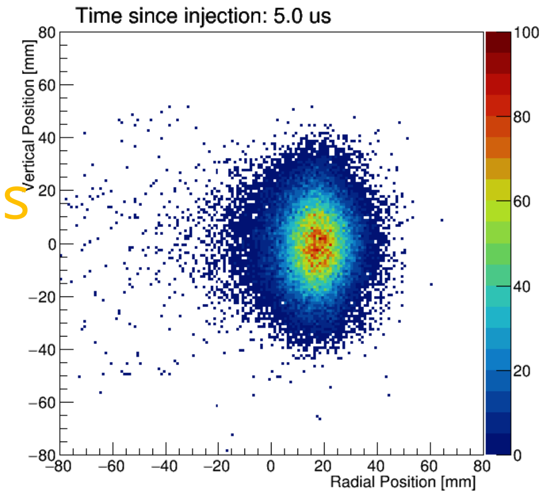

$$\frac{\omega_a}{\tilde{\omega}'_p} = \frac{f_{\rm clock}\,\omega_a^{\rm meas}(1+C_e+C_p+C_{ml}+C_{pa})}{f_{\rm calib}\langle M(x,y,\phi)\,\omega'_p(x,y,\phi)\rangle\,(1+B_k+B_q)}$$

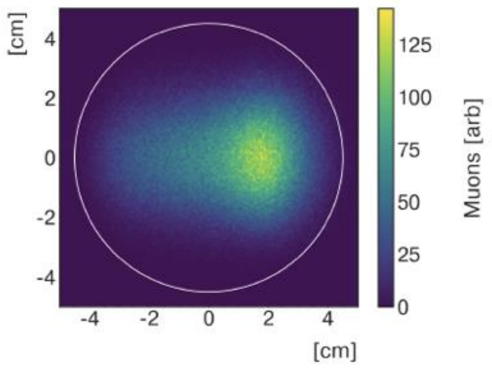

Spatial muon distribution

Spatial distribution of magnetic field

Transient magnetic fields

Calibration

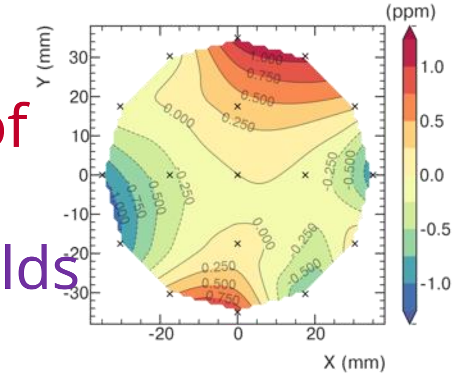

1.45 T vertical magnetic field

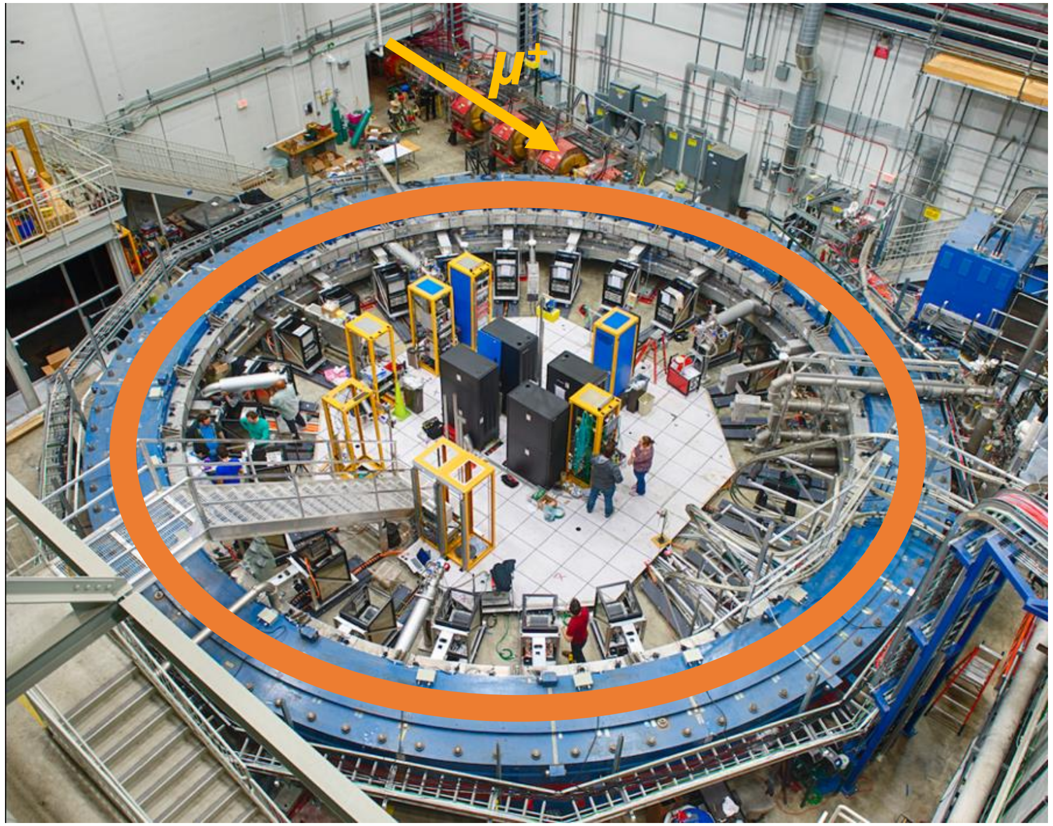

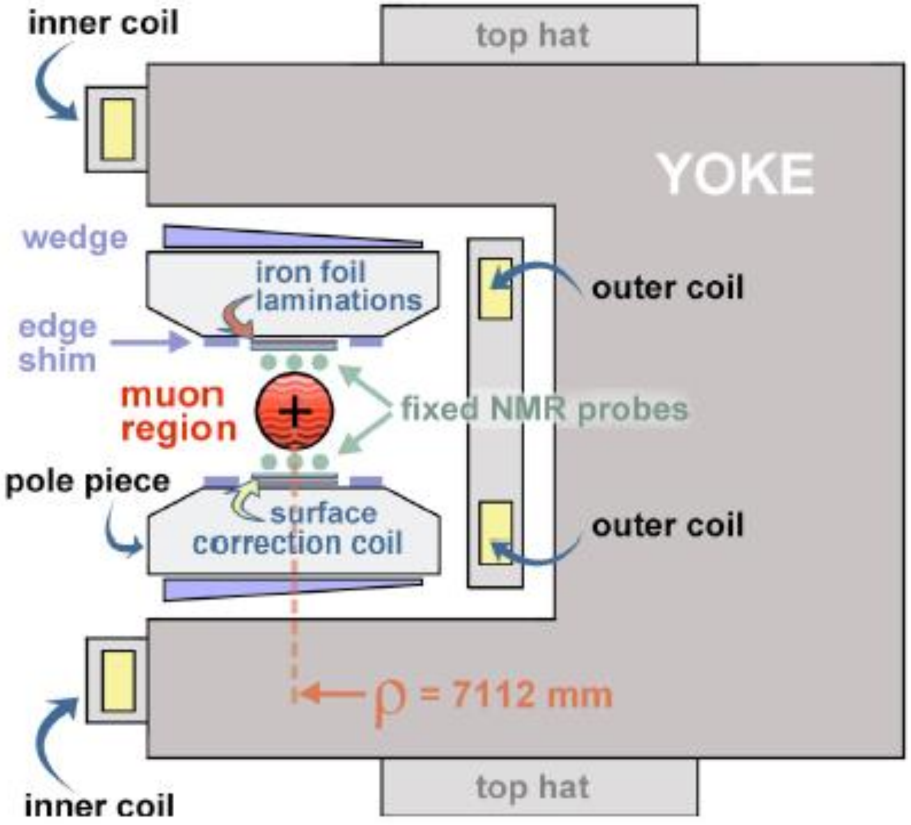

Nuclear Magnetic Resonance (NMR) technique

Material in external magnetic field

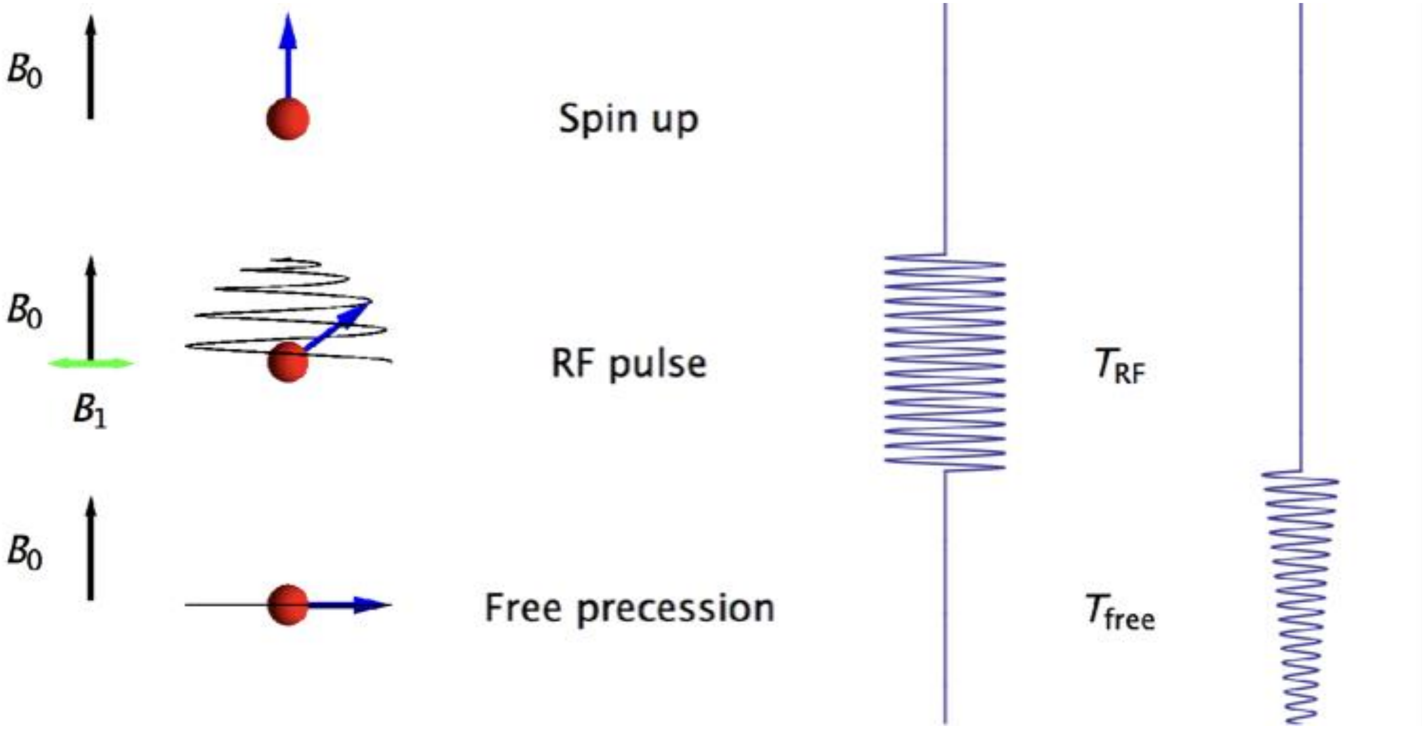

thermal equilibrium polarization: ~ 10^{-6}

RF pulse perpendicular to main field close to proton Larmor frequency tilts the p spin

Pick up induction signal of precising magnetization with the excitation coil

NMR technique

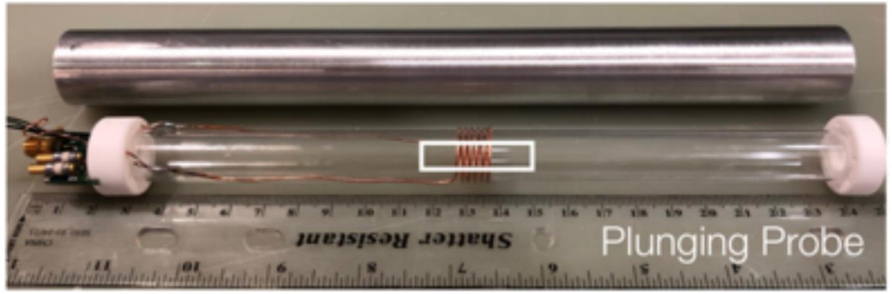

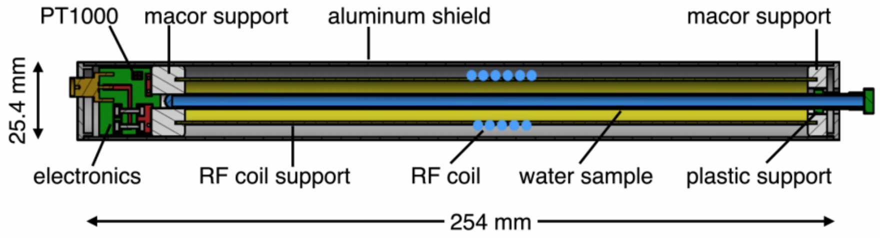

- Lamor precession frequency

$$\omega_L = -\gamma B$$

  with gyromagnetic ratio γ

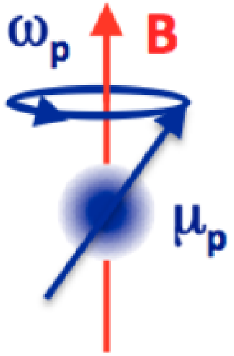

- Gyromagnetic ratio of free proton is 2.6752218744 $\cdot 10^8$ Hz/T

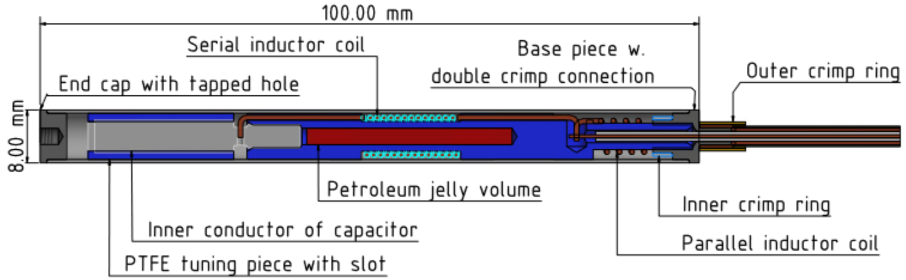

- Reference gyromagnetic ratio of pure water in spherical sample

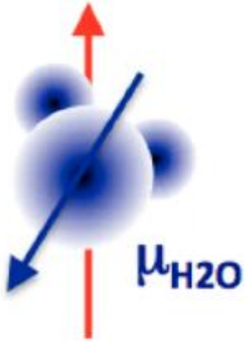

- Two types of probes
  - Ultra pure water in cylinder volume for calibration
  - Petroleum jelly in cylinder volume for normal measurement

Free Induction Decay

- At 1.45 T field proton spin precession frequency if about 61.79 MHz
- Mixed down frequency to ~50kHz for digitization
- Free induction decay signal oscillates at Lamor frequency
- Decoherence of spins in sample lead to envelop decay
- Using Hilbert transformation to extract phase
- Frequency is given by slope of phase at time t=0
- Subtract template → measure field differences

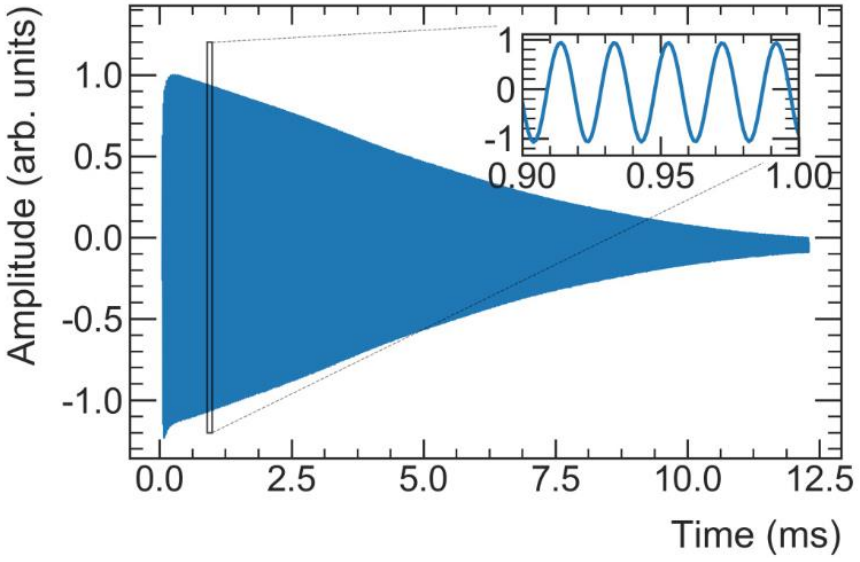

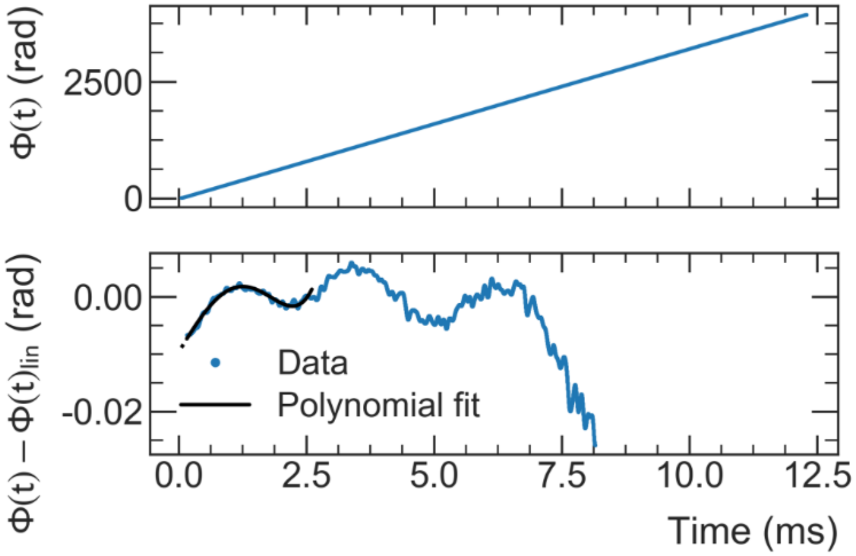

Shimming trolley

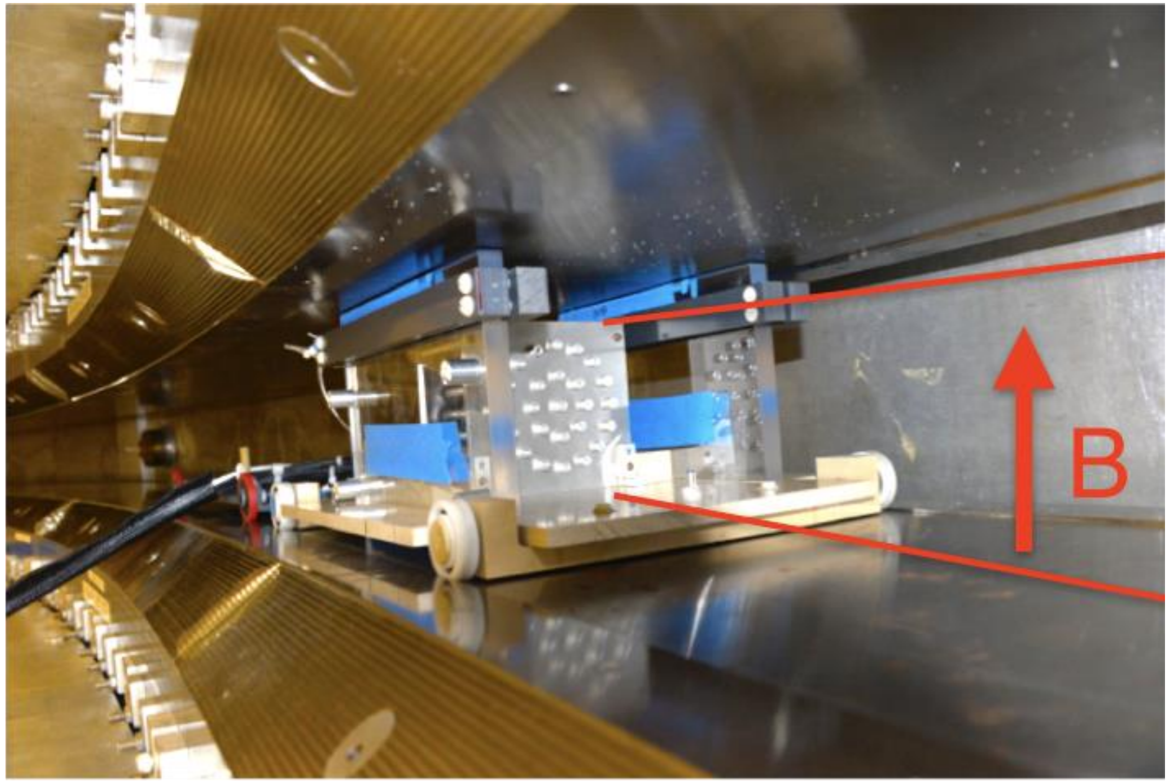

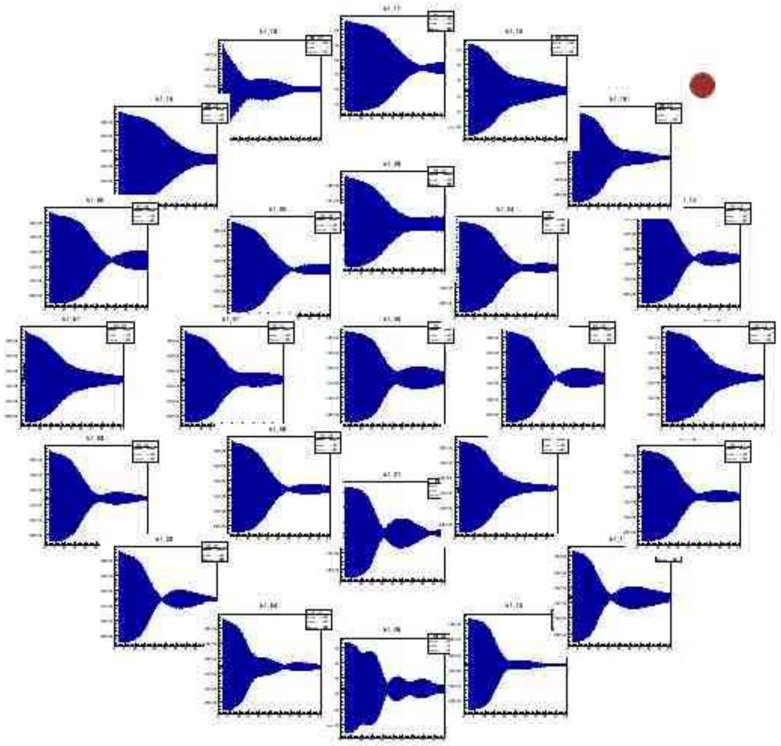

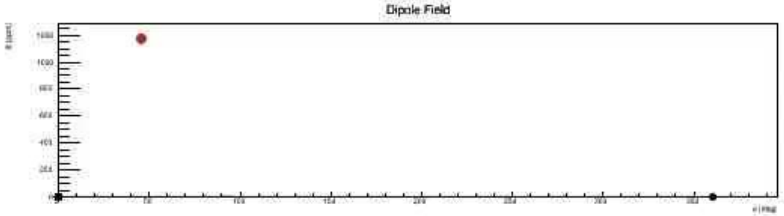

- 25 NMR probes on movable platform
- Used to measure field while assembly

Getting a homogeneous field

First adjust height and tilt of pole pieces

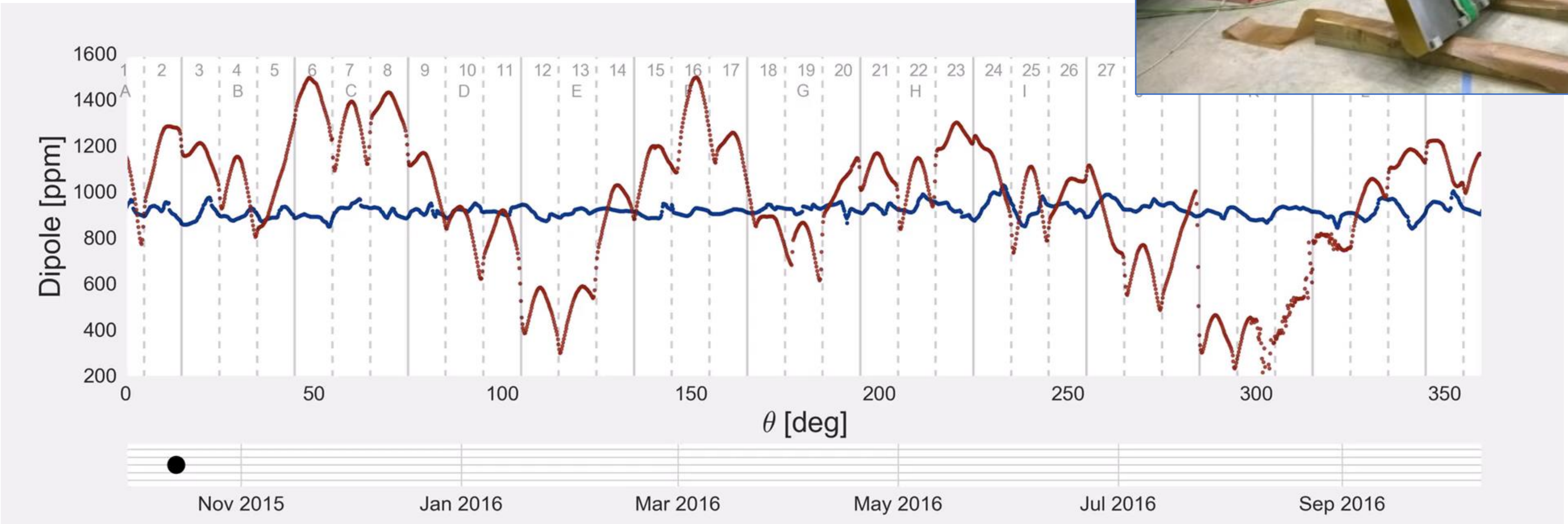

Getting a homogeneous field

Second top hats and wedge shims

Top hats gap changes effective permeability in the magnetic circuit

Radial position of wedges to adjust dipole and compensate quadrupole

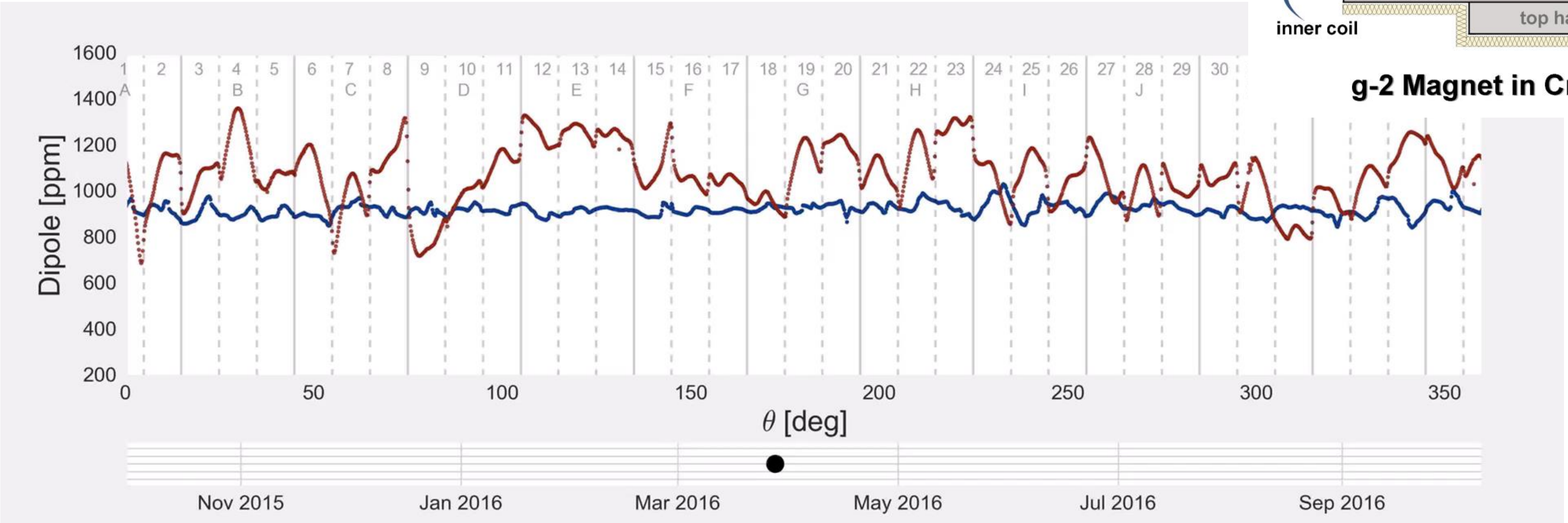

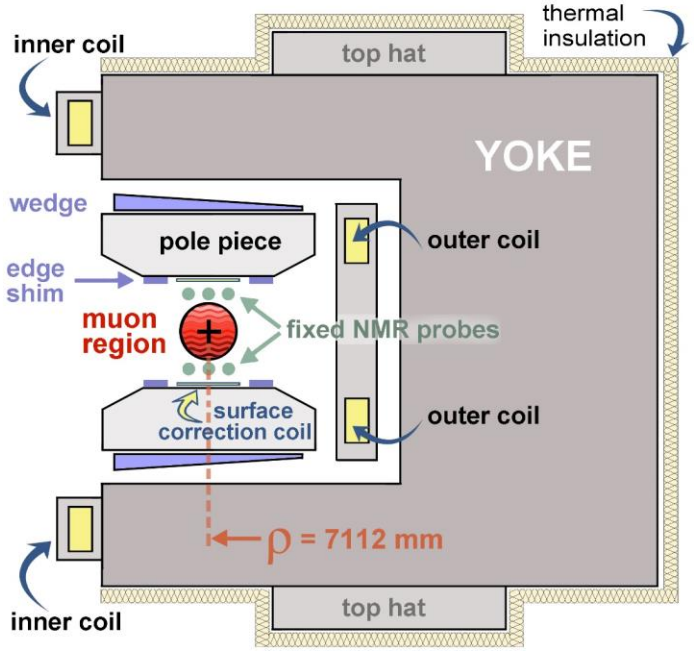

g-2 Magnet in Cross Section

Getting a homogeneous field

Add IR laser cut iron foils

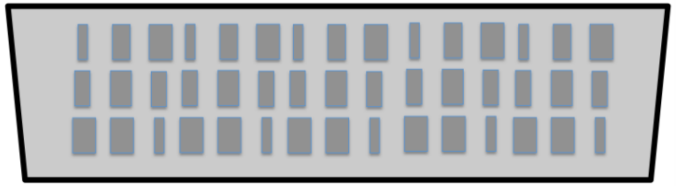

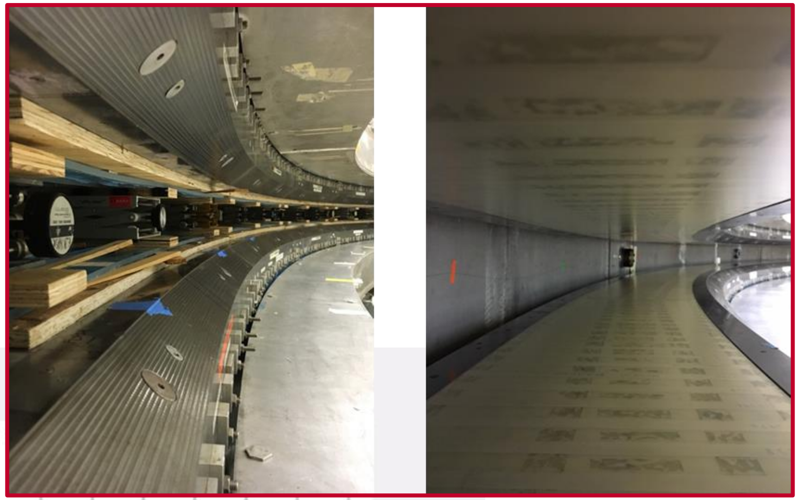

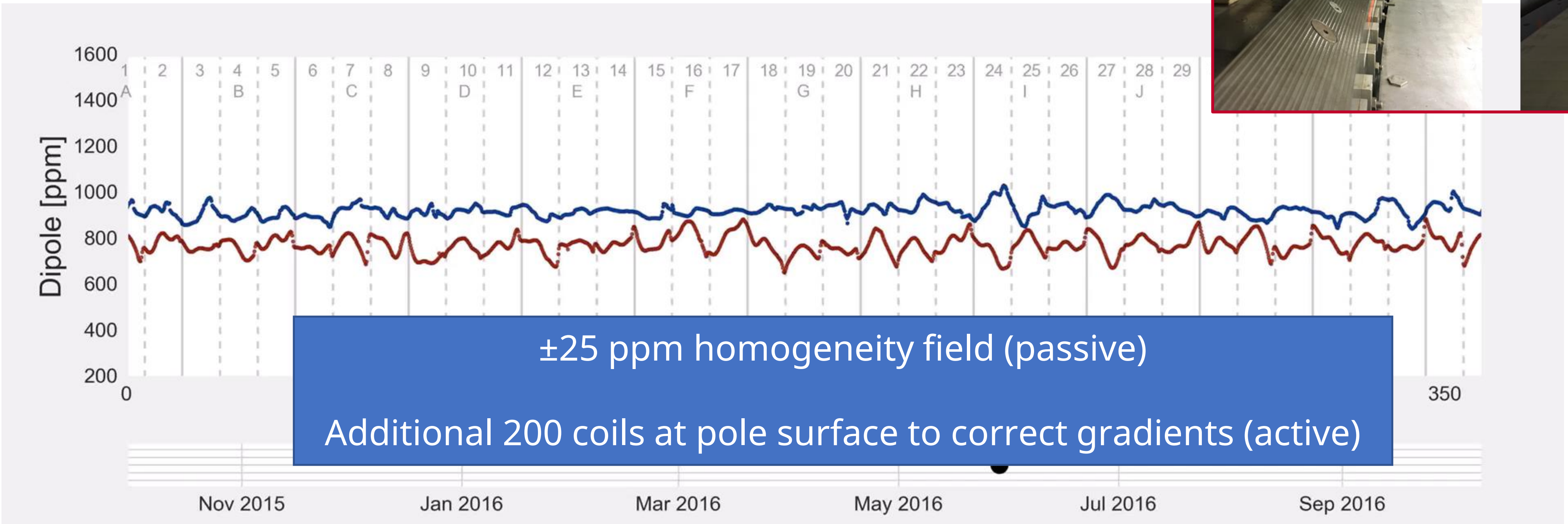

±25 ppm homogeneity field (passive)

Additional 200 coils at pole surface to correct gradients (active)

Trolley System

- 17 NMR probes
- Measures spatial field distribution in storage region
- Pulled through ring every ~3 days

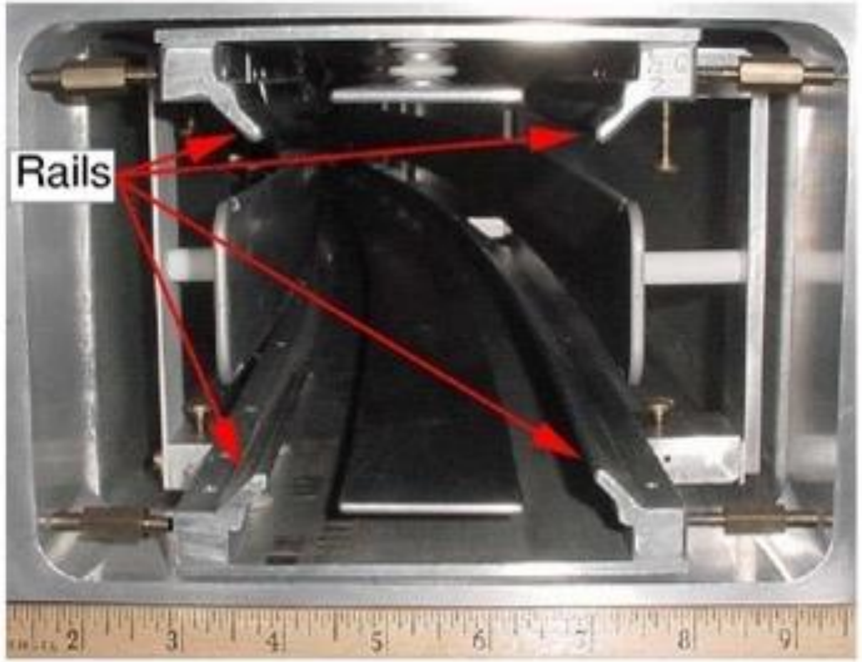

Spatial distribution of field

$$B(r,\theta) = B_0 + \sum_{n=1}^{4} \left(\frac{r}{r_0}\right)^n [a_n \cos(n\theta) + b_n \sin(n\theta)]$$

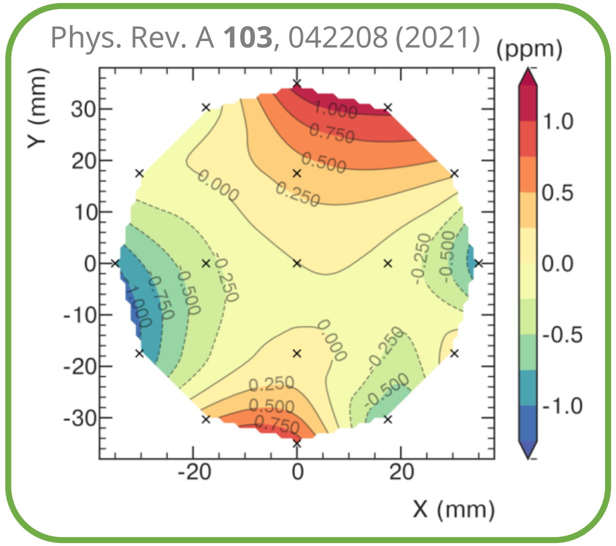

azimuthal slice

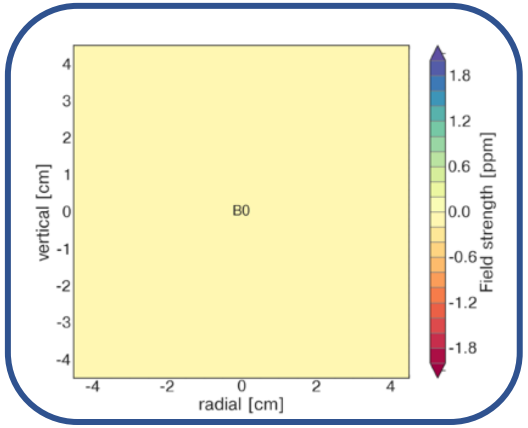

dipole

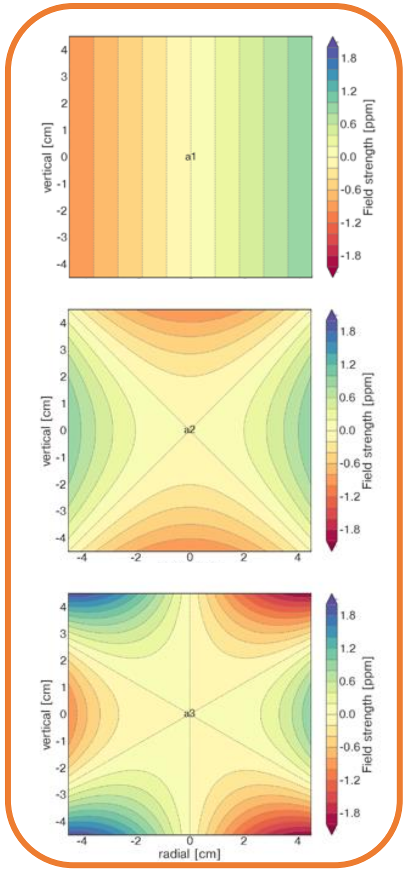

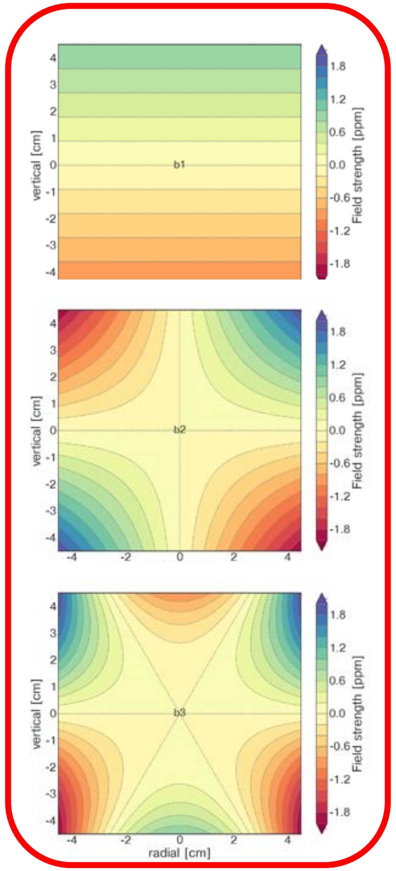

quadrupole

sextupole

octupole

Trolley measurements

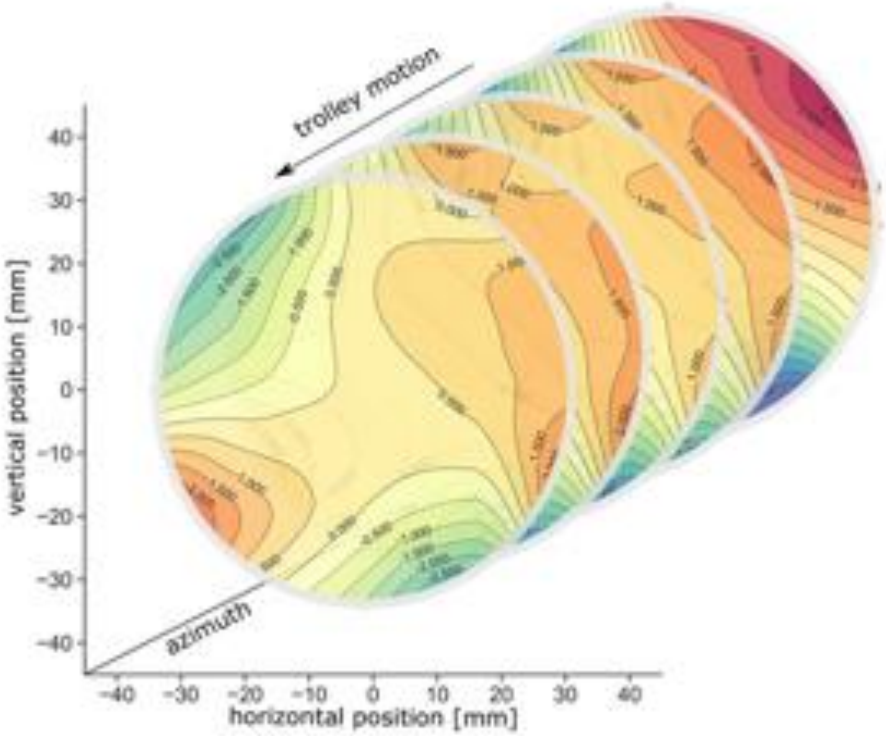

>8000 azimuthal locations

Phys. Rev. A **103**, 042208 (2021)

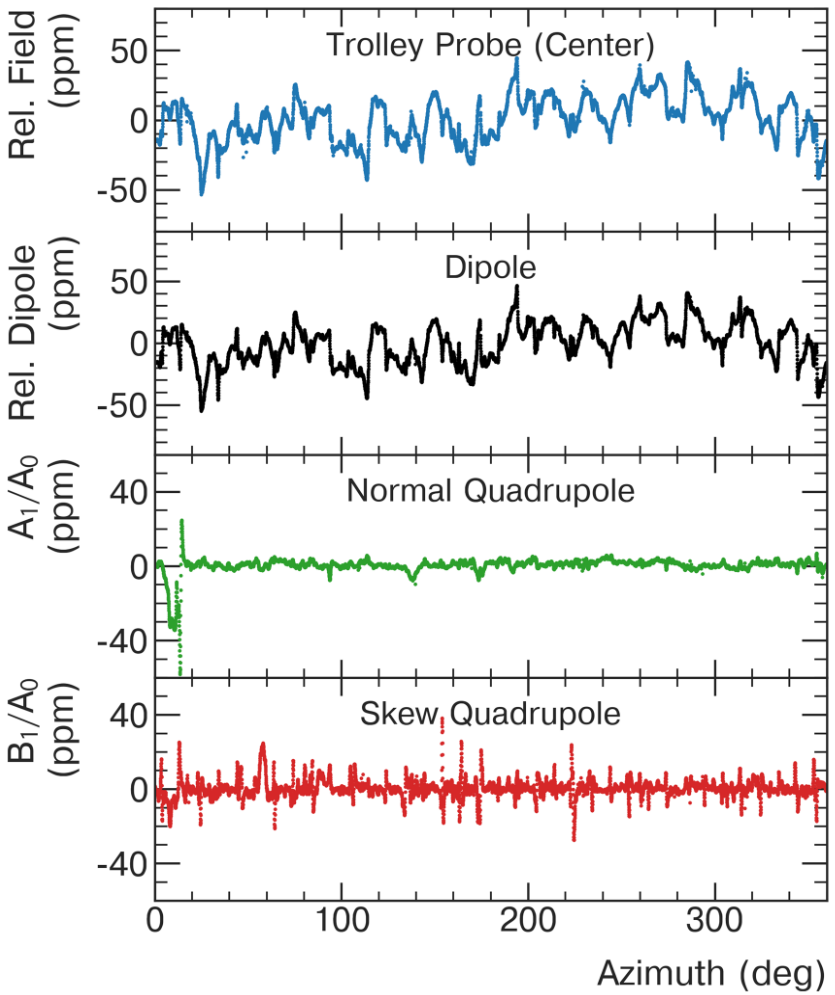

Trolley measures spatial distribution, but can not measure while muon beam

Fixed Probe System

- 72 azimuthal location (stations)
- allows to extract 4/5 multipole moments
- tracks field drift 24/7
- measures field differences

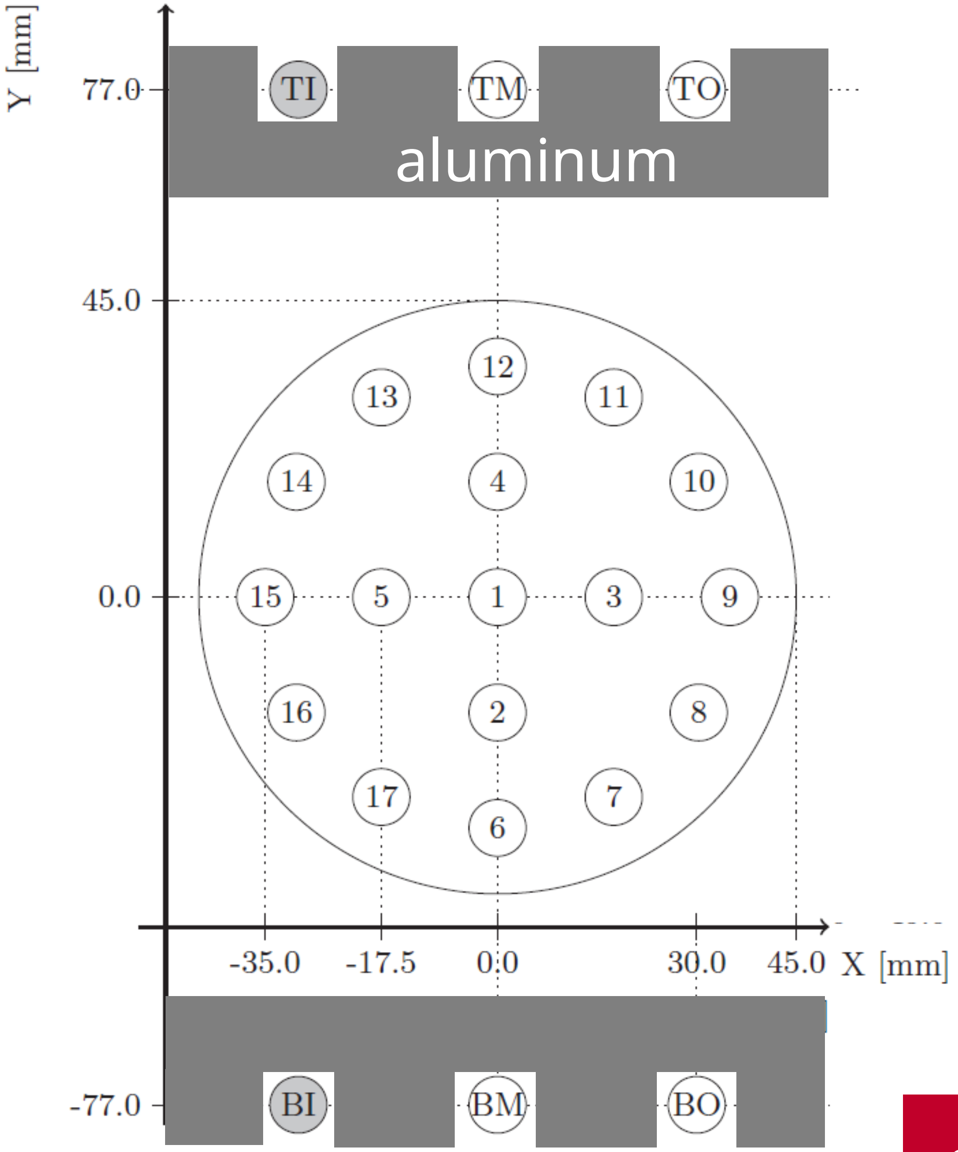

Trolley Footprint Removal

Phys. Rev. A **103**, 042208 (2021)

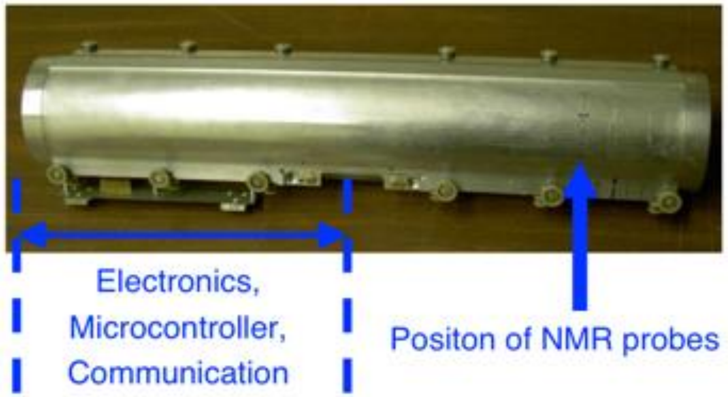

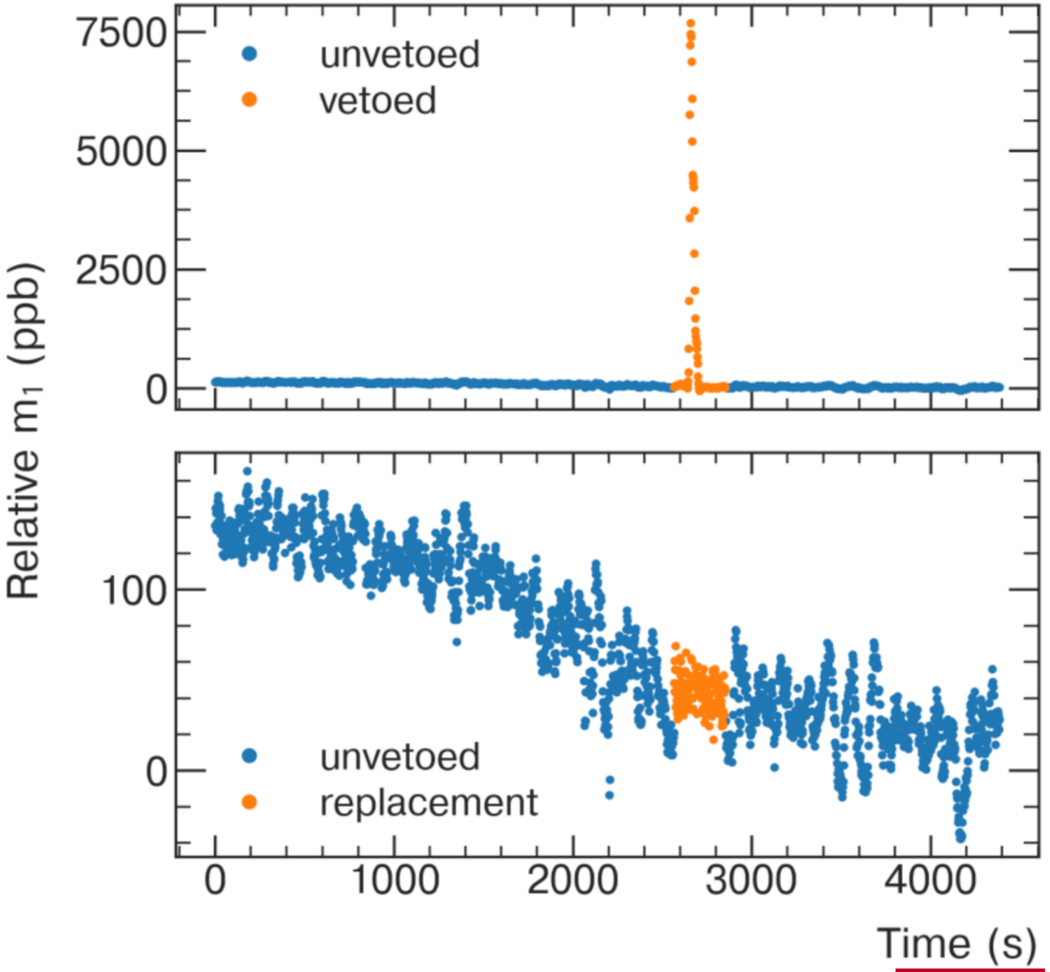

- trolley electronics disturbs field (footprint)
- veto measurements
- interpolate from neighboring probes
- Aligns trolley and fixed probe measurements

Time tracking

Phys. Rev. A **103**, 042208 (2021)

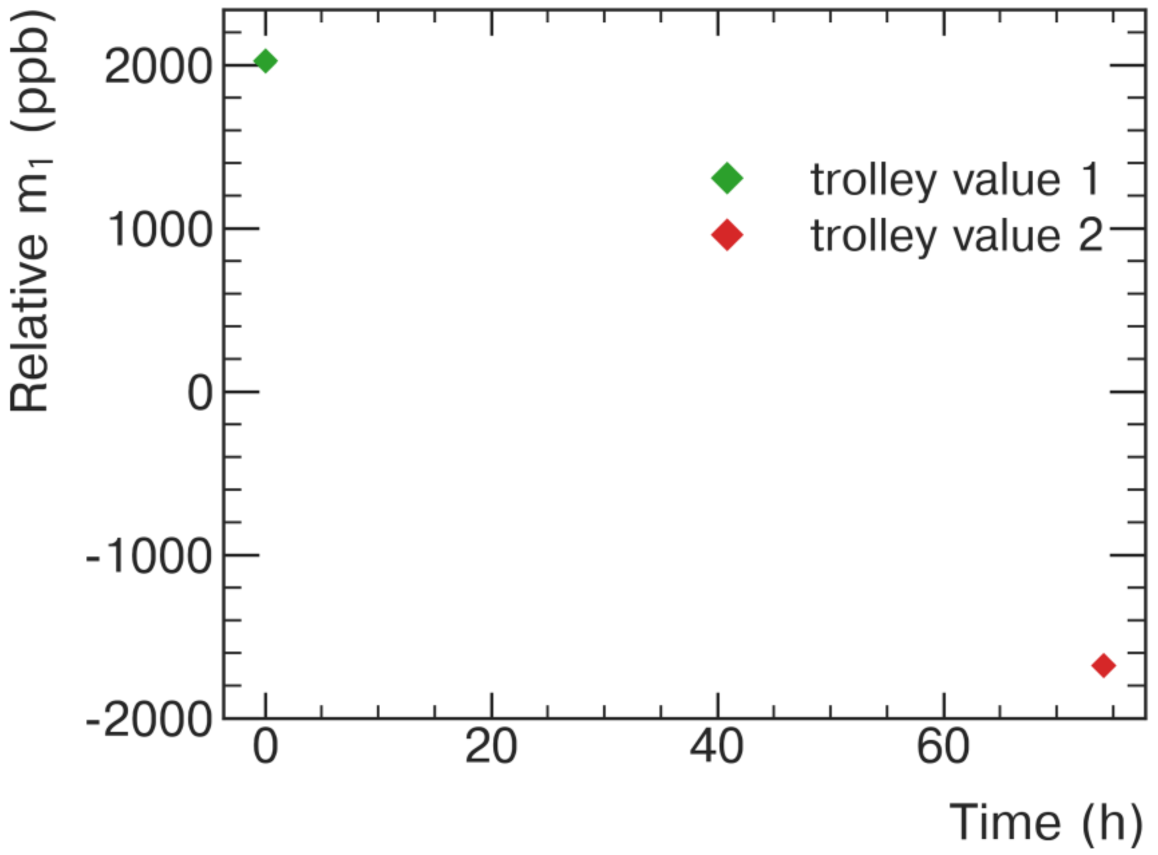

Time tracking

Phys. Rev. A **103**, 042208 (2021)

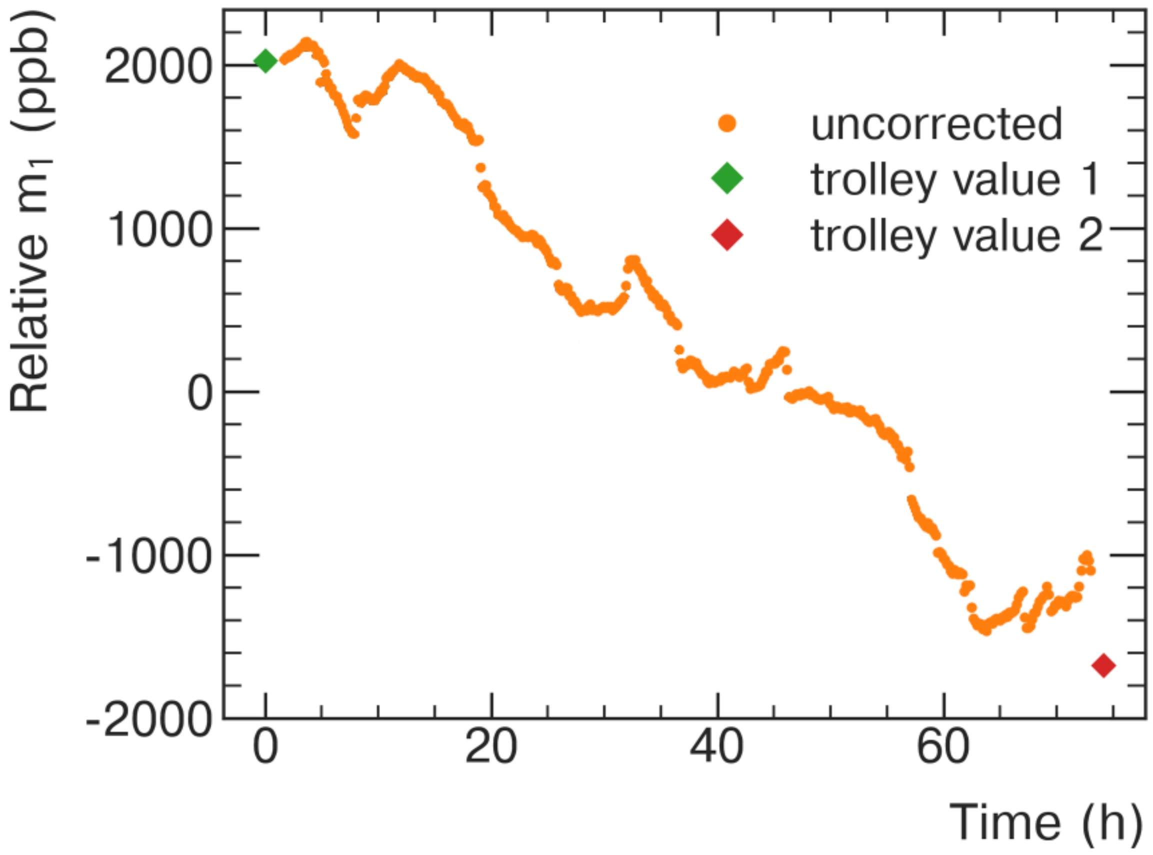

Time tracking

Phys. Rev. A **103**, 042208 (2021)

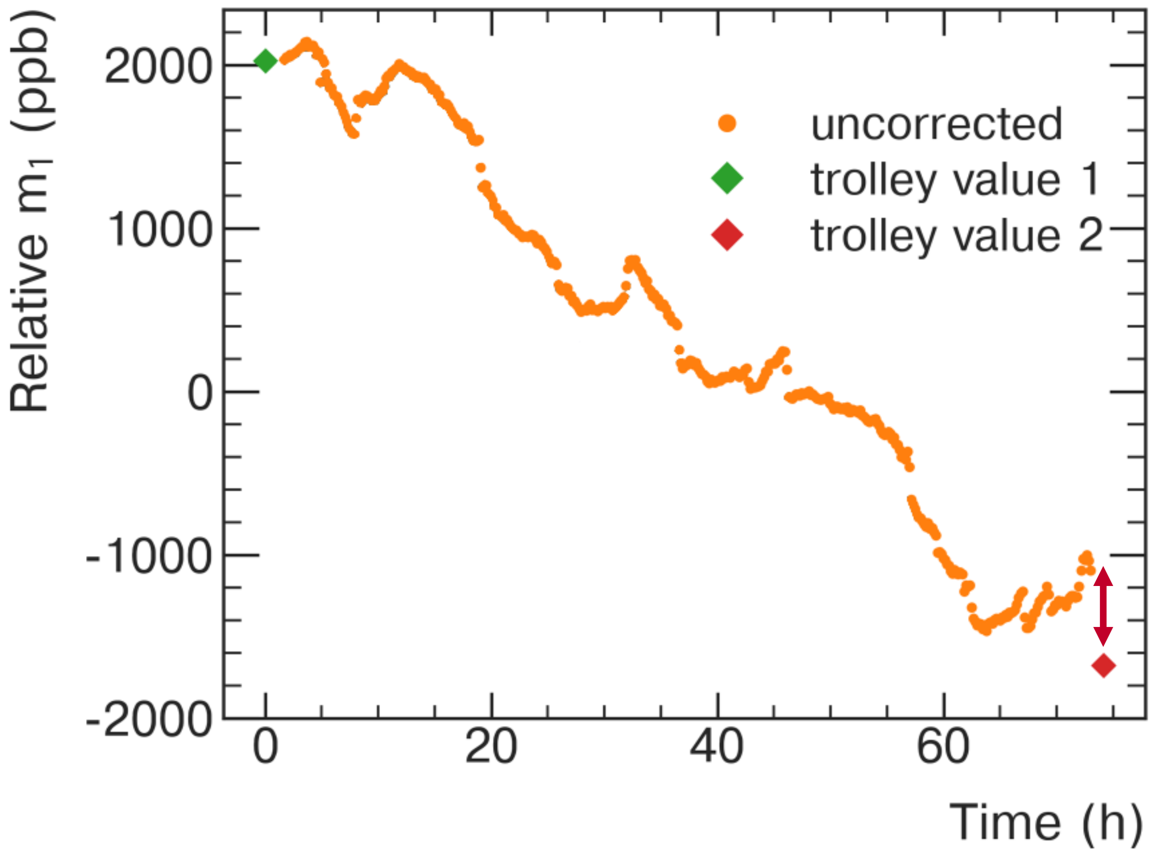

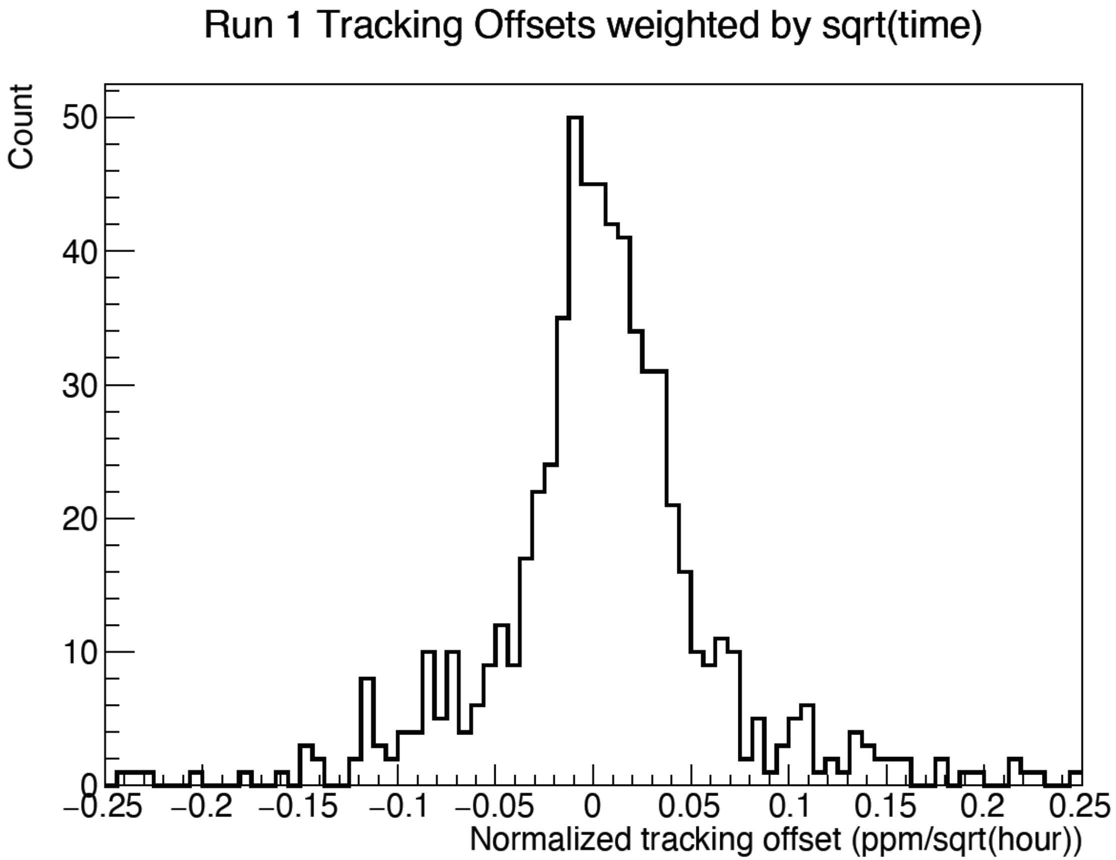

drifts in higher order moments lead to **tracking offset**

Time tracking

Phys. Rev. A **103**, 042208 (2021)

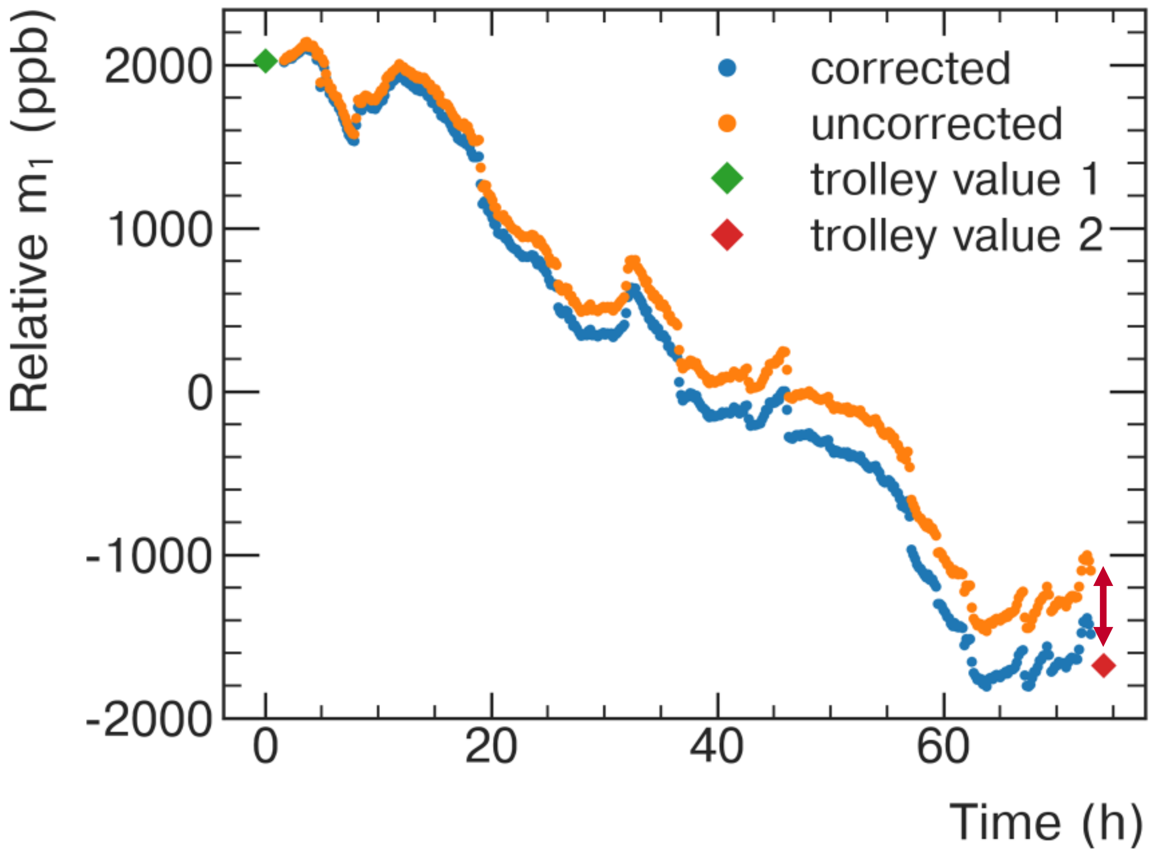

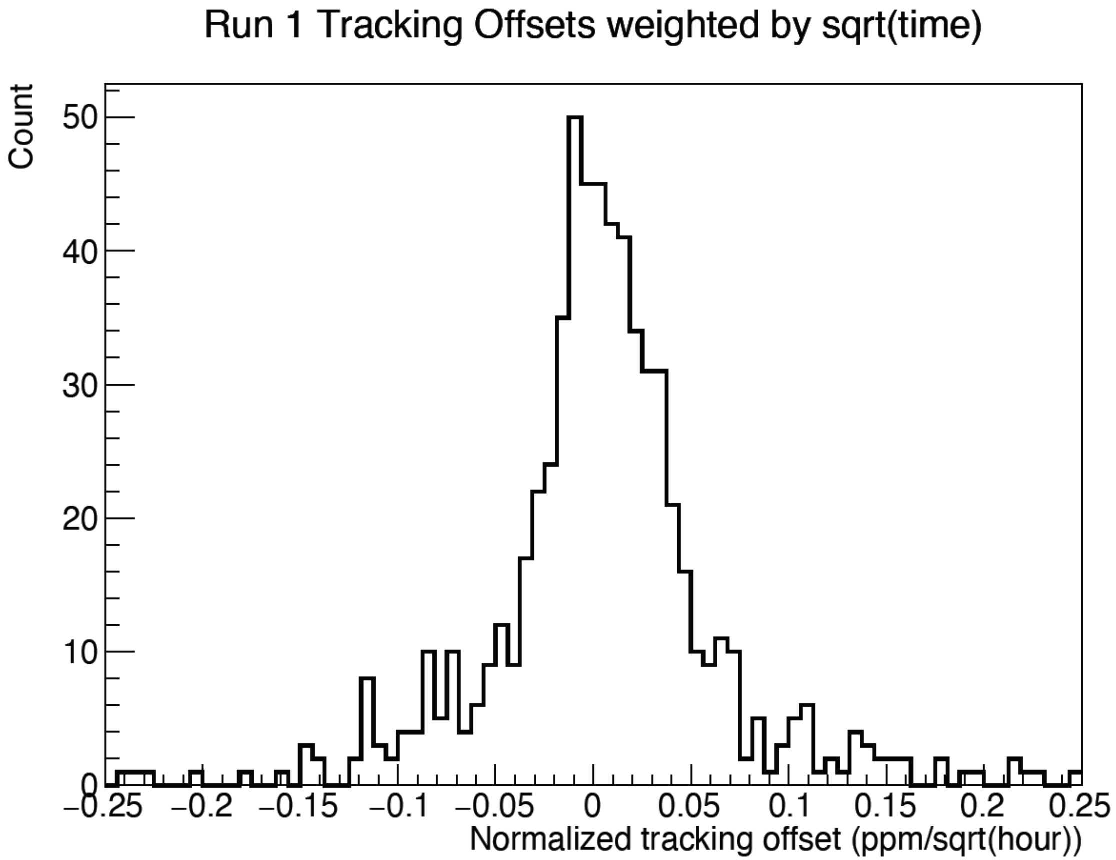

drifts in higher order moments lead to **tracking offset**

Tracking Uncertainty

- Fixed Probe drift: Random walk
- End point known: Brownian bridge

$$\sigma(t_1, t_2) = M\frac{(T - t_2)t_1}{T}$$

drift rate parameter

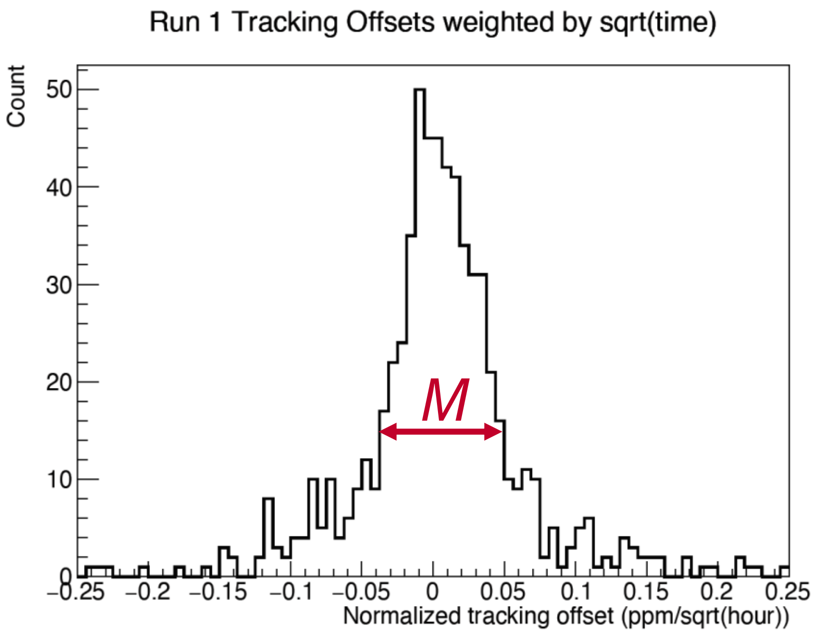

assumes *M* is constant in the ring

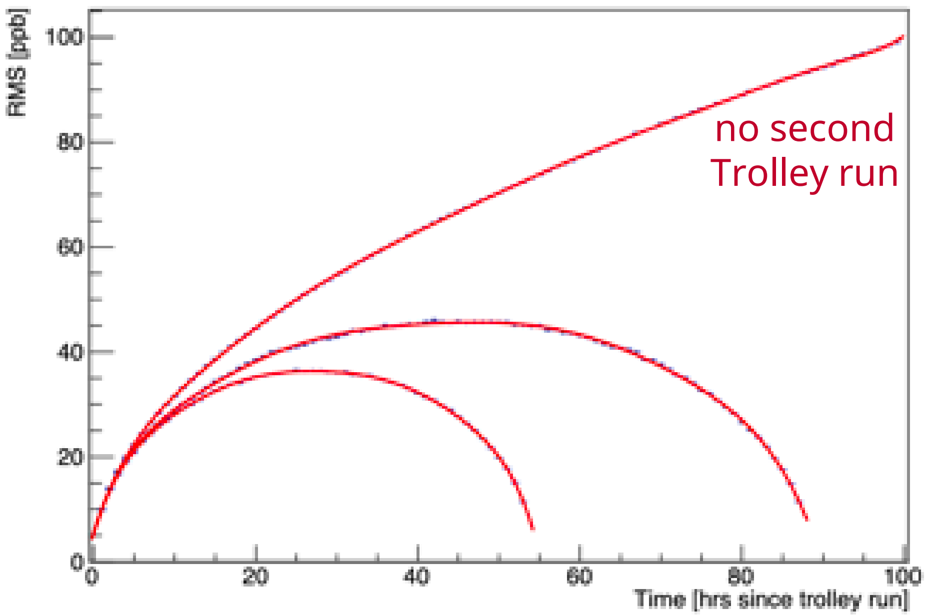

Uncertainty vs time

Field calibration

- Trolley is main device to measure the field
  - Trolley probes based on petroleum jelly
  - Needs calibration

- Alignment of plunging probe & trolley probe
  - Measure field
  - Apply gradient field by surface coils
  - Re-measure field
  - ΔB give position information
- Scan field around probe trolley position
  - Can correct for remaining gradients
- Measure field with both probes by swapping

- Calibration constant per trolley probe

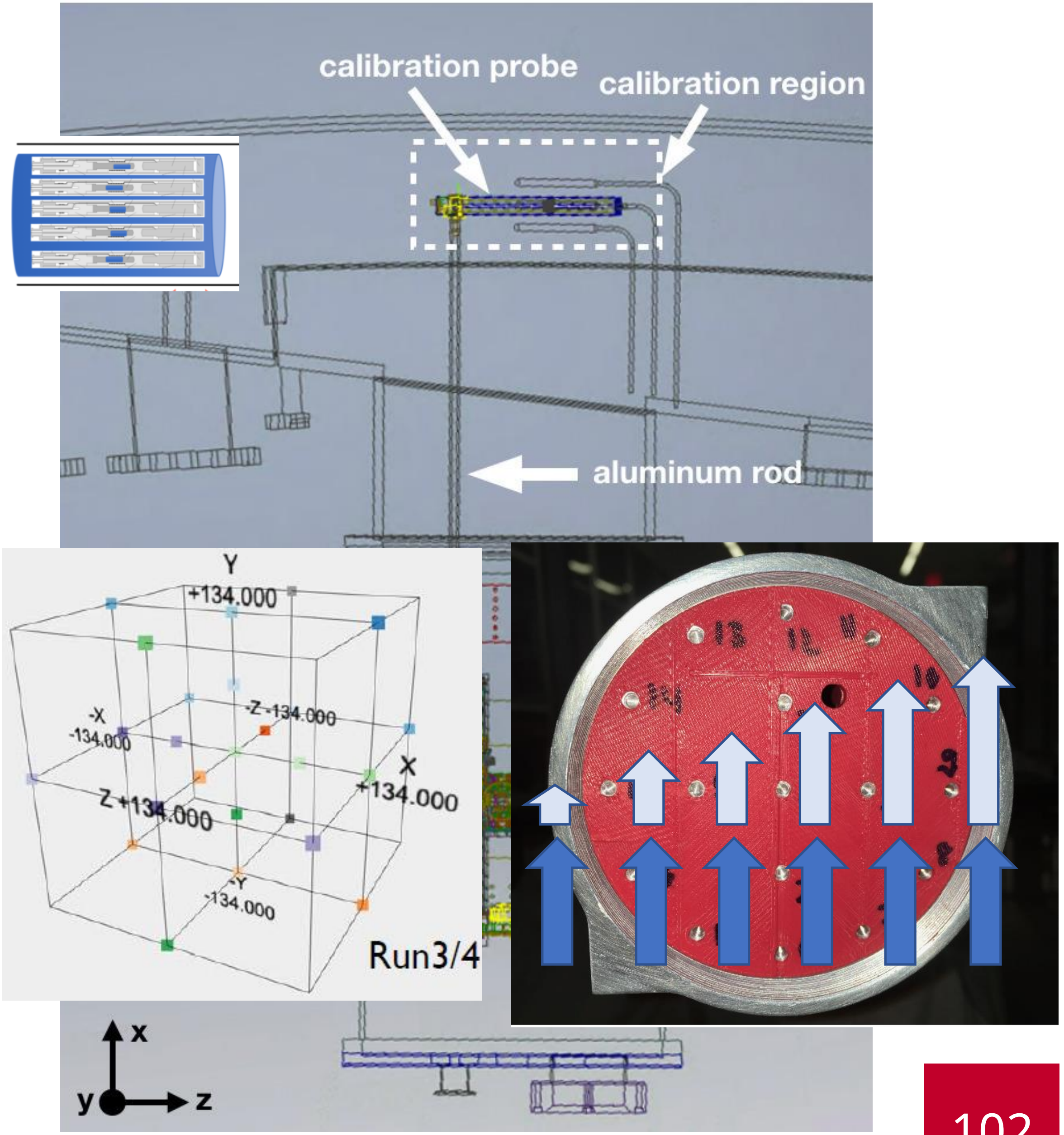

Muon weighted magnetic field

- We need the field seen by the muons
- Tracking magnetic field multipole moments
- Muon distribution given by tracker data and beam dynamics simulation
- Can be decomposed in multipoles as well

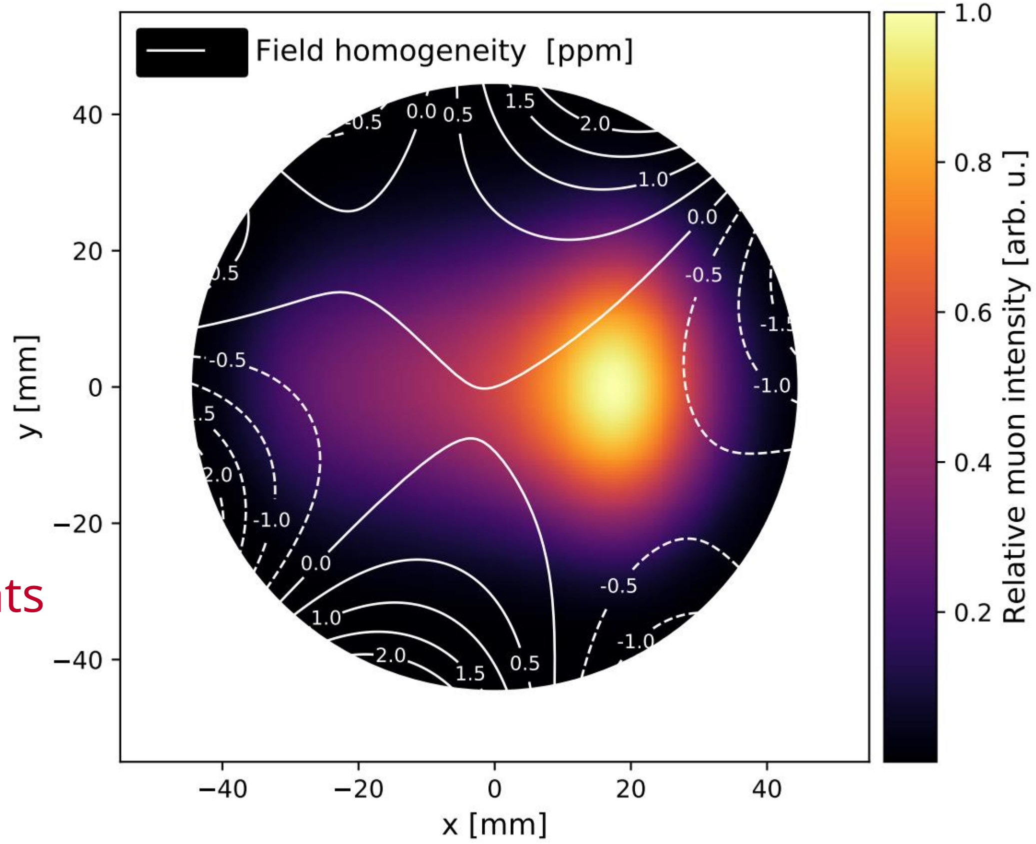

Muon distribution moments

Magnetic field moments

$$\tilde{\omega}'_p = \left\langle \sum_i k_{i,q,j} m_{i,q,j} \right\rangle_{q,j}$$

Time & azimuth index

Magnetic field quadrupole transients

Pulsing electrostatic quadrupoles for beam confinement leads to magnetic field transient.

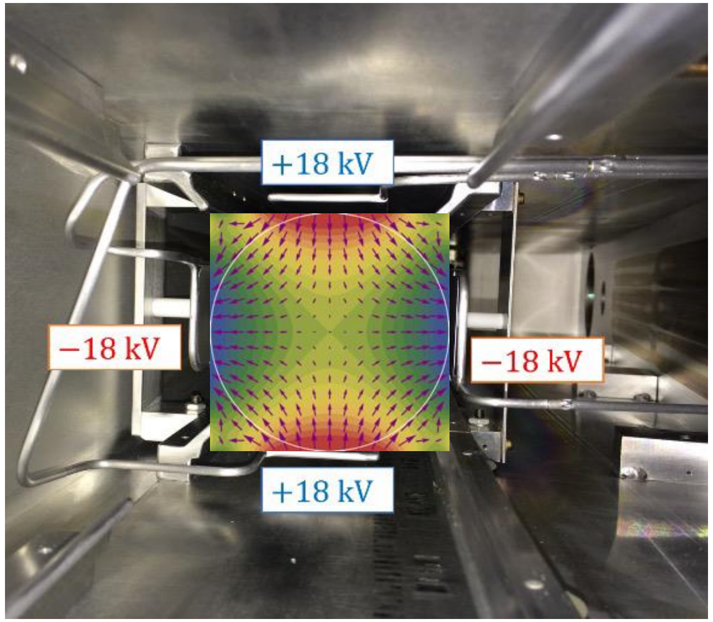

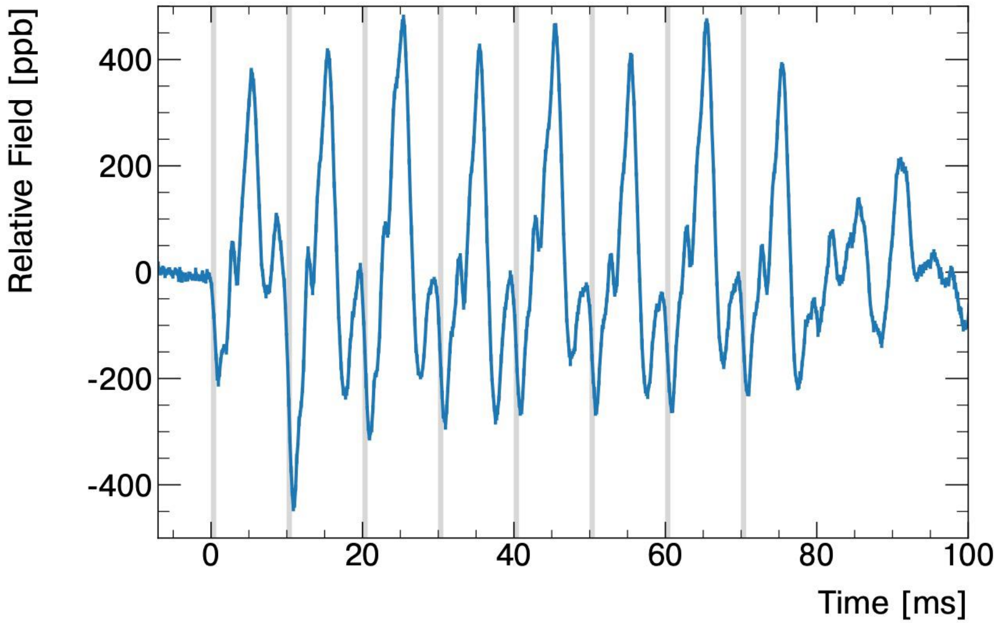

NMR probes run asynchronous with beam injection
Fast transient fields are shielded by aluminum in vacuum chambers

Magnetic field quadrupole transients

Pulsing electrostatic quadrupoles for beam confinement leads to magnetic field transient.

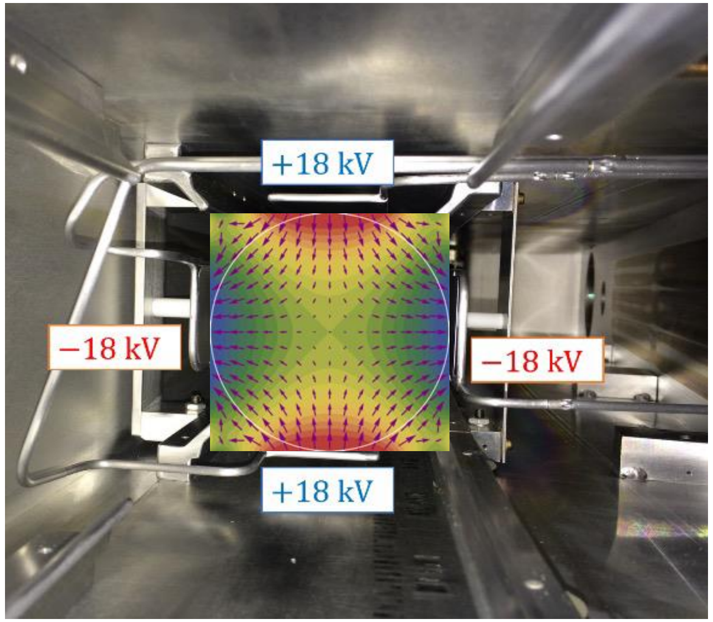

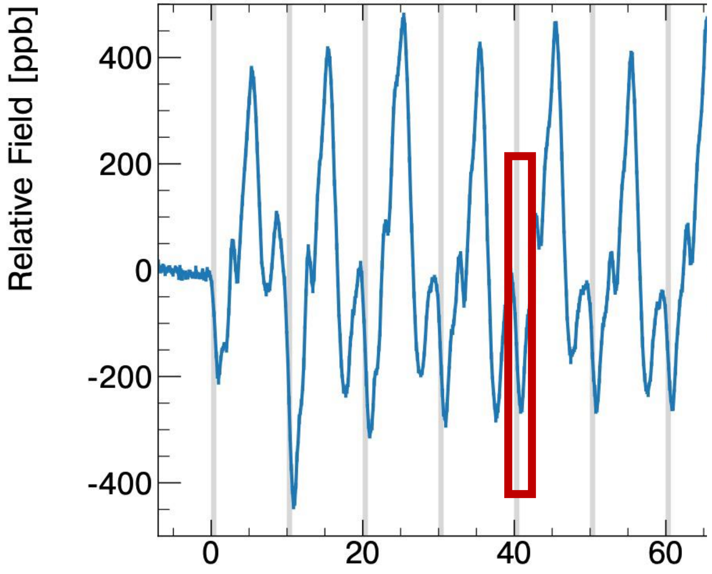

μ present

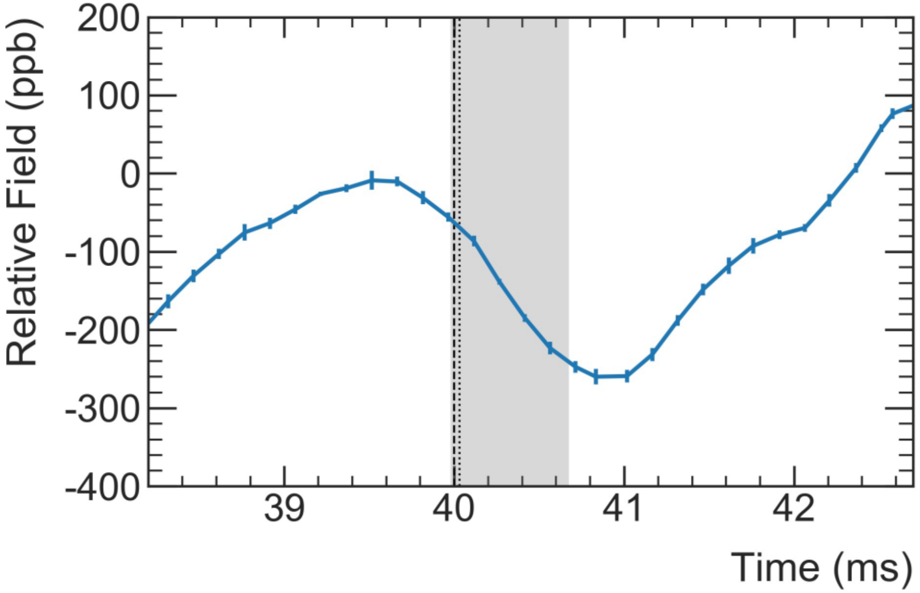

NMR probes run asynchronous with beam injection
Fast transient fields are shielded by aluminum in vacuum chambers

Needs correction

Magnetic field kicker transients

Kicker pulse induces 22mT field in radial direction
NMR technique not fast enough to resolve transient

Measurement based on optical faraday rotation in optical TGG cristal

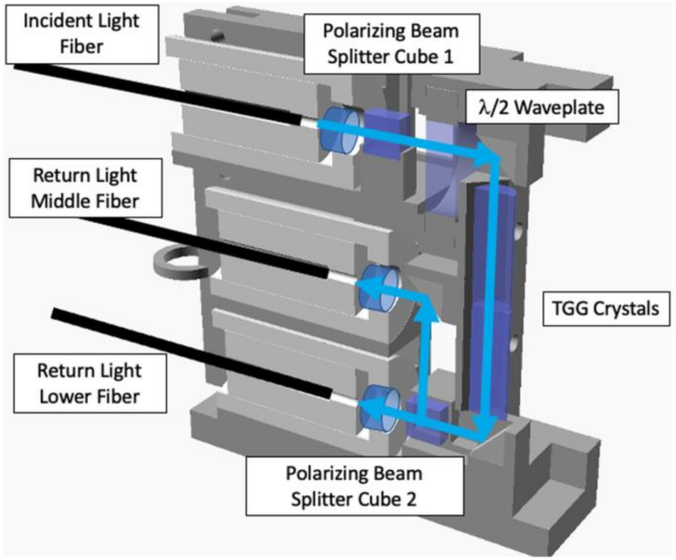

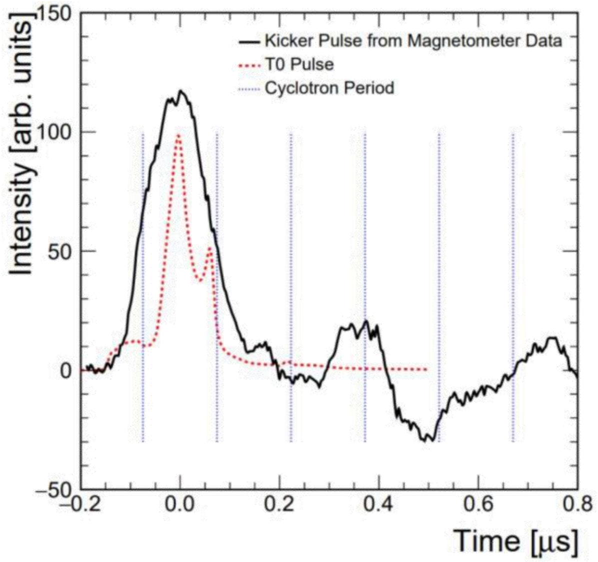

Adds correction factor

Extracting a_μ

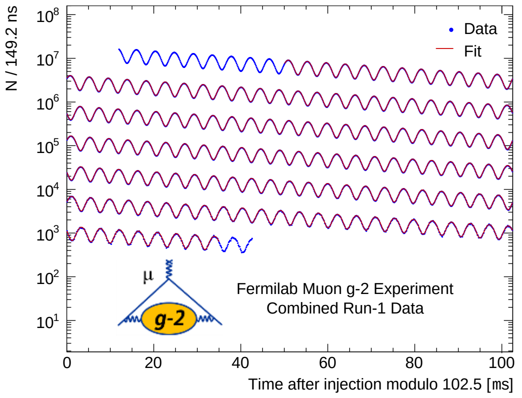

Anomalous spin precession frequency

Clock blinding

Muon beam dynamics corrections

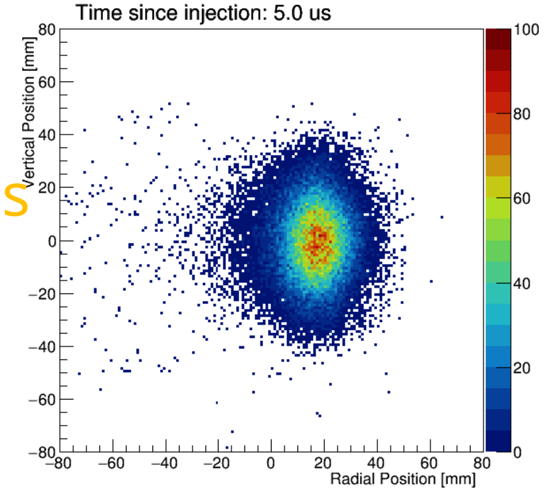

$$\frac{\omega_a}{\tilde{\omega}'_p} = \frac{f_{\mathrm{clock}}\, \omega_a^{\mathrm{meas}} (1 + C_e + C_p + C_{ml} + C_{pa})}{f_{\mathrm{calib}} \langle M(x,y,\phi) \times \omega'_p(x,y,\phi) \rangle (1 + B_k + B_q)}$$

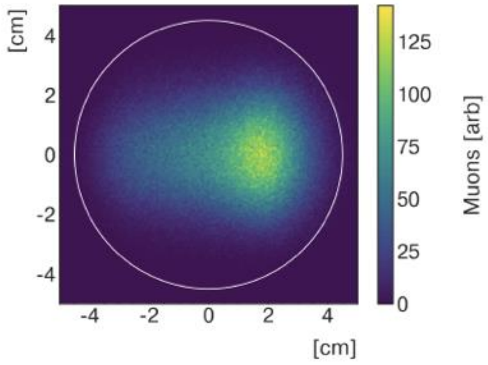

Spatial muon distribution

Spatial distribution of magnetic field

Transient magnetic fields

Calibration

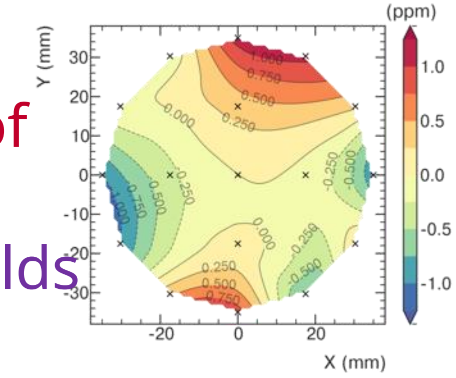

Run 1 datasets

Quantity	Correction Terms (ppb)	Uncertainty (ppb)
ω_a^m (statistical)	–	434
ω_a^m (systematic)	–	56
C_e	489	53
C_p	180	13
C_{ml}	-11	5
C_{pa}	-158	75
$f_{\text{calib}}\langle\omega_p(x,y,\phi)\times M(x,y,\phi)\rangle$	–	56
B_k	-27	37
B_q	-17	92
$\mu_p'(34.7^\circ)/\mu_e$	–	10
m_μ/m_e	–	22
$g_e/2$	–	0
Total systematic	–	157
Total fundamental factors	–	25
Totals	544	462

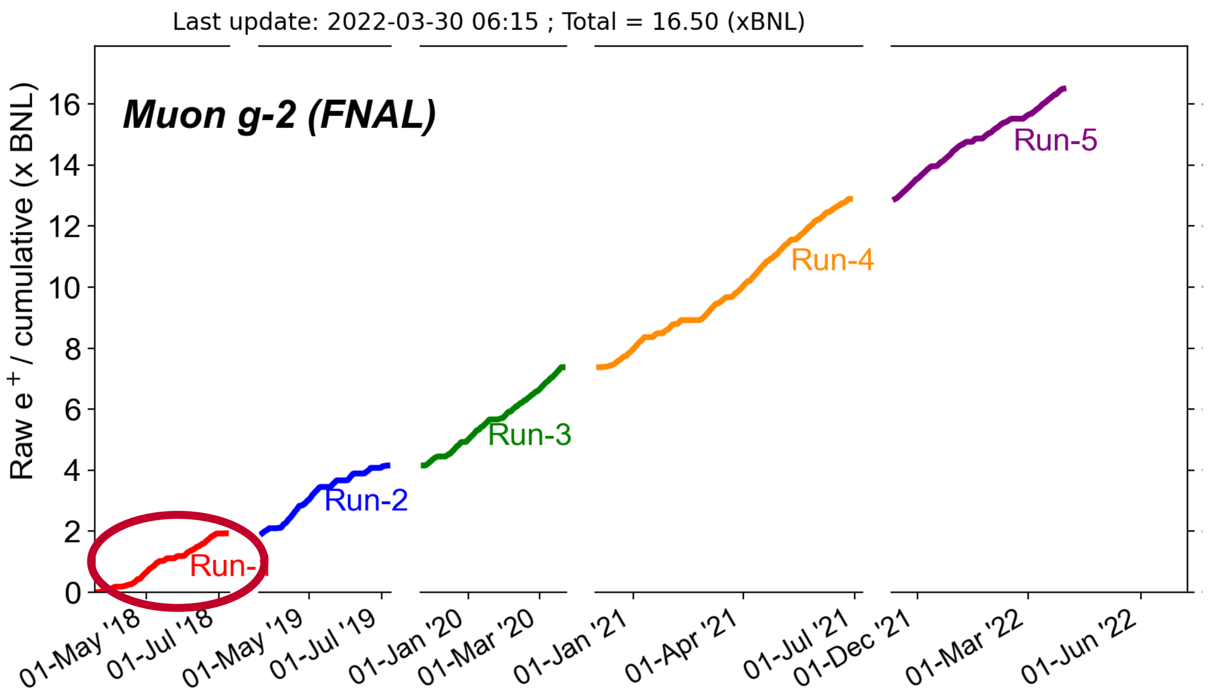

Dataset	Field index n ESQ HV [kV]	Kicker HV [kV]	Number of positrons
1a	0.108 / 18.3	130	0.9×10^9
1b	0.120 / 20.4	137	1.3×10^9
1c	0.120 / 20.4	132	2.0×10^9
1d	0.108 / 18.3	125	4.0×10^9

Blinded results from 4 data periods

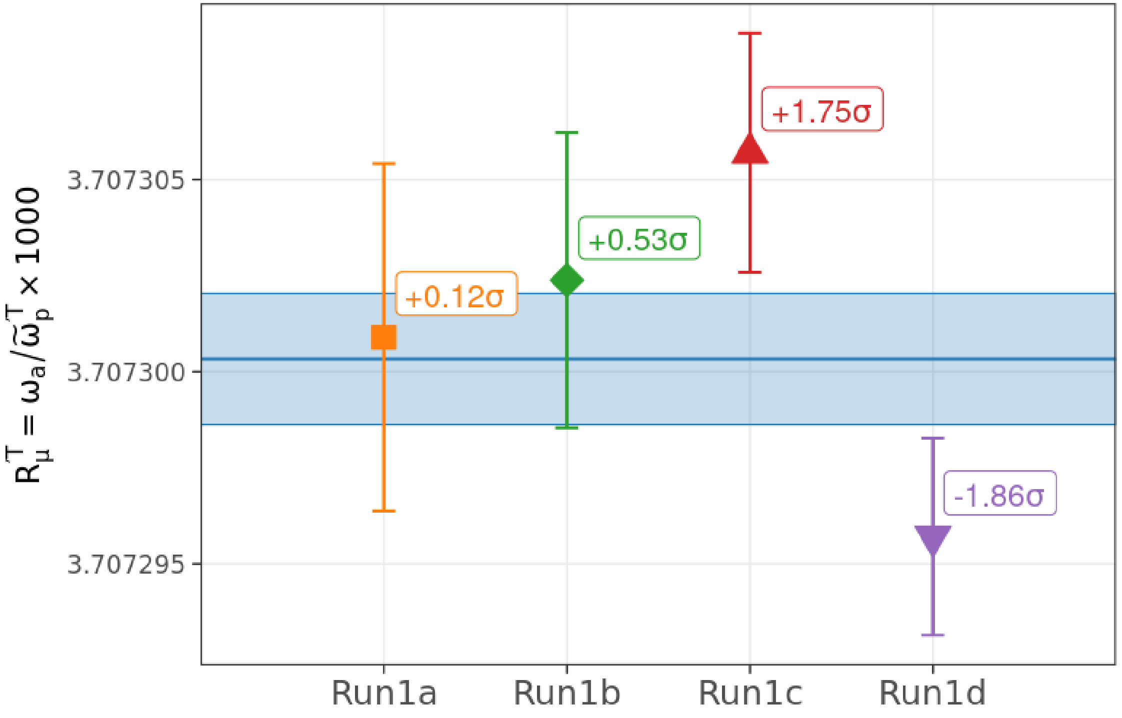

- Correction factors and analysis depend on kicker strength and ESQ HV settings (beam tune)
- Four different settings in run 1
- Results consistent with c^2/ndf=6.8/3 P(c^2)=7.8%
- Result still hardware blinded

Blinding of master clock

… by Greg Bock and Joe Lykken in 2018 (no members of Muon g-2 collaboration)

ω_a reference clock supposed to be at 40 MHz but slightly detuned

$$\frac{\omega_a}{\tilde{\omega}'_p} = \frac{f_{\mathrm{clock}}\,\omega_a^{\mathrm{meas}}\left(1 + C_e + C_p + C_{ml} + C_{pa}\right)}{f_{\mathrm{calib}}\left\langle M(x,y,\phi)\,\omega'_p(x,y,\phi)\right\rangle\left(1 + B_k + B_q\right)}$$

Muon g-2 ready for unblinding

... on February 25th, 2021!

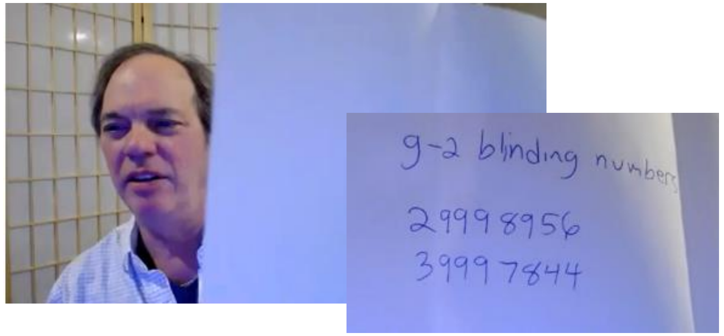

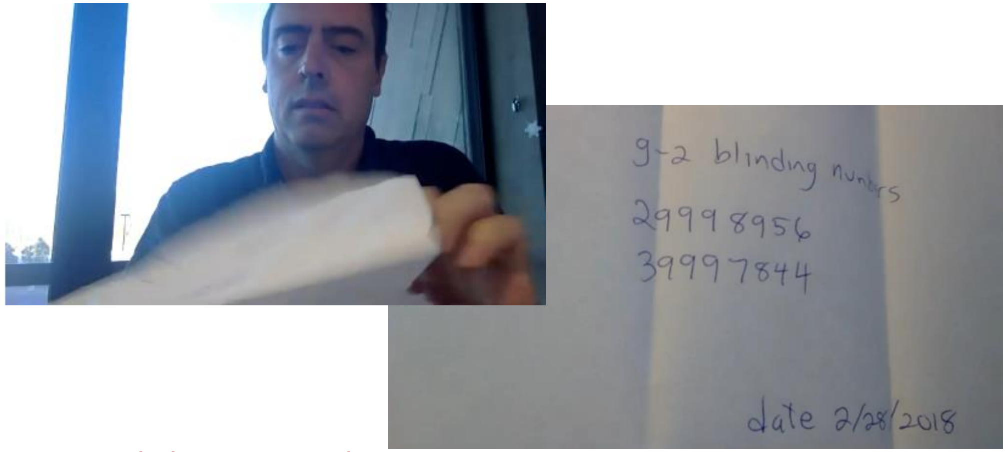

The 40 MHz clock was really set to:
39 997 844 MHz

$$\frac{\omega_a}{\tilde{\omega}'_p} = \frac{f_{\text{clock}}\, \omega_a^{\text{meas}} \left(1 + C_e + C_p + C_{ml} + C_{pa}\right)}{f_{\text{calib}} \left\langle M(x,y,\phi)\, \omega'_p(x,y,\phi) \right\rangle \left(1 + B_k + B_q\right)}$$

Run 1 Result

- Muon g-2 collaboration published Run 1 result
  B. Abi *et al.* (Muon g−2 Collaboration) Phys. Rev. Lett. **126**, 141801, 2021

$$a_\mu(\mathrm{FNAL}) = 116\,592\,040(54) \times 10^{-11} \quad (0.46\,\mathrm{ppm})$$

- Uncertainty in theory calculation dominated by calculation of hadronic vacuum polarization

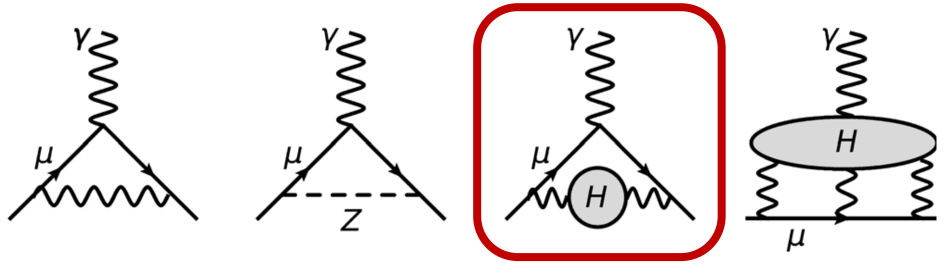

- Dispersive approach, 4.2σ tension
  T. Aoyama *et al.*, Phys. Rept. **887** (2020) 1-166

- Latice QCD approach , 1.5σ tension
  Borsányi *et al.*, Nature **593**, 51–55, 2021 and arXiv:2002.12347

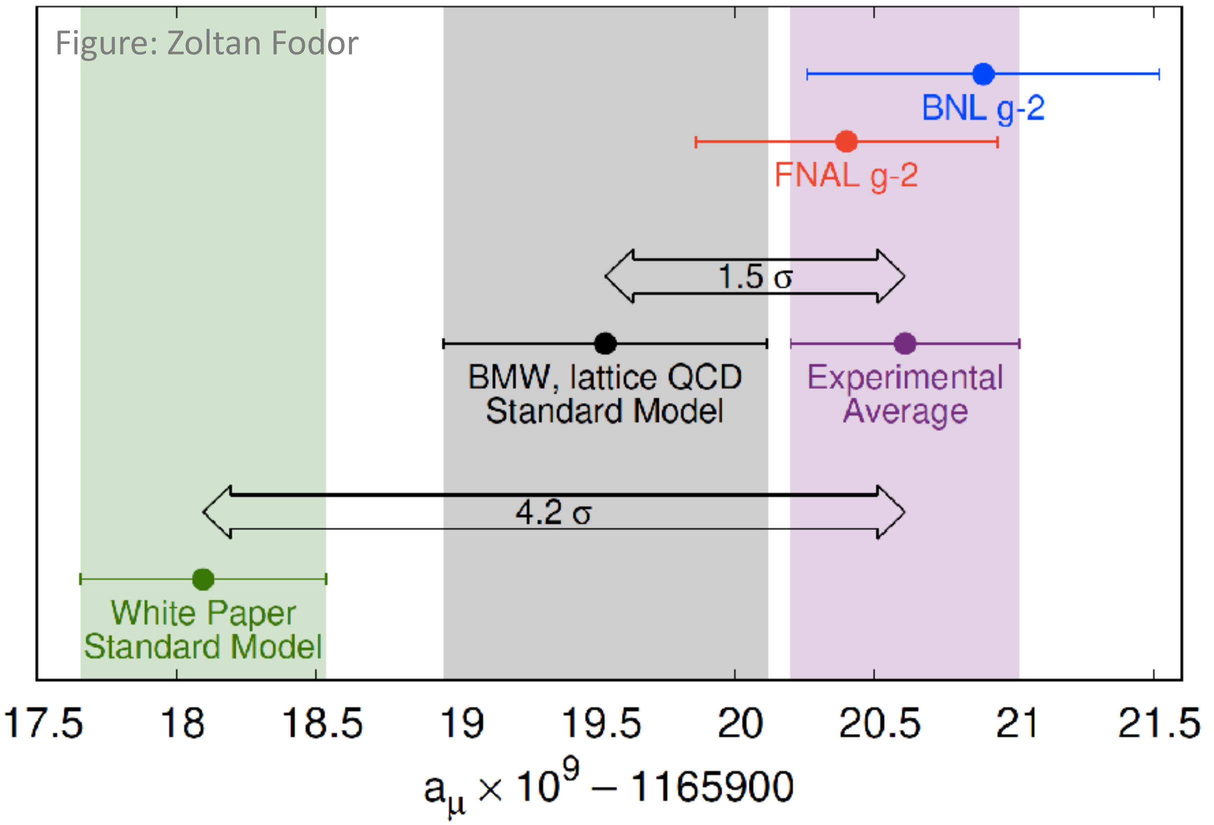

A new era of a_μ comparisons

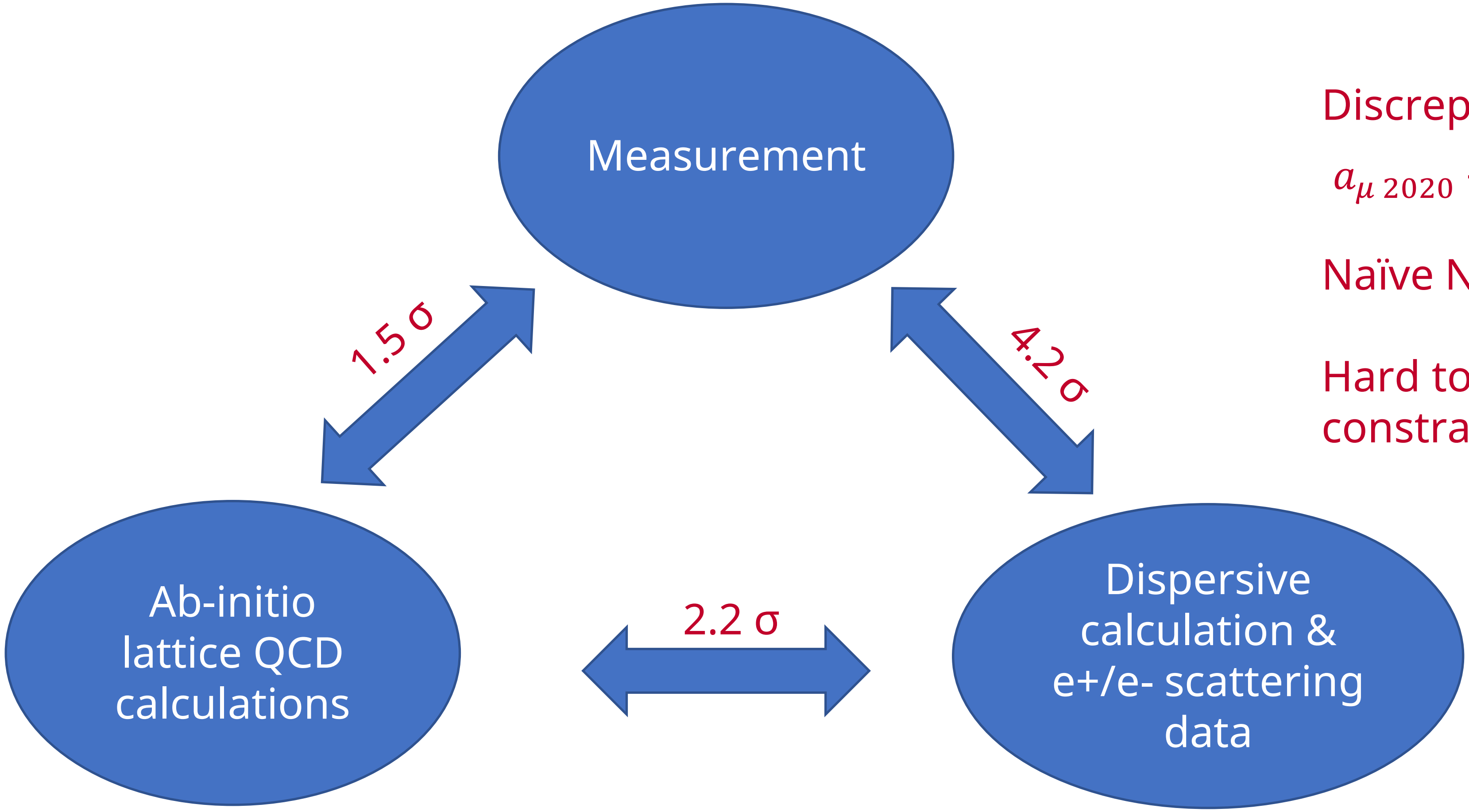

Discrepancy is large

$a_{\mu\,2020} - a_{\mu\,dispersive} \sim 1.7\; a_{\mu\,Weak}$

Naïve NP scaling $M_{BSM} < O(2.1\text{ TeV})$

Hard to accomodate with LHC and DM constraints

Dispersive approach

The diagram to be evaluated:

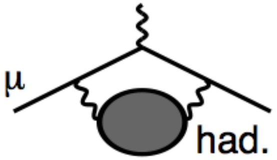

pQCD not useful. Use the dispersion relation and the optical theorem.

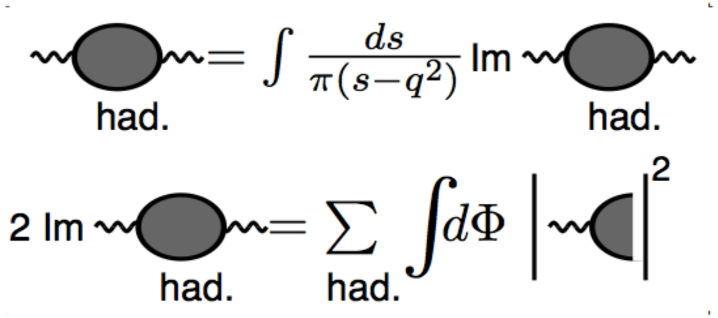

$$a_\mu^{\mathrm{had,LO}} = \frac{m_\mu^2}{12\pi^3} \int_{s_{\mathrm{th}}}^{\infty} ds \, \frac{1}{s} \hat{K}(s) \sigma_{\mathrm{had}}(s)$$

Credit: Thomas Teubner

Follows from causality → analyticity

Follows from unitarity of scattering matrix

Weight function K(s) from loop integral $\int d^4q$

Low energies more important

$\pi^+ \pi^-$ contribute 73% to LO

need to know total hadronic cross-section $\sigma_{had}(s)$

Dispersive approach

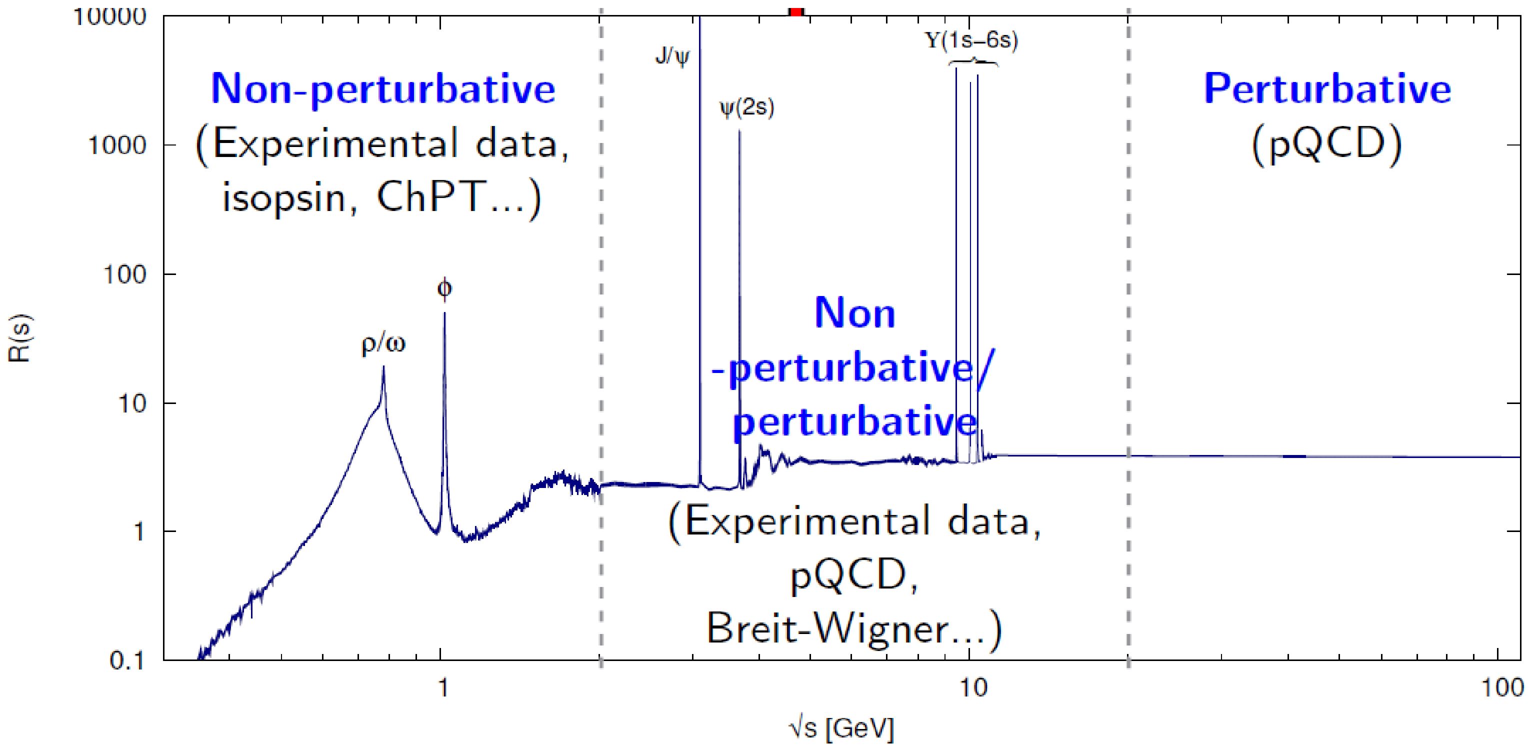

- >100 datasets from e^+e^- → hadrons in > 35 final states
- Data from BELLE-II, BES-III, KLOE, BaBar, SND, CMD-3 and KEDR

Uncertainties for Run 1

$$\frac{\omega_a}{\tilde{\omega}'_p} = \frac{f_{\rm clock}\,\omega_a^{\rm meas}\,(1 + C_e + C_p + C_{ml} + C_{pa})}{f_{\rm calib}\,\langle M(x,y,\phi)\,\omega'_p(x,y,\phi)\rangle\,(1 + B_k + B_q)}$$

Quantity	Correction Terms (ppb)	Uncertainty (ppb)	Design goal
ω_a^m (statistical)	–	434	100 ppb
ω_a^m (systematic)	–	56	70 ppb (with C_e, C_p, C_{ml}, C_{pa})
C_e	489	53	
C_p	180	13	
C_{ml}	-11	5	
C_{pa}	-158	75	
$f_{\rm calib}\langle\omega_p(x,y,\phi)\times M(x,y,\phi)\rangle$	–	56	70 ppb (with B_k, B_q)
B_k	-27	37	
B_q	-17	92	
$\mu'_p(34.7°)/\mu_e$	–	10	
m_μ/m_e	–	22	
$g_e/2$	–	0	
Total systematic	–	157	100 ppb
Total fundamental factors	–	25	
Totals	544	462	140 ppb

- Improve statistics
  → take more data
- Systematics must be improved to achieve design goal
  → Reduce systematics in operations
  → Improve understanding of systematic effects

Summary

- FNAL Run 1 results
    - agrees with BNL measurement
    - statistics limited
    - systematic above design goal
- Increased statistic by factor of ~8
- First time a three-way comparison of a_μ
- Independent measurement of muon g-2 at J-PARC
    - Different experimental technique (no electrostatic focusing)
    - Different beam energy → different magnetic field
- Further theory developments
    - Improved precision of lattice QCD results
    - Proposed new data-driven HVP determination: MUonE at Cern
- This summer Muon g-2 will switch from μ^+ to μ^- (can test LV / CPT invariance)

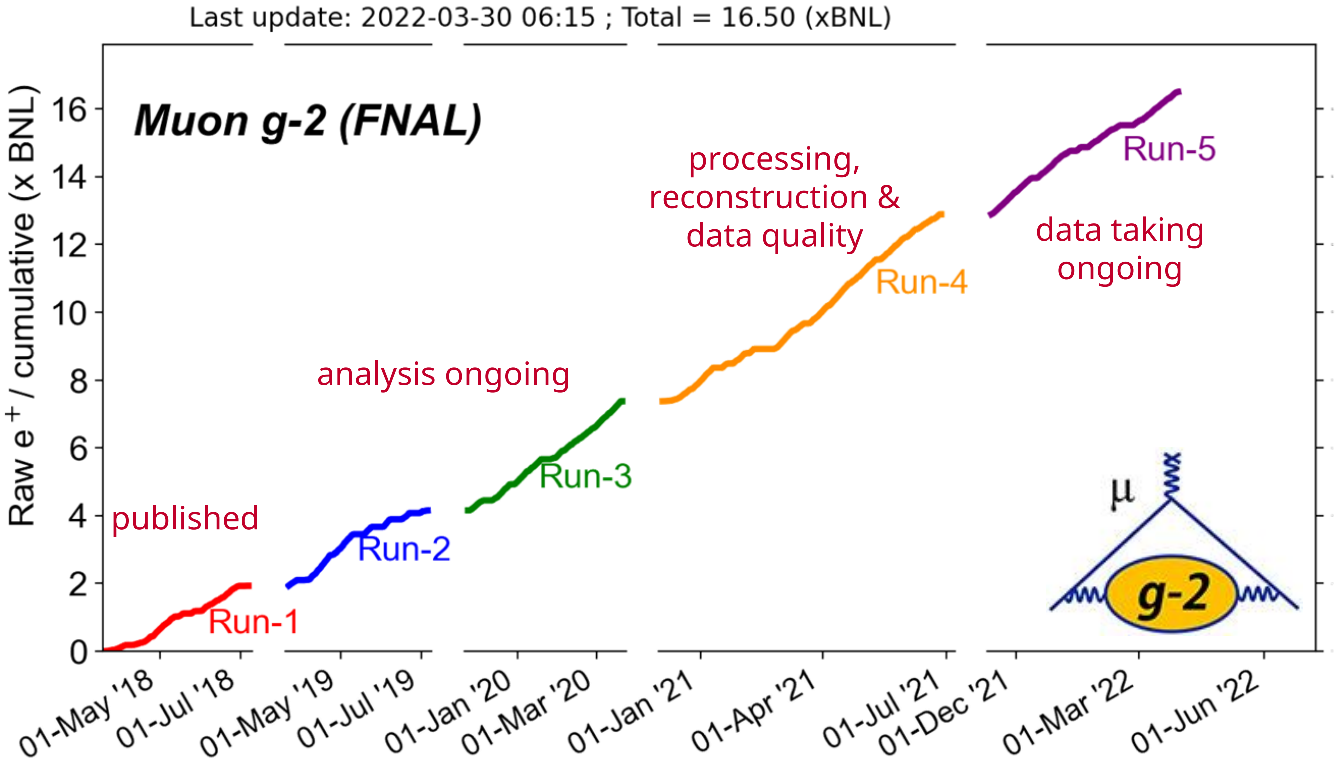

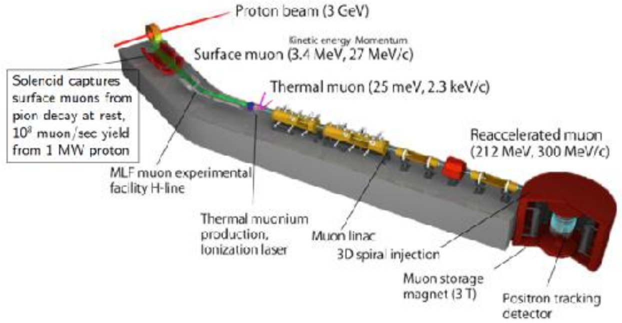

Backup

Lattice approach

- BMW20: First sub% calculation of HVP contribution on lattice

- Calculation of “1 particle Irreducible diagrams”

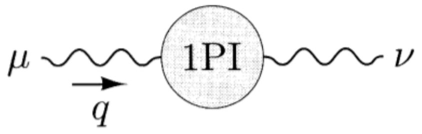

$$\equiv i\Pi^{\mu\nu}(q),$$

- Large systematics from **continuum limit**

➢ upper right panel: limit and uncertainty estimation

➢ lower right panel: limit for central window compared to other lattice and data-driven results

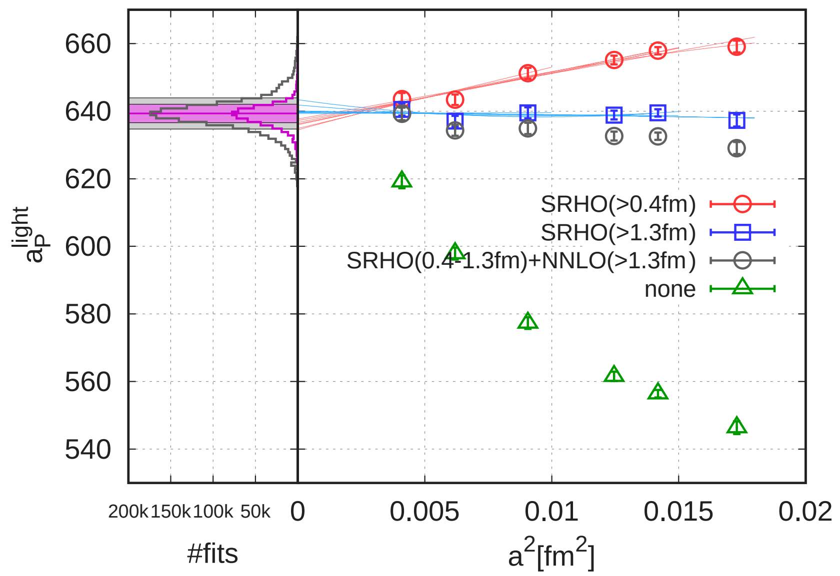

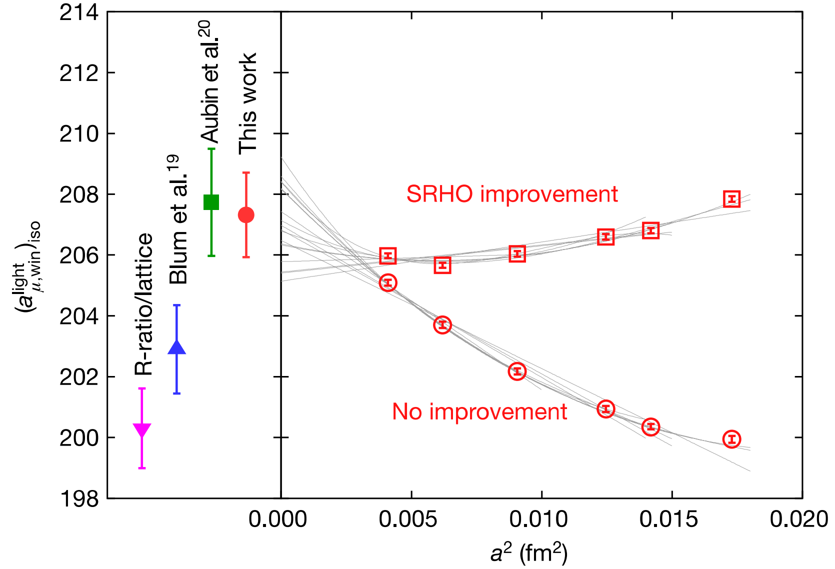

BMW20 [Borsanyi et al, arXiv:2002.12347, 2021 Nature]

Lattice approach

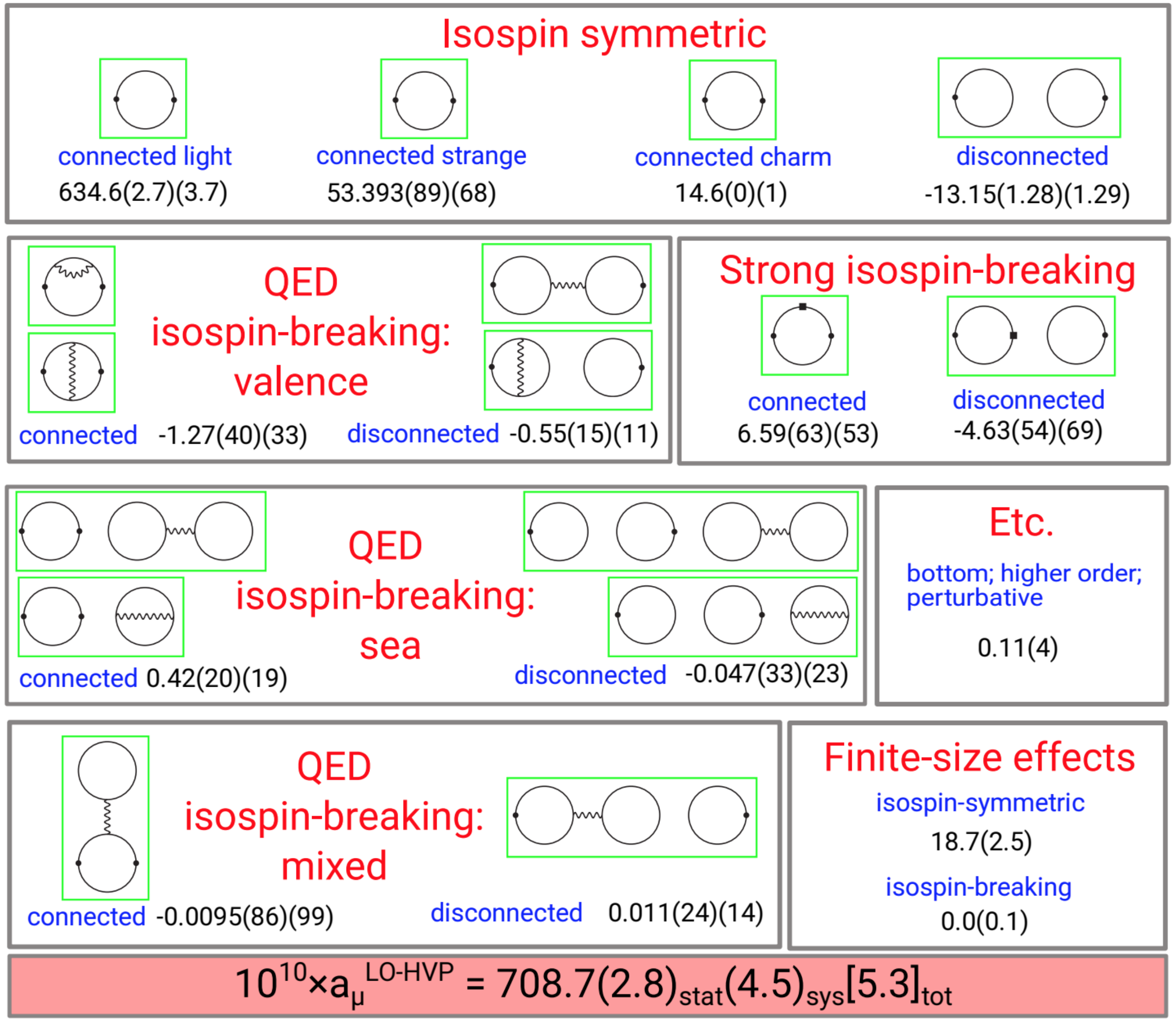

BMW20 [Borsanyi et al, arXiv:2002.12347, 2021 Nature]